2024-06-19

Taphonomic comparison of Hypacrosaurus stebingeri (Hadrosauridae: Lambeosaurinae) bonebeds from the upper Campanian Oldman and Two Medicine formations of Alberta and Montana

Joubarne, Tristan

UNIVERSITY OF CALGARY

Taphonomic comparison of *Hypacrosaurus stebingeri* (Hadrosauridae: Lambeosaurinae) bonebeds from the upper Campanian Oldman and Two Medicine formations of Alberta and Montana

by

Tristan Joubarne

A THESIS

SUBMITTED TO THE FACULTY OF GRADUATE STUDIES

IN PARTIAL FULFILMENT OF THE REQUIREMENTS FOR THE

DEGREE OF MASTER OF SCIENCE

GRADUATE PROGRAM IN GEOSCIENCE

CALGARY, ALBERTA

JUNE, 2024

ABSTRACT

Hadrosaurid social structure is still poorly understood. Evidence from bonebeds suggests that juvenile individuals lived apart from herds composed of older individuals, a phenomenon called age segregation. However, the timing at which juvenile individuals became segregated and later rejoined a multigenerational herd is still unknown. Three monodominant bonebeds that preserve the remains of multiple individuals of the lambeosaurine hadrosaurid *Hypacrosaurus stebingeri* at different ontogenetic stages offer an opportunity to better understand the timing of the age structuring in this species' social structure. One of the three bonebeds, known as the Devil's Coulee juvenile hadrosaur bonebed (JBB) from the Oldman Formation of Alberta (Canada), studied here for the first time, preserves a minimum of four similar-sized late juvenile individuals. The two other bonebeds, Blacktail Creek North (BCN) and Lambeosite (LS) from the Two Medicine Formation of Montana (U.S.A.), preserve a minimum of 23 nestling individuals, and four similar-sized late juvenile individuals with one adult, respectively. These bonebeds show uniform taphonomic signatures throughout the assemblage, characterized by little to no weathering and abrasion, uniform style of fracturing, and rare tooth marks in the assemblages. All three bonebeds are interpreted as mass-mortality assemblages. Histological data indicates that the late juvenile individuals from the JBB were three years old at the time of death, similar to the slightly larger late juvenile individuals from the LS, whereas the individuals from the BCN were less than one year old. A taphonomic comparison with osteological considerations of the three bonebeds reveal that *Hypacrosaurus stebingeri* individuals became segregated when they were less than one year old, and rejoined a multigenerational herd when they were three years old, as evidenced by the presence of an adult with four three-year-old individuals in the LS.

Furthermore, the smaller number of individuals associated with later ontogenetic stages reveals that group size appears to decrease as *Hypacrosaurus stebingeri* individuals grew older.

PREFACE

This thesis is original, unpublished, independent work by the author, T. Joubarne.

ACKNOWLEDGEMENTS

I would like to thank my supervisors, Dr Darla Zelenitsky and Dr François Therrien, for their guidance throughout the project. I would also like to thank Dr Corwin Sullivan and Dr Glenn Dolphin for being a part of my examination committee and for reviewing this thesis. For access to the specimens at the Royal Tyrrell Museum, I thank Brandon Strilisky, Tom Courtenay, and Becky Sanchez. I would like to thank Don Brinkman, Caleb Brown, and James Gardner for their help in identifying microvertebrate fossils. For access to the specimens at the Museum of the Rockies, I thank Eric Metz and John Scannella. For taking the time to scan and share histological thin sections from the Museum of the Rockies, I would like to thank Ellen-Thérèse Lamm and Dane Johnson. I am grateful to John Issa, Amer Dzindic, Kirstin Brink, and Laura Rooney for providing information on the *Hypacrosaurus stebingeri* localities. I would like to acknowledge Eamon Drysdale for sharing histological resources with me. I would like to thank Jared Voris for his help using statistical analysis software. I am also grateful to him for the many hiking trips over the years. Finally, I would like to thank my family for their constant support during my studies.

I would like to acknowledge my funding sources, which consist of a FRQNT Master's Research Scholarship, a Roger Soderstrom Scholarship, two University of Calgary FGS Summer Funding Scholarships, an Alberta Graduate Excellence Scholarship, and a NSERC Discovery Grant (awarded to Dr Darla Zelenitsky).

DEDICATION

This thesis is dedicated to my parents, François Joubarne and Joès Turgeon. Their constant love and support throughout the years kept me going and helped me focus on my work.

TABLE OF CONTENTS

LIST OF TABLES AND FIGURES

CHAPTER 1: INTRODUCTION

Hadrosauridae is a highly diverse group of herbivorous dinosaurs consisting of two major subclades, Saurolophinae and Lambeosaurinae, that lived during the Late Cretaceous. Hadrosaurids are extremely common with over 40 species currently recognized worldwide. Their remains include skeletal elements from individuals of various ontogenetic stages (i.e., embryonic remains, nestlings, juveniles, subadults, and adults) known from isolated skeletons and bonebeds, some of which preserve integument (e.g., Bell, 2012, 2014; Drumheller et al., 2022; Joubarne et al., 2022; Libke et al., 2022), as well as trackways (e.g., Carpenter, 1992; Fiorillo et al., 2014). Their abundance in the fossil record has allowed us to improve our understanding of hadrosaurid behavior such as parental care (Horner and Makela, 1979), migratory patterns (e.g., Carpenter, 1992; Fiorillo et al., 2014), and social structure (e.g., Lauters et al., 2008; Wosik and Evans, 2022). The objective of this thesis is to reconstruct the taphonomic history of three bonebeds from a single lambeosaurine species, *Hypacrosaurus stebingeri*, known from various ontogenetic stages, to better understand the social behavior of this species throughout its lifetime.

Lambeosaurines are notable for their bony cranial ornamentation (i.e., hollow cranial crest). Although lambeosaurines are known widely from the Upper Cretaceous of Eurasia and North America (e.g., Brown, 1913, 1914; Parks, 1922; Young, 1958; Horner and Currie, 1994; Godefroit et al., 2003, 2004; Evans and Reisz, 2007; Gates et al., 2007; Pereda-Suberbiola et al., 2009; Cruzado-Caballero et al., 2010), an unusually high number of species are found in Alberta, Canada (Mallon et al., 2012). Most species from Alberta have been recovered from the Belly River Group, and the highly fossiliferous Dinosaur Park Formation in particular (Ryan and

Evans, 2005). Of all the lambeosaurine species known (n = 7) from the Belly River Group, only one, *Hypacrosaurus stebingeri*, has been recovered from the Oldman Formation, and this species also occurs in the time-equivalent Two Medicine Formation of Montana (Horner and Currie, 1994).

Hypacrosaurus stebingeri has the best represented growth series among lambeosaurines and is known primarily from bone concentrations or bonebeds preserving remains of embryos, nestlings, juveniles, subadults, and adult individuals (Varricchio and Horner, 1993; Horner, 1994; Horner and Currie, 1994; Brink, 2009; Brink et al., 2011, 2014). Most of the embryonic remains, often associated with eggs, are from Alberta (Horner and Currie, 1994; Brink, 2009), whereas specimens of nestling, juvenile, subadult, and adult individuals are mainly from Montana (Varricchio and Horner, 1993; Horner, 1994; Horner and Currie, 1994; Brink, 2009). Dense concentrations of embryonic remains (often nests) of *Hypacrosaurus stebingeri* are known mainly from the Devil's Coulee locality in southernmost Alberta (Horner and Currie, 1994), and bonebeds of nestling-size individuals are primarily known from Glacier County, Montana (Horner and Currie, 1994; Brink, 2009). Devil's Coulee has also yielded a bonebed that contains mid-sized juvenile individuals of *Hypacrosaurus stebingeri* (Brink, 2009), and bonebeds from Glacier County in northern Montana have been reported with both mid-size juvenile and adult individuals, some of which are monodominant for *Hypacrosaurus stebingeri* (Varricchio and Horner, 1993), while others are multitaxic but still contain some *Hypacrosaurus stebingeri* elements (Varricchio and Horner, 1993; Varricchio, 1995).

Despite reports of the existence of several juvenile *Hypacrosaurus stebingeri* bonebeds, limited information has been published on their depositional setting and taphonomy (e.g., Varricchio and Horner, 1993; Varricchio, 1995; Brink, 2009). Here, we present a detailed

sedimentologic and taphonomic analysis of a juvenile bonebed from Devil's Coulee, along with taphonomic comparisons with two additional bonebeds from Montana preserving nestling, juvenile, and adult individuals, to gain a better understanding of the depositional environment and the sequence of events that led to the preservation of young hadrosaurids and to provide insight into the social structure of lambeosaurines.

1.1 LITERATURE REVIEW

1.1.1 Bonebeds

Bonebeds consist of large accumulations of disarticulated, fossilized bones that represent multiple individuals preserved together. Bonebeds are generally described as either monodominant, in which case most of the faunal component represents a single species, or as multitaxic, in which a wide variety of taxa are represented. The study of dinosaur bonebeds can shed light on multiple aspects of dinosaur paleoecology, including social behavior, interspecific interactions, and environmental conditions that may have led to the death of these animals.

Among dinosaurs, monodominant bonebeds are known from various groups, including tyrannosaurs (Eberth and Currie, 2010), ankylosaurs (e.g., Botfalvai et al., 2021), and sauropodomorphs (e.g., Sander, 1992; Storrs et al., 2012), but mainly from ceratopsians (e.g., Ryan et al., 2001; Chiba et al., 2015; Scott et al., 2022b) and hadrosaurids (e.g., Varricchio and Horner, 1993; Lauters et al., 2008; Scherzer and Varricchio, 2010; Holland et al., 2021; Scott et al., 2022a). Hadrosaurid bonebeds have been found in North America (e.g., Varricchio and Horner, 1993; Bell and Campione, 2014; Evans et al., 2015; Holland et al., 2021), Europe (e.g., Gaete Harzenetter, 2021), and Asia (e.g., Bell et al., 2018; Hone et al., 2014b), and are known

from many different species of both saurolophines and lambeosaurines. Most monodominant hadrosaurid bonebeds are located in the Upper Cretaceous (upper Campanian and Maastrichtian) strata of Alberta (Canada) and Montana (U.S.A), where hadrosaurid bonebeds preserved in floodplain (e.g., Bell and Campione, 2014; Holland et al., 2021; Scott et al., 2022a) and debris flow deposits (e.g., Scherzer and Varricchio, 2010; Evans et al., 2015) are common. These bonebeds are often interpreted as resulting from flooding events, which is a potential cause of death commonly invoked to explain the formation of bonebeds. The numerous *Centrosaurus apertus* bonebeds located in Dinosaur Provincial Park are inferred to be the result of large-scale storm-induced flooding events (Eberth and Getty, 2005), an interpretation also invoked for the formation of three *Edmontosaurus regalis* bonebeds from the Horseshoe Canyon Formation of Alberta (Evans et al., 2015). Another cause of death commonly proposed for the individuals preserved in bonebeds is droughts. Such events can often result in the congregation of individuals near a water source, which facilitates the burial of multiple individuals together (Rogers, 1990; Varricchio and Horner, 1993; Hone et al., 2014a). Drought as a mass-kill mechanism has been inferred from several hadrosaurid and ceratopsian bonebeds from the Upper Cretaceous (upper Campanian) Two Medicine Formation of Montana (U.S.A.) (Rogers, 1990; Varricchio and Horner, 1993). However, in the absence of geologic or taphonomic evidence supporting one cause of death over another, it is often impossible to ascertain the cause of death of the individuals preserved in a bonebed. Nonetheless, valuable information on the paleoecology of these animals can still be gained despite the uncertainty of the cause of death.

Bonebeds are generally categorized as representing either mass-death assemblages or time-averaged, attritional assemblages. Mass-death assemblages are formed as a result of catastrophic events that cause the death of a group of individuals. In these assemblages, the cause of death is

indiscriminate of the age of the individuals. As such, the age profile of the individuals in the resulting assemblage reflects that of a population. On the other hand, attritional assemblages, whether monodominant (e.g., Lauters et al., 2008) or multitaxic (e.g., Varricchio, 1995), are formed of individuals that died from independent, unrelated events such as predation or diseases and that accumulate over time in the same area. These assemblages will typically show an age profile biased towards very young and very old individuals that have the highest mortality rate (Varricchio and Horner, 1993; Lyman, 1994; see supp. data of Erickson et al., 2006; Erickson et al., 2010; Lauters et al., 2008). However, social behavior of the individuals can generate a departure from this theoretical model. An assemblage composed of herding animals that perished from a catastrophic event can be biased towards certain ontogenetic stages depending on the herd structure of this animal. Thus, a proper taphonomic consideration is required to accurately infer the type of assemblage represented by the bonebed. Since mass-death assemblages are composed of individuals that died together, the bones from these individuals share a common taphonomic history and undergo the same physical and chemical processes. On the other hand, time-averaged, attritional bonebeds are composed of individuals that may have perished over long periods of time from independent causes. Consequently, the bones from these individuals can experience vastly different physical and chemical processes, resulting in a non-uniform distribution of taphonomic signatures throughout the assemblage (Behrensmeyer, 1978; Varricchio and Horner, 1993; Ryan et al., 2001; Chiba et al., 2015).

1.1.2 Taphonomy

Following the death of an animal, several physical processes can affect the carcass and alter its taphonomic history and its preservation potential. Processes such as scavenging, subaerial

exposure, and transport all play major roles in altering carcasses prior to burial and shaping the resulting assemblage.

Consumption of the carcass by scavengers may leave traces such as tooth marks on the bones. Such tooth marks can vary in shape, size, and depth, depending on the tracemaker and the manner in which the teeth contact the bones. While tooth marks are a good indicator of an interaction between teeth and bones, determining the mechanism that formed a set of tooth marks can be challenging. Tooth marks on bones can be produced from various types of behavior, including agonistic behavior in carnivorous dinosaurs (e.g., Brown et al., 2022), predation, prey bone utilization ("gnawing") (e.g., Brown et al., 2021), and scavenging (e.g., Eberth and Getty, 2005; Gangloff and Fiorillo, 2010; Hone and Watabe, 2010), all of which can result in similar-looking marks, usually in the form of punctures or score marks (also referred to as "drag marks" or "bite-and-drag marks", sensu Hone and Watabe [2010]). Tooth marks that show signs of healing indicate that the prey survived the encounter in which the wound was produced and lived long enough for healing to occur. Thus, behavior such as prey bone utilization ("gnawing") and scavenging can be ruled out when healing is observed, as it would be more consistent with agonistic behavior (e.g., Brown et al., 2022) or a failed hunting attempt. On the other hand, the absence of signs of healing indicates that the animal either perished from the encounter that produced the tooth marks before healing could occur, in the instance where hunting is the cause, or that the animal was already dead when the tooth marks were produced, in which case prey bone utilization ("gnawing") or scavenging are likely scenarios. Scavenging is often inferred from tooth marks in mass death assemblages, in which the cause of death can occasionally be identified as environmental influences (e.g., Ryan et al., 2001; Eberth and Getty, 2005; Chiba et al., 2015) or diseases (e.g., Varricchio, 1995). The rarity of tooth marks in mass death

assemblages can be explained by the overabundance of food that a high number of carcasses would produce, which would decrease the odds of scavenger teeth making contact with the bones of any one of the carcasses (Eberth and Getty, 2005; Hone and Rauhut, 2010).

Once exposed to subaerial conditions, bones start to undergo weathering, which causes them to decay over time. Weathering occurs mainly as a result of cyclical variations in temperature and humidity (Behrensmeyer, 1978). To better understand the timing and rate at which this process occurs, Behrensmeyer (1978) studied modern mammal bones in the Amboseli Basin (Kenya) over a period of more than 15 years and noticed a sequence of alteration features on the bones. These weathering characteristics were split into six weathering stages, indicative of increasing alteration related to increasing time of exposure after death: Stage 0 refers to pristine bones (0-1 year of exposure); Stage 1 is characterized by longitudinal cracking of the bone surface (0-3 years of exposure); Stage 2 is characterized by flaking of the bone surface (2-6 years of exposure); Stage 3 is characterized by a removal of the outermost layers of the bone, resulting in the presence of rough patches (4-15+ years of exposure); Stage 4 is characterized by deep alteration and splintering of the bone (6-15+ years of exposure); Stage 5 is characterized by heavy alteration that causes the bone to easily fall apart (6-15+ years of exposure) (Behrensmeyer, 1978). Interestingly, while bone alteration due to weathering follows these same stages in order, bones of small and juvenile individuals exhibit a higher rate of weathering than bones of large and adult individuals (Behrensmeyer, 1978). Recognizing the potential of using weathering as a tool to infer exposure time, Behrensmeyer (1978) established the methodology used to record weathering stages: these stages should be assessed on regions of the bones, such as the shaft of limb bones or the flat surfaces of flat bones, that undergo little physical alteration, and the most advanced weathering stage that covers at least 1 cm^2 of the bone must be

considered. For a better application to fossil assemblages, Fiorillo (1988) adapted the weathering stages defined by Behrensmeyer (1978) based on comparisons with a Miocene mammal assemblage (Hazard Homestead Quarry). This new classification system accounts for the absence of soft tissue in fossil assemblages and the low preservation potential of heavily weathered bones by dropping stages 4 and 5 as defined by Behrensmeyer (1978). Recent taphonomic studies of fossil assemblages still rely on the amended classification by Fiorillo (1988) to assess the extent of weathering (e.g., Ryan et al., 2001; Gangloff and Fiorillo, 2010; Chiba et al., 2015; Holland et al., 2021; Scott et al., 2022a)

Bone abrasion occurs as a result of the interaction of bones with sediments or other bones during hydraulic transport. To assess the extent of abrasion, Fiorillo (1988) proposed a classification based on the alteration observed on the surface and the edges of the bones. Similar to weathering, abrasion is classified into four stages: Stage 0 represents pristine bones; Stage 1 is characterized by slight abrasion that results in slight rounding of the edges; Stage 2 is characterized by moderate abrasion producing well-rounded edges and a somewhat polished surface; Stage 3 is characterized by extensive abrasion resulting in barely recognizable bones (Fiorillo, 1988). This type of bone modification feature is often seen as an indicator of distance of transport experienced by bones in fluvial settings, as more transport results in more interaction between the bones and the sediments. However, recent experiments in annular flumes have shown that abrasion is also dependant on the size and angularity of the sediments that interact with the bones (Griffith et al., 2016), the duration of the interaction with the sediments (Thompson et al., 2011), and the mode of transport experienced by the sediments which, in turn, depends on flow velocity (Thompson et al., 2011). These experiments showed that under similar conditions, fresh bones experience the most abrasion as the sediments are transported by

saltation (Thompson et al., 2011). The extent of abrasion also increases with the grain size of the sediments, although this relationship is more complex with sand grains due to the formation of scour pits around the bones, which hinder abrasion (Thompson et al., 2011; Griffith et al., 2016). These studies highlight the fact that bone abrasion is a complex process influenced by many different factors and a direct correlation between the degree of bone abrasion and the distance of transport cannot be established. Nonetheless, this bone modification feature provides some valuable taphonomic information regarding the interaction between the bones and the sediments under fluvial influence.

During fluvial transport, some bones can be preferentially removed from an assemblage. Using modern sheep and coyote bones, Voorhies (1969) examined the susceptibility to hydraulic transport of bones and their dispersal patterns under fluvial influence, and noticed that some bones were transported further from their starting position than others. Bones were classified into three dispersal groups, now commonly referred to as “Voorhies groups”, based on their susceptibility to hydraulic transport and their modes of transportation: group I contains bones that are most easily transported by flotation or saltation, group II contains bones that are progressively removed and transported by traction, and group III contains bones that are left as lag deposits (Voorhies, 1969). The application of this classification to fossil assemblages is useful to infer the extent of fluvial influence on the formation of the bonebed. However, the applicability of these groups as defined by Voorhies (1969) to dinosaur bonebeds has been questioned (e.g., Lauters et al., 2008; Gangloff and Fiorillo, 2010; Holland et al., 2021; Blob et al., 2023). While the approach is robust, the classification of each bone into the three Voorhies groups was originally based on the dispersal pattern of modern mammalian bones. Significant differences between dinosaur bones and mammalian bones could result into a different grouping

than that proposed by Voorhies (1969). For example, Voorhies (1969) observed that the fused pelvis of mammals belongs to group II. In dinosaurs, the three bones forming the pelvis (ilium, ischium, and pubis) are unfused, which implies that they may behave differently from one another under fluvial influence, which would result in them being classified in different groups and would consequently alter the expected proportions for each group. To account for these differences, Holland et al. (2021) proposed an amended grouping for juvenile hadrosaurids by taking into account inferred susceptibility to hydraulic transport and the lack of skeletal fusion, and adjusting the expected proportions for each group based on the count for each skeletal element in a complete hadrosaurid skeleton. As such, all cranial elements were moved from group III to group I, with the exception of the dentary and the maxilla which were moved to group II. The three bones forming the pelvis were placed in different groups: the ischium was placed in group I, the pubis in group II, and the ilium in group III. Phalanges were moved from group II to group I, and all other limb bones were moved to group III, with the exception of the tarsals and metapodials which remained in group II (Holland et al., 2021).

A recent study testing the dispersal patterns of alligator bones under fluvial influence has shown a different grouping from mammal and hadrosaurid bones, highlighting the fact that susceptibility to hydraulic transport for each skeletal element may vary significantly between taxa (Blob et al., 2023). In this study, group I consisted of the ilium, ischium, scapula, coracoid, and vertebrae. Group II consisted of the ulna, tibia, humerus, rib, fibula, and radius. Group III consisted of the pubis and the femur. The susceptibility to hydraulic transport of the skull and the mandible varied significantly depending on the orientation of these elements relative the direction of the flow (Blob et al., 2023). Despite the differences observed in bone dispersal between taxa, this approach is still informative and widely used in taphonomic analyses as it

relies on differences in susceptibility to hydraulic transport of the bones of an individual. Bones under fluvial influence will tend to follow a general dispersal pattern affected notably by their density, shape, and initial orientation (Blob et al., 2023), regardless of the taxon. These dispersal patterns can inform on the extent of hydraulic sorting that an assemblage underwent. For example, an assemblage composed mainly of bones classified into Voorhies group III (lag deposits) suggests that the assemblage is autochthonous and that light, easily transported skeletal elements were preferentially removed from the assemblage through hydraulic winnowing, whereas an assemblage composed exclusively of bones classified into Voorhies group I (easily transported by flotation or saltation) would be indicative of an allochthonous assemblage. To evaluate the relative proportions of each Voorhies group, Fiorillo (1991) suggested that the observed proportions in an assemblage should be compared with the expected proportions from complete, unaltered skeletons of the same species, a method also followed in recent studies (e.g., Ryan et al., 2001; Lauters et al., 2008; Holland et al., 2021). A perfect match between the observed and expected proportions would indicate that the assemblage experienced little to no fluvial influence or, at least, that no bones from the assemblage experienced preferential removal through hydraulic winnowing.

1.1.3 Behavior

Behavior in extinct animals is often challenging to infer due to the lack of direct evidence. Despite being impossible to observe directly, certain types of behavior can be reflected in trace fossils and fossil accumulations. Some of the strongest evidence for social behavior in dinosaurs comes from the study of trackways, nesting sites, and bonebeds.

Dinosaur behavior is best understood in hadrosaurids due to their abundance in the fossil record. The first evidence of parental care among hadrosaurids came with the discovery of a group of 15 baby *Maiasaura peeblesorum* individuals associated with eggshells in a nest (Horner and Makela, 1979). Based on the fact that these young individuals were preserved in a nest, Horner and Makela (1979) concluded that parental care must have occurred, either to bring food to the nest, or to escort them back to the nest in the instance that they were able to forage themselves. Based on osteological and histological data from embryonic and neonate individuals, *Maiasaura peeblesorum* is thought to be an altricial species, implying that the nest-bound neonates would require extensive parental care to survive (Horner and Weishampel, 1988). It is still unclear whether young hadrosaurid individuals stayed within groups alongside individuals of all ages as they grew up, or would have formed segregated groups with conspecifics of the same age. Trackways from the Upper Cretaceous Cantwell Formation of Alaska (U.S.A.) support the idea that some hadrosaurids lived in multigenerational herds composed of individuals of all ages (Fiorillo et al., 2014). This tracksite is unique in preserving hadrosaurid footprints with a wide size range, from very small footprints likely produced by juvenile individuals, to very large footprints produced by adult individuals, indicating that individuals of all growth stages lived and traveled together (Fiorillo et al., 2014). Interestingly, hadrosaurid trackways from the Mesaverde Group of Utah and Colorado (U.S.A.) show a separation between tracks produced by young individuals and those produced by subadult and adult individuals (Carpenter, 1992). The absence of small tracks associated with large footprints in these trackways could be indicative of young individuals living and traveling apart from groups composed of older individuals, or it could be explained by the small weight of juvenile individuals which would have prevented them

from pressing the substrate hard enough to produce a well-defined footprint that could be preserved (Carpenter, 1992; Fiorillo et al., 2014).

Evidence from bonebeds supports a scenario in which juvenile hadrosaurids were segregated from very young and old individuals (e.g. Lauters et al., 2008; Scherzer and Varricchio, 2010; Holland et al., 2021; Scott et al., 2022a). While individuals of all ontogenetic stages (i.e., nestlings, early juveniles, late juveniles, subadults, and adults) are known from hadrosaurid bonebeds, their distribution tends to be biased towards one ontogenetic stage. For example, some bonebeds preserve exclusively late juvenile individuals (e.g., Gangloff and Fiorillo, 2010; Scherzer and Varricchio, 2010; Holland et al., 2021), whereas others preserve exclusively subadult and adult individuals (e.g., Varricchio and Horner, 1993; Evans et al., 2015). This pattern can be explained by the type of assemblage that is represented by the bonebed (Varricchio and Horner, 1993; Lyman, 1994; see supp. data of Erickson et al., 2006; Erickson et al., 2010; Lauters et al., 2008), or by the social behavior of the individuals preserved in the bonebed (e.g., Gangloff and Fiorillo, 2010; Scherzer and Varricchio, 2010; Holland et al., 2021). The near monospecificity of these bonebeds and their uniform taphonomic signatures suggest that these assemblages are the result of mass-mortality events and that their composition reflects true hadrosaurid behavior. As such, the absence of juvenile individuals in most bonebeds and their exclusive preservation in others suggest that age segregation was a life strategy employed by these dinosaurs. However, despite the plethora of hadrosaurid bonebeds that support this inference (e.g., Lauters et al., 2008; Scherzer and Varricchio, 2010; Evans et al., 2015; Holland et al., 2021; Scott et al., 2022a), the timing at which young individuals wandered off to form segregated groups of their own and later joined a multigenerational herd is still poorly understood, in part due to the fact that few hadrosaurid species are known from multiple

bonebeds that preserve individuals of all growth stages. To date, a single study has tackled this issue for the saurolophine *Edmontosaurus annectens* (Wosik and Evans, 2022). Using a histological comparison among several bonebeds, Wosik and Evans (2022) determined that nestling and early juvenile *Edmontosaurus annectens* individuals likely formed segregated groups that would rejoin the multigenerational herd during their second year of life. The life-history of lambeosaurines is still poorly understood, despite many reports of lambeosaurine bonebeds in the upper Campanian (Upper Cretaceous) strata of North America (e.g., Varricchio and Horner, 1993; Horner and Currie, 1994; Scherzer and Varricchio, 2010; Holland et al., 2021).

CHAPTER 2: MATERIALS AND METHODS

To better understand the life history and social behavior of juvenile *Hypacrosaurus stebingeri* individuals, the taphonomy of three bonebeds that preserve individuals at different ontogenetic stages was studied. One bonebed is from the upper Oldman Formation in the Devil's Coulee area in southernmost Alberta (Canada), whereas the other two are from the upper Two Medicine Formation of northwestern Montana (U.S.A.). As part of this project, we conducted field work at only one of the three sites, where stratigraphic and sedimentologic data had never been collected before. Specimens collected during the excavations of the bonebeds in the late 1980s were examined first-hand in the collections of the Royal Tyrrell Museum of Palaeontology (Drumheller, Alberta, Canada) and the Museum of the Rockies (Bozeman, Montana, U.S.A.).

2.1 FIELD OBSERVATIONS

Specimens from the juvenile hadrosaur bonebed (JBB) at Devil's Coulee, referred to as 'Juvenile Bonebed' or 'Juvie Camp' in the RTMP collections database, were collected over the course of excavations conducted in 1988 and 1989 by the Royal Tyrrell Museum of Palaeontology. All specimens from the JBB are accessioned at the Royal Tyrrell Museum of Palaeontology (TMP 1988.151 and TMP 1989.151 series). Although a quarry map was produced during excavation of the JBB, it could not be located for our current research (i.e., more than 30 years after the excavation). While the map would have been useful to determine preferential orientation and distribution of the skeletal elements in the bonebed, its absence does not preclude a detailed taphonomic study of the bonebed.

The JBB locality was revisited in June 2022 to examine exposures and measure two stratigraphic sections of the bonebed-hosting interval (Figure 1) in order to conduct a detailed study of the depositional environment. The stratigraphic sections were measured at the northern and southern extremities of the bonebed to understand the lateral variations of the JBB-hosting interval. The stratigraphic interval was trenched with a hand pick to expose fresh rocks, allowing for a complete description of the strata. The precise coloration of the rocks was determined using the Munsell Soil Color Charts (Munsell, 2000). The thickness of the strata has been measured using a tape measure.

The Blacktail Creek North and Lambeosite bonebeds were excavated in 1988 and 1985, respectively (E. Metz, pers. comm., 2022), and all specimens from both bonebeds were accessioned at the Museum of the Rockies in Bozeman, Montana (MOR 548 and MOR 355, respectively). While the material recovered from these bonebeds was re-examined for this study, the localities were not revisited. As such, all information pertaining to the depositional environments, including potential causes of death inferred from sedimentology, presented here is based on published literature.

Figure 1. Map of Alberta (Canada) and Montana (U.S.A.) illustrating the geographic location of the bonebeds (red stars).

2.2 TAPHONOMY

Material from the three *Hypacrosaurus stebingeri* bonebeds was examined here in the context of a rigorous taphonomic study. Despite having been excavated in 1988 and 1989, the JBB has never been subject to a taphonomic analysis and is analyzed here in this context for the first time. The taphonomy of the Blacktail Creek North (MOR 548) and Lambeosite (MOR 355) bonebeds has been briefly described over 30 years ago (see Varricchio and Horner, 1993; Horner, 1994; Horner and Currie, 1994). Since then, additional material from these two bonebeds has been prepared and was available for study. All specimens from both bonebeds were re-examined to obtain an updated taphonomic profile and allow for a rigorous comparison among these *Hypacrosaurus stebingeri* bonebeds.

In this study, the term "specimen" refers to any individual bone, tooth, or element collected from the bonebeds. Since a few specimens remain unprepared, descriptions of bone modification features are based on the number of prepared specimens (NPSP). "Identifiable specimens" refers to those that are sufficiently complete to be recognized as part of a specific skeletal element. "Skeletal elements" refers to the individual bones that make up the skeleton (e.g., humerus, ulna, vertebra). The total number of skeletal elements preserved in the assemblages is estimated based on the number of identifiable specimens (NISP) with no overlapping parts: various fragmentary specimens of a given skeletal element that do not overlap with each other are assumed to represent a single skeletal element. The minimum number of individuals (MNI) preserved in each bonebed was estimated based on the number of the most abundant unique skeletal element (i.e., element that is present only once in any given individual, e.g., right scapula, left humerus) in the assemblage. For consistency, the ontogenetic status of the individuals from each bonebed was estimated based on the length of limb bones (see Horner et al. [2000] and Ullmann et al.

[2017]) due to the scarcity of cranial elements in two of the three bonebeds examined (JBB and Lambeosite), which precluded determination of ontogenetic status based on skull length as typically done (e.g., Evans [2010], Holland et al. [2021]).

Specimens were visually examined for signs of bone modification features, including weathering (Behrensmeyer, 1978; Fiorillo, 1988), abrasion (Fiorillo, 1988), breakage, fractures (Haynes, 1983), wet rot (Andrews and Ersoy, 1990; Scherzer and Varricchio, 2010), and tooth marks (Hone and Watabe, 2010). Two specimens (TMP 1988.151.98 and TMP 1993.76.1) were excluded from this analysis due to heavy modern alteration. To estimate the duration of subaerial exposure of the bones prior to burial, weathering was assessed and staged based on the extent of modification to the bone. Weathering of a specimen was recorded on a scale from stage 0 to stage 3, as originally defined by Behrensmeyer (1978) and subsequently adapted for fossil deposits by Fiorillo (1988), by assessing the most advanced weathering stage that covers a surface of at least one cm^2 of the specimen (sensu Behrensmeyer, 1978): stage 0 represents an intact bone surface; stage 1 is characterized by light cracks parallel to the bone surface; stage 2 is characterized by flaking and cracking of the outermost layer of the bone; and stage 3 is characterized by the removal of the outermost bone layers and presence of deep cracks. Bone abrasion, which results from interaction with sediments during transport (Behrensmeyer, 1982, 1991; Fiorillo, 1988), was recorded on a scale from stage 0 to stage 3: stage 0 is characterized by intact and well-defined edges; stage 1 is characterized by slight abrasion resulting in slight rounding of the edges; stage 2 is characterized by moderate abrasion resulting in well-rounded edges; and stage 3 is characterized by extreme abrasion resulting in rounded and unidentifiable bone fragments (sensu Fiorillo, 1988). The presence of fractures was assessed for each specimen, and the fracture pattern and location on the element was recorded (sensu Haynes, 1983). Tooth marks were

described following the terminology established by Hone and Watabe (2010), and the number, position, and morphology of tooth marks in the assemblage were recorded for each specimen.

Susceptibility to hydraulic transport and sorting of skeletal elements is dependent on the shape and density of the bones, and on their orientation relative to the direction of the flow (Voorhies, 1969; Behrensmeyer, 1982, 1991; Blob et al., 2023). Due to a differential susceptibility to transport among skeletal elements, sorting of the elements increases with the distance of transport (Voorhies, 1969; Behrensmeyer, 1991). To account for the possibility of pre-transport breakage and to obtain a conservative estimate of the number of elements initially preserved in the assemblage, the extent of hydraulic transport and sorting was assessed for each bonebed based on the total number of skeletal elements (as defined above), including non-prepared elements, rather than the NPSP. Each skeletal element was assigned to its respective dispersal group, often referred to as "Voorhies groups". These groups, indicative of a skeletal element's susceptibility to hydraulic transport, were experimentally established by Voorhies (1969) and subsequently adapted for juvenile lambeosaurine hadrosaurids by Holland et al. (2021: table 2) to account for the unique shape of their bones, the size of the skeletal elements, and the unfused condition of the bones in juvenile individuals. As such, the assignment of skeletal elements to Voorhies groups in this study is based on Holland et al. (2021). The observed proportions of each Voorhies group in the bonebeds were compared to the expected proportions for complete lambeosaurine hadrosaurid skeletons (see Holland et al., 2021: table 2). To determine if a significant difference existed between the observed and expected proportions of each Voorhies group, a chi-square goodness of fit test has been conducted using R v4.3.2.

Preferential orientation of the elements was tested for the Blacktail Creek North bonebed based on an unprepared field jacket on display at the MOR since a complete quarry map of the

bonebed could not be found. A total of 96 identifiable specimens (two maxillae, one jugal, 32 vertebral elements [29 isolated centra and three cervical vertebrae with neural arches], 32 ribs, five scapulae, one coracoid, four sternal plates, five humeri, three ulnae, one radius, one metacarpal, one ilium, two ischia, two femora, three tibiae, one fibula) are exposed in the field jacket, although more unexposed specimens could be present. Orientation of the specimens relative to North was measured towards the East (i.e., all measurements ranged from 0° to 180°) on specimens that showed a clear linear axis (54 specimens: all ribs and most limb bones) using ImageJ v1.53k, with the direction of the North based on a partial illustration of the field jacket (see Horner, 1994: fig. 8.4). Orientation data were plotted on a mirror-image rose diagram using GeoRose v0.5.1 with intervals of 10 degrees. A Rao's spacing test of uniformity was performed in R v4.3.2 using the CircStats package. Since directional data of bones is diametrically bimodal, the dataset used to conduct the Rao's spacing test of uniformity was doubled to include the diametrical opposites of every measurement in order to avoid obtaining an erroneous result that would indicate departure from directional uniformity simply due to the lack of data in the western quadrants. Orientation of the bones could not be analyzed for the JBB and Lambeosite in the absence of a quarry map or an unprepared jacket containing numerous elements.

2.3 HISTOLOGY

The presence of lines of arrested growth (LAGs) and annuli are commonly used to determine the biologic age of extinct animals such as dinosaurs (e.g., Cooper et al., 2008; Erickson et al., 2007; Griebeler et al., 2013; Horner et al., 1999). Since dinosaurs exhibit cyclical growth (Chinsamy-Turan, 2005), each LAG or annulus is interpreted to represent one year. As such, counting the number of LAGs and annuli on cross-sections of limb bones provides an estimate

for the biologic age of the individuals. To assess the biological age of the individuals preserved in the three bonebeds examined as part of this study, histological thin sections of select limb bones were examined. Bones from the JBB were sent to Calgary Rock and Materials Services Inc. (Calgary, Alberta) for sectioning. Thin sections from the JBB were produced from the mid-diaphysis of four left fibulae (TMP 1988.151.4, TMP 1988.151.23, TMP 1988.151.45, TMP 1988.151.81), elements that served as the basis for the MNI, to ensure that each bone sampled represented a different individual. These thin sections were examined using a Leica DM 2500P microscope and photographed with Leica MC190 HD camera. Thin sections from the Blacktail Creek North and Lambeosite bonebeds were scanned and digitally shared with us by the MOR collections. These thin sections were produced from a fibula (in the case of the Blacktail Creek North bonebed) and a tibia (for Lambeosite). Histological features of the bones were measured using ImageJ v1.53k.

CHAPTER 3: TAPHONOMY OF THE THREE *HYPACROSAURUS STEBINGERI* BONEBEDS

3.1 GEOLOGICAL SETTING

3.1.1 Belly River Group

The Belly River Group (Upper Cretaceous: upper Campanian) of Alberta consists of an eastward-thinning clastic wedge that represents paralic and non-marine environments on the western margin of the Western Interior Seaway (Eberth and Hamblin, 1993; Eberth, 2005). It is underlain by the marine shales of the Pakowki Formation and overlain by the marine shales of the Bearpaw Formation (Eberth and Hamblin, 1993). The Belly River Group is subdivided, in ascending order, into the Foremost (170 m thick in Dinosaur Provincial Park [DPP], no exposure in DPP), Oldman (40 m thick in DPP, partially exposed), and Dinosaur Park (70 m thick in DPP) formations in the Alberta plains (Eberth and Hamblin, 1993; Eberth, 2005). The Foremost Formation is composed of paralic sediments deposited during the regression of the Pakowki Sea. It is characterized by a succession of coarsening-upwards parasequences marked by marine shales at the bottom and terrestrial carbonaceous shales at the top (Ogunyomi and Hills, 1977; Eberth and Bergman, 1997; Gordon, 2000; Eberth, 2005). The Oldman Formation conformably overlies the Foremost Formation and consists of a northeastward-thinning sequence of terrestrial sediments deposited by northeast-trending, low-sinuosity, ephemeral fluvial streams in an arid to semi-arid environment with seasonal wetlands (Eberth and Hamblin, 1993; Hamblin, 1997; Eberth, 2005; Therrien et al., 2014; Therrien et al., 2015). The formation is subdivided into a lower, a middle (the Comrey Sandstone zone), and an upper unit. The lower and upper units are dominated by pedogenically-modified mudstone containing pedogenic carbonate nodules (i.e., caliches), and lenticular channel deposits reflecting moderate accommodation during the

regression of the Pakowki Sea (regressive system tract) and the transgression of the Bearpaw Sea (transgressive system tract), respectively; in contrast, the Comrey sandstone zone is dominated by multi-meter-thick channel sandstone deposits, interpreted as amalgamated paleochannel-fills, reflecting low accommodation in an early transgressive system tract following maximum eustatic drop (lowstand system tract) (Brinkman et al., 2004; Eberth, 2005). A regional discontinuity separates the Oldman Formation from the overlying Dinosaur Park Formation (Eberth and Hamblin, 1993; Eberth, 2005). The Dinosaur Park Formation is composed of sediments transported by southeast-trending meandering and straight rivers (Eberth and Hamblin, 1993; Hamblin, 1997; Eberth, 2005). It represents a transition from terrestrial to paralic deposits during the transgression of the Bearpaw Sea (Eberth and Bergman, 1997; Brinkman et al., 2004; Eberth, 2005). Paleochannel deposits, represented by sandstones exhibiting trough-cross stratification, inclined heterolithic stratification, and inclined bedding, are abundant throughout the formation. Fine-grained facies of the Dinosaur Park Formation consist mainly of mudstones interpreted as hydromorphic paleosols, bentonite beds derived from volcanic ashes, mudstone-filled incised valleys, and coal beds, the latter two being present exclusively in the Lethbridge Coal Zone (Eberth and Hamblin, 1993; Eberth, 1996; Eberth, 2005). The Dinosaur Park Formation thins in a southward direction while the Oldman Formation thickens, resulting in the upper Oldman Formation of southernmost Alberta being stratigraphically-equivalent and contemporaneous with the Dinosaur Park Formation in DPP (Eberth and Hamblin, 1993; Brinkman et al., 2004; Therrien et al., 2015).

3.1.2 Two Medicine Formation

The Two Medicine Formation consists of an approximately 550 m-thick, eastward-thinning clastic wedge representing terrestrial deposits exposed in northwestern Montana. It is underlain by the Virgelle Formation, representing shoreface deposits on the western margin of the Western Interior Seaway, and overlain by the marine Bearpaw Formation (Rice, 1980; Lorenz, 1981; Rogers, 1998; Trexler, 2001). The Two Medicine Formation consists of fluvial and deltaic deposits in a semi-arid environment (Rogers, 1990; Rogers, 1998; Trexler, 2001). It can be separated into a lower unit (100 m-thick), a middle unit (220 m-thick), and an upper unit (roughly 225 m-thick) (Lorenz, 1981). The lower unit is composed of alternating fine to medium-grained sandstones exhibiting cross-bedding and ripples and massive, greenish-grey mudstone. The upper limit of this unit is characterized by the presence of a muddy sandstone containing gastropods and bivalve shells (Lorenz, 1981). The middle unit of the Two Medicine Formation is characterized by lenticular sandstone bodies separated by grey mudstone with carbonate nodules (Lorenz, 1981). The upper unit of the Two Medicine Formation is marked by the presence of mudstone (grayish-purple and red-brown) and thick, lenticular, cross-bedded sandstone bodies. This unit contains abundant vertebrate fossils (Lorenz, 1981; Trexler, 2001).

3.1.3 Correlations among *Hypacrosaurus stebingeri* bonebeds

Hypacrosaurus stebingeri is known from Devil's Coulee in the upper Oldman Formation of southern Alberta, as well as from 10 localities in the upper 80 m of the Two Medicine Formation of Montana (Horner and Currie, 1994; Trexler, 2001; Brink, 2009). Of these localities, the Blacktail Creek North bonebed (MOR 548) and the Lambeosite bonebed (MOR 355) from Montana studied here have yielded specimens that have been referred to *Hypacrosaurus*

stebingeri (Horner and Currie, 1994). The scarcity of cranial material from the JBB in Devil's Coulee makes a specific identification based on morphology impossible (as also noted by Brink [2009]). However, the material from this bonebed is also considered referrable to *Hypacrosaurus stebingeri* (Brink, 2009). These specimens possess characteristics diagnostic of Lambeosaurinae, such as a distal expansion of the ischium (TMP 1989.151.55) and a strong ventral deflection of the dentary symphysis observable on all dentaries that retain the rostral portion (TMP 1988.151.5 [right], TMP 1988.151.75, TMP 1988.151.88, and TMP 1988.151.158: Figure 2) (Horner et al., 2004; Brink, 2009; Brink et al., 2011). Additionally, embryonic remains of *Hypacrosaurus stebingeri* have been identified at the Little Diablo's Hill locality in Devil's Coulee (Horner and Currie, 1994; Brink, 2009), which is located stratigraphically approximately 10 meters below the JBB. *Hypacrosaurus stebingeri* is also the only known lambeosaurine hadrosaurid from the upper Oldman Formation of Alberta or from the upper Two Medicine Formation of Montana (Trexler, 2001; Horner et al., 2004).

The Devil's Coulee locality, situated south of the depositional edge of the Dinosaur Park Formation (Eberth, 2024), is roughly time-equivalent to the localities that preserve *Hypacrosaurus stebingeri* individuals from Montana (Figure 3). Although difficult to locate exactly in terms of stratigraphic level within the upper Oldman Formation due to the limited exposure at the locality, Devil's Coulee is located within 100 m of the Oldman – Bearpaw Formation contact (Eberth [pers. com.] in Brink [2009]). Both the Blacktail Creek North bonebed and the Lambeosite bonebed are located approximately 45 m below the Two Medicine – Bearpaw Formation contact (Brink, 2009). A radiometric date of 75.05 ± 0.08 Ma was produced from a bentonite sample from the upper Oldman Formation at Devil's Coulee (reported by Eberth and Deino [pers.com.] in Horner and Currie [1994]). Recent radiometric dating of a

bentonite sample recovered 40 m below the Two Medicine – Bearpaw Formation contact at the type locality of the Two Medicine Formation, approximately 10 km north of the Blacktail Creek North bonebed, produced an age of 75.259 ± 0.027 Ma (Ramezani et al., 2022). Although it is unknown how the Bearpaw contact with the Oldman Formation of southern Alberta and with the Two Medicine Formation of Montana relate to one another stratigraphically or chronologically, the difference may be minimal due to their relative proximity, as the three sites studied here are located within 100 km of one another. As such, the age of the upper Oldman Formation at the Devil's Coulee locality is roughly consistent with that of the interval of the upper Two Medicine Formation of Montana from which *Hypacrosaurus stebingeri* is known.

Figure 2. Dentaries (medial view) from the Devil's Coulee juvenile hadrosaur bonebed (JBB) showing a strong ventral deflection of the symphysis characteristic of lambeosaurines. Top left, TMP 1988.151.5; Top right, TMP 1988.151.75; Bottom left, TMP 1988.151.88; Bottom right, TMP 1988.151.158.

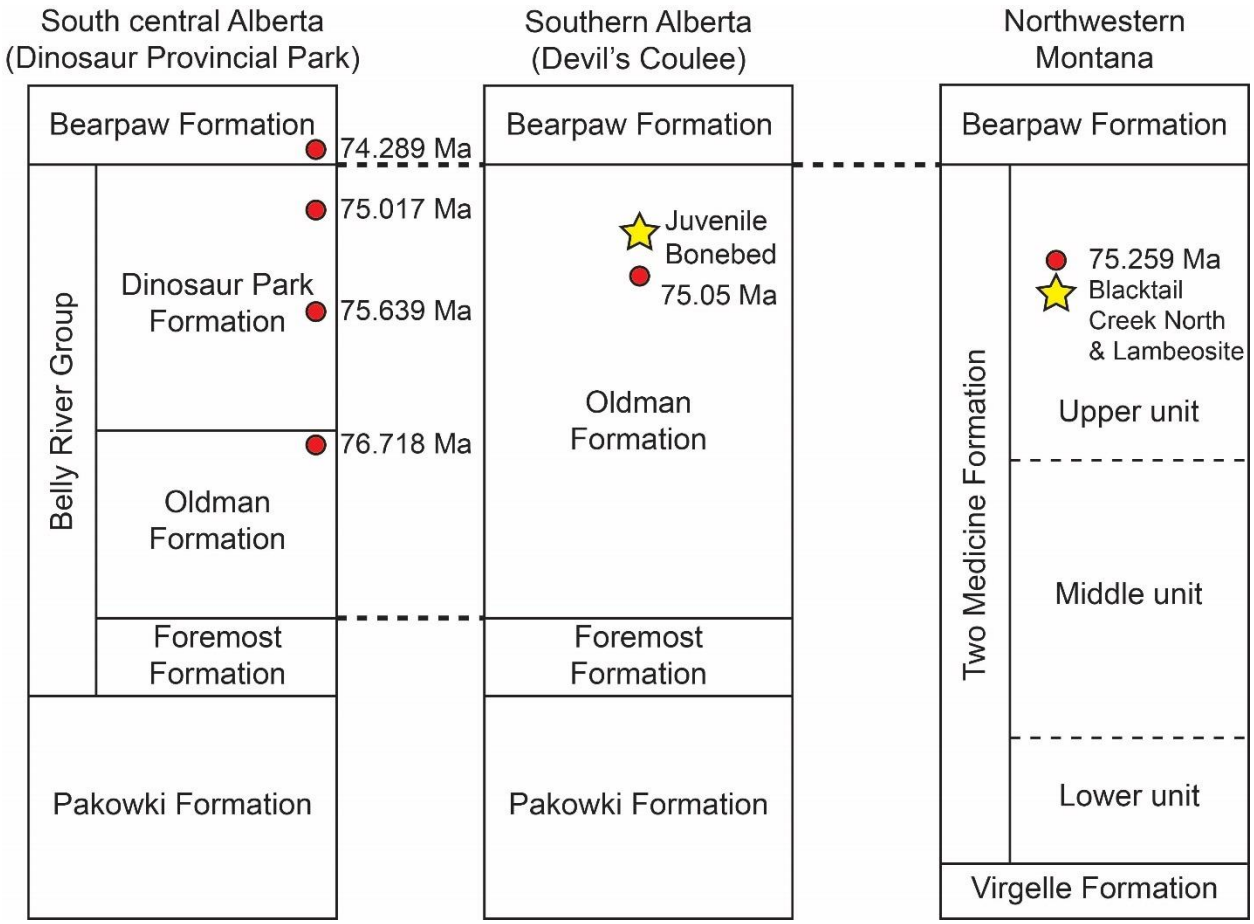

Figure 3. Stratigraphic correlation of the Belly River Group of Alberta (Canada) and the Two Medicine Formation of Montana (U.S.A.). The thickness of the northwestern Montana section is not proportional to the thickness of the Alberta sections. Radiometric ages from South central Alberta and Northwestern Montana are from Ramezani et al. (2022). Radiometric age from Southern Alberta is from Eberth and Deino (pers.com. in Horner and Currie [1994]).

3.2 RESULTS

3.2.1 Stratigraphy and sedimentology of the JBB (Alberta)

The JBB is exposed over a lateral extent of roughly 11 meters along the western wall of a coulee (Figure 4). The stratigraphic section measured at the southern extremity of the JBB spans an interval of roughly 9 meters and includes strata underlying and overlying the bonebed, whereas the section measured at the northern extremity spans roughly two meters and includes fewer strata surrounding the JBB-hosting interval due to the limited access (Figure 5).

The 9 m-thick stratigraphic interval studied can be subdivided into a lower and upper unit based on lithological differences (Figure 5). The JBB is situated near the top of the lower unit of the stratigraphic section. The lower unit is dominated by greenish-grey, gleyed siltstones and mudstones (5GY 4/1, 5GY 5/1, 5GY 6/1, 10 GY 5/1, 10Y 3/1, 10Y 4/1, 10Y 6/1, 10Y 7/1; Munsell, 2000). There are abundant bivalve and gastropod fragments disseminated throughout the matrix of most mudstone and siltstone layers, as well as occasional fossil plant fragments (<1 cm in length) and burrows (2 to 4 cm in length on average). These siltstones and mudstones (23 to 91 cm thick) are interbedded with very fine- to fine-grained sandstones (17 to 93 cm thick). Similarly, the upper unit consists of massive siltstone and mudstone layers (18 to 69 cm thick) interbedded with very fine- to fine-grained sandstone layers (17 to 29 cm thick). Contrary to the lower unit, however, the mudstones and siltstones are mostly light to dark brown (5Y 4/2, 5Y 5/2, 5Y 6/2, 5Y 7/2, 5Y 8/2; Munsell, 2000) in coloration. At the top of the upper unit, a >50 cm thick, blocky, fining-upward sandstone exhibiting large-scale trough cross-stratification and plant fragments at its base is present. Vertebrate remains, gastropod fragments, and bivalve fragments are absent in the upper unit.

The lithofacies change evident between the lower and upper units suggests a shift in paleoenvironmental conditions, from poorly-drained wetlands to well-drained paleoenvironments. The abundance of gley colors in the lower unit is indicative of iron depletion and suggests those deposits were subjected to extended periods of reducing conditions due to a high water table (Leckie et al., 1989; Vepraskas and Sprecher, 1997; Therrien and Fastovsky, 2000; Sprecher, 2001; Vepraskas, 2001; Driese and Ober, 2005; Therrien et al., 2009; Rosenau et al., 2013; Retallack, 2019). Based on the presence of pedogenic features (i.e., burrows, gleyed profiles) and sedimentological evidence (i.e., abundant mudstones and siltstones), the lower unit is interpreted as representing a low-energy, wetland paleoenvironment. Due to the highly fissile and brittle nature of the rock, other pedogenic features commonly associated with poorly-drained environments or alternating wet and dry periods (e.g., slickensides, redoximorphic features; Rosenau et al., 2013; Retallack, 2019) could not be observed. The lack of evidence of iron depletion (i.e., absence of gleyed horizons) in the upper unit suggests better drainage conditions than in the lower unit.

During field work in 2022, small hadrosaurid bone fragments (ischium fragment [TMP 2022.14.1] and rib fragment [TMP 2022.14.2]), bivalve and gastropod shell fragments, and plant debris were recovered from a 23 cm-thick, gleyed, greenish-grey siltstone (10Y 4/1; Munsell, 2000) at the level of the bonebed. This siltstone bed overlies a thick, sideritized layer (maximum thickness of 33 cm) that pinches laterally to the north. Comparison with matrix still attached to some JBB bones (TMP 1989.151.79, TMP 1989.151.97, TMP 1989.151.145, TMP 1989.151.156, TMP 1989.151.136, TMP 1989.151.150, TMP 1989.151.93) collected in 1988-1989 reveals they were encased in a very fine-grained sandstone. As a lithologically similar sandstone layer was not encountered in either of our measured stratigraphic sections, the

presence of such matrix suggests the bones were likely preserved in a lenticular sandstone body of limited lateral extent (<11 m), laterally-equivalent to the gleyed siltstone that produced hadrosaurid bones in 2022, that was likely entirely excavated in 1988-1989. Thus, the fine-grained nature and lenticular morphology of the bonebed host sandstone and the presence of bone fragments in the laterally-equivalent, gleyed, fine-grained deposit suggests that the hadrosaurid bones accumulated in a channel and on its margin in a poorly-drained paleoenvironment (Figure 6).

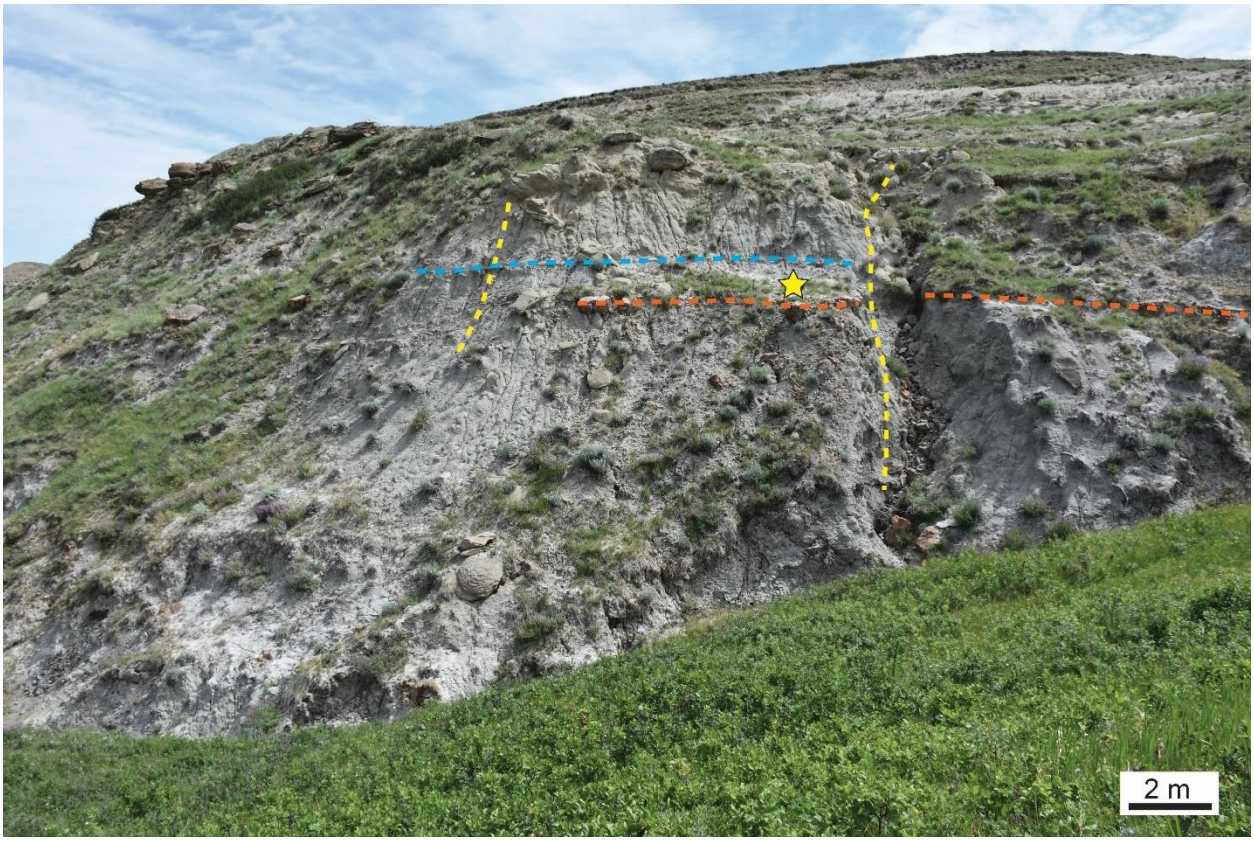

Figure 4. Photo of the Devil's Coulee juvenile hadrosaur bonebed (JBB) facing East. Yellow star indicates the position of the bonebed. Yellow dashed lines show the position of the two measured stratigraphic sections (left: North end of the bonebed; right, South end of the bonebed). Blue dashed line marks the volcanic ash layer overlying the bonebed. Orange dashed line marks the position of the sideritized layer underlying the bonebed.

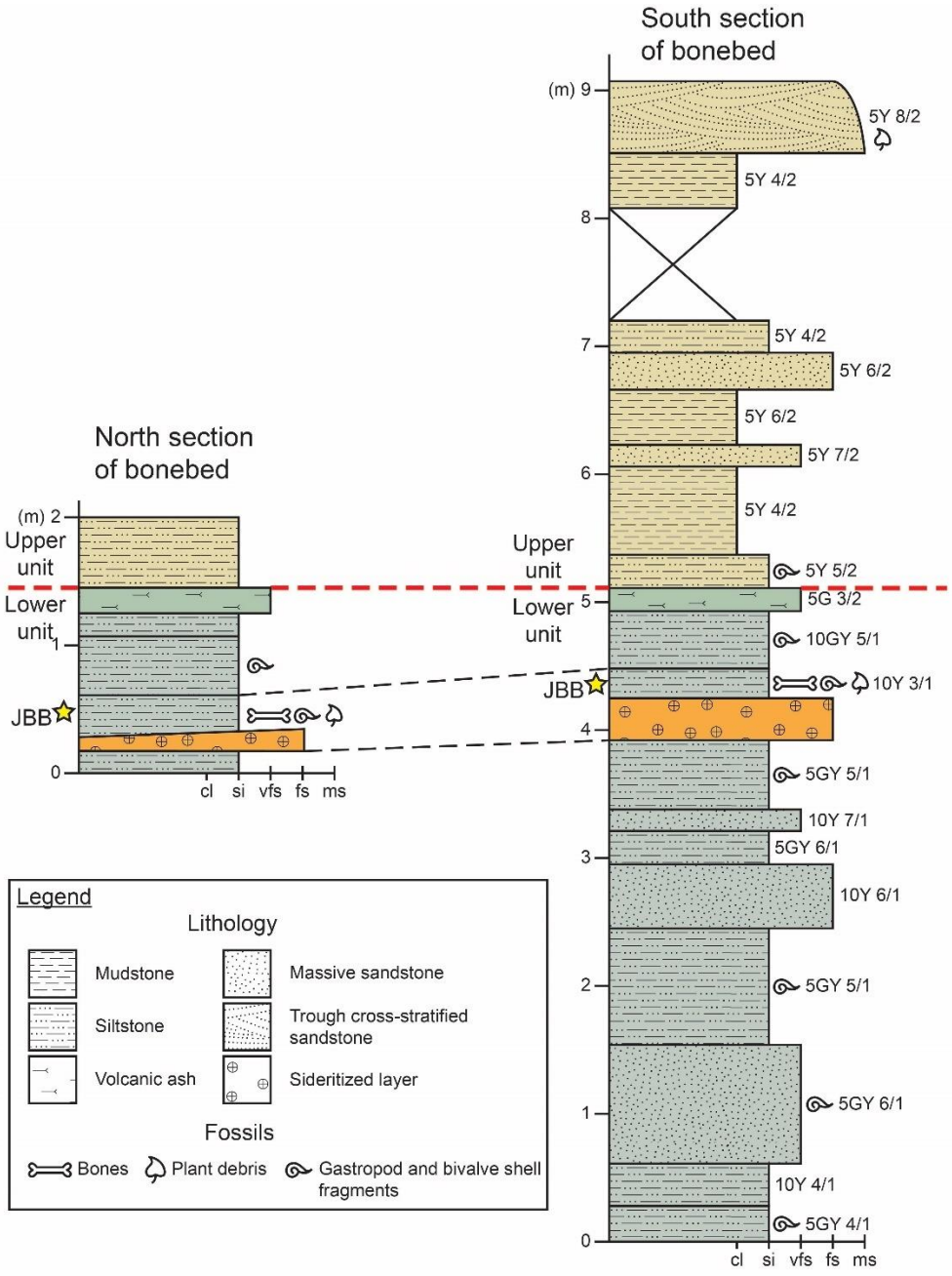

Figure 5. Stratigraphic column of the Devil's Coulee juvenile hadrosaur bonebed (JBB). Red dashed line indicates the boundary between the lower and the upper units.

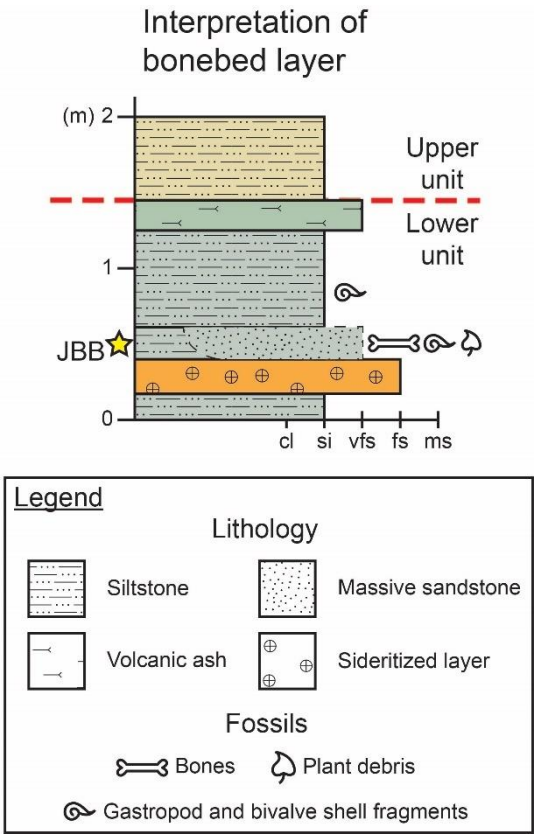

Figure 6. Stratigraphic interpretation of the bonebed layer inferred from the two stratigraphic sections in Figure 5. Red dashed line indicates the boundary between the lower and the upper units.

3.2.2 Faunal composition of the JBB

A total of 312 specimens were recovered from the JBB, 15 of which remain unprepared. The JBB is a mixed assemblage (sensu Eberth et al., 2007) of fully disarticulated macrovertebrate fossils (n = 229), microvertebrate fossils (n = 68), and invertebrate fossils. (Table 1; Appendix A). The macrovertebrate portion of the bonebed consists of a low-diversity, monodominant assemblage containing 219 prepared hadrosaurid specimens (NPSP = 219), four of which are unidentifiable due to heavy breakage; as such, the number of identifiable specimens (NISP) is 215. Based on the definition presented above (see Materials and Methods), the number of skeletal elements preserved in the bonebed is 203 (Table 2). From the number of left fibulae (TMP 1988.151.23, TMP 1988.151.4, TMP 1988.151.81, and TMP 1988.151.45), a minimum of four hadrosaurid individuals (MNI) are preserved in the JBB (Figure 7A). The microvertebrate assemblage is highly diverse and consists of isolated teeth (Ankylosauridae, Crocodylia, Dromaeosauridae, Hadrosauridae, Osteichthyes) and scales (*Lepisosteus*), as well as fragments of ossified tendons (Hadrosauridae), dermal scutes (Ankylosauria, Crocodylia), carapace and plastral elements (*Basilemys*, Chelydridae, Tryonichidae), and other small bones (*Champsosaurus,* Squamata). The invertebrate fossils preserved in the bonebed layer consist of abundant gastropod and broken bivalve shell fragments.

	Taxa	Number of specimens
Macrovertebrate remains	Hadrosauridae *Hypacrosaurus stebingeri*	221 (96.5%)
	Tyrannosauridae (vertebral element, phalanges)	1 (0.4%)
	Tyrannosauridae (phalanges)	2 (0.9%)
	Dromaeosauridae (furcula)	1 (0.4%)
	Ornithomimidae (phalanges)	1 (0.4%)
	Theropoda (vertebral elements)	2 (0.9%)
	Crocodylia (scute)	1 (0.4%)
Microvertebrate remains	Hadrosauridae (teeth and ossified tendons)	12
	Tyrannosauridae (teeth)	7
	Dromaeosauridae (teeth)	6
	Ankylosauria (scute fragments)	1
	Ankylosauridae (teeth)	8
	Crocodylia (teeth, scute fragments)	8
	Basilemys Turtle (shell fragments)	1
	Chelydridae (shell fragments)	2
	Tryonichidae (shell fragments)	2
	Lepisosteus (scales)	4
	Osteichthyes (teeth)	1
	Osteichthyes (bone fragments)	8
	Squamata (bone fragments)	5
	Champsosaurus (bone fragments)	3
Invertebrate remains	Bivalvia (shell fragments)	Abundant
	Gastropoda (shell fragments)	Abundant

Table 1. Taxonomic identifications of specimens present in the Devil's Coulee juvenile hadrosaur bonebed (JBB).

	Category	Element	Count	Total	Observed Proportion (%)
Group I	Light cranial elements		15	148	72.9
	Digital elements	Pedal phalanges	19		
		Manual phalanges			
	Ribs		34		
	Vertebral elements	With centra	47		
		Other processes	29		
	Pelvic elements	Ischia	4		
Group II	Pectoral elements	Sternal plates	1	29	14.3
		Scapulae	3		
	Dense cranial elements	Maxillae	4		
		Dentaries	6		
	Tarsals and metapodials	Metacarpals	5		
		Metatarsals	5		
		Astragali	1		
	Pelvic elements	Pubes	4		
Group III	Limb bones	Humeri	5	26	12.8
		Radii	5		
		Ulnae	4		
		Femora	1		
		Tibiae	3		
		Fibulae	5		
	Pelvic elements	Ilia	3		

Table 2. Hadrosaurid elements preserved in the Devil's Coulee juvenile hadrosaur bonebed (JBB). Categorization of the skeletal elements to Voorhies groups is based on Holland et al. (2021).


A
TMP 1988.151.4
TMP 1988.151.81
TMP 1988.151.23
TMP 1988.151.45
10 cm
B
5 cm
C
MOR 355-8-22-5-6
MOR 355-8-25-5-5
MOR 355-8-24-5-8
MOR 355-8-27-5-2
MOR 355
5 cm

Figure 7. Skeletal elements used to determine the minimum number of individuals (MNI) preserved in each bonebed. **A**, Left fibulae (lateral view) of late juvenile individuals from the Devil's Coulee juvenile hadrosaur bonebed (JBB) revealing a MNI of four; **B**, right dentaries (lateral view) of nestling individuals from the Blacktail Creek North bonebed revealing a MNI of 23; **C**, left humerus (lateral view) of an adult individual (MOR 355-8-22-5-6) and right humeri (lateral view) of late juvenile individuals from the Lambeosite bonebed revealing a MNI of five.

3.2.3 Taphonomic features of the JBB (Alberta)

Size distribution- With the exception of a single adult pedal phalanx III-1 (TMP 1989.151.150), the hadrosaurid skeletal elements preserved in the JBB belong to juvenile individuals of similar body size (Figure 8A). Two complete tibiae (TMP 1988.151.92 and TMP 1988.151.6) show a difference in length of less than 9% (54.5 cm vs 59.3 cm in length, respectively). Although breakage is frequent in the bone assemblage (i.e., bones are commonly incomplete, see below), no major size difference is visible between different specimens of a same skeletal element. Based on tibia size (TMP 1988.151.6 [length = 59.3 cm] and TMP 1988.151.92 [length = 54.5 cm]), the JBB individuals are approximately 51% to 56% of the size of a fully-grown adult (MOR 355-8-25-5-4, tibia length = 106.0 cm; see Horner and Currie, 1994), and are in the size range of late juveniles according to the categories established by Horner et al. (2000) and Ullmann et al. (2017).

Bone completeness- Evidence of breakage is present predominantly on large skeletal elements (limb bones and ribs), which may be missing either the proximal or distal end, or both. Most small elements (e.g., phalanges, metapodials, vertebral centra) are complete and show no sign of breakage. Half of the maxillae from the JBB (n = 2, TMP 1994.666.80 and TMP 1988.151.84) and half of the dentaries (n = 3, TMP 1988.151.88, TMP 1988.151.5 [left and right]) preserve articulated teeth. The lingual sheets of bone associated with these two maxillae are also preserved.

Sorting- Light skeletal elements (e.g., phalanges and vertebrae: Voorhies group I) are under-represented in the JBB (observed proportion of 72.9% vs expected proportion of 90.0%: χ^2 = 77.604, df = 2, $p < 0.001$). Elements that belong to Voorhies group II (e.g., pectoral elements and dense cranial elements) are over-represented (observed proportion of 14.3% vs expected

proportion of 6.6%). Heavy skeletal elements (e.g., limb bones: Voorhies group III) are over-represented (observed proportion of 12.8% vs expected proportion of 3.4%) (Figure 9A; Table 2). This discrepancy suggests that light skeletal elements were preferentially removed from the assemblage.

Weathering and Abrasion- Weathering features are present on very few specimens in the JBB assemblage (Figure 9B). Most specimens (93.1% of NPSP, n = 202) exhibit no sign of weathering (stage 0; sensu Fiorillo, 1988). Small longitudinal cracks (weathering stage 1) are present on the surface of a few specimens (2.8% of NPSP, n = 6) (Figure 10A). A small number of specimens (3.2% of NPSP, n = 7) exhibit stage 2 weathering, and rare specimens (only 0.9% of NPSP, n = 2) exhibit extensive weathering (stage 3). Early weathering (stage 1) predominantly occurs on flat bones (i.e., shaft of ribs and scapular blade), whereas advanced weathering (stages 2 and 3) is most common on vertebral centra, phalanges, and metacarpals.

Most specimens (84.0% of NPSP, n = 184) show no sign of abrasion and preserve well-defined edges (stage 0; sensu Fiorillo, 1988). Evidence of abrasion is observed only on 16% (n = 35) of the prepared hadrosaurid specimens (Figure 9C): 12.3% of NPSP (n = 27) exhibit stage 1 of abrasion and are characterized by slight rounding of their edges, and 3.7% of NPSP (n = 8) exhibit advanced rounding of their edges (stage 2); stage 3 of abrasion is not represented in the assemblage. The majority of the abraded specimens (approximately 83%) are light, easily transported bones, such as phalanges and vertebrae (Voorhies group I), indicating that light skeletal elements have experienced the most transport. Abrasion occurs predominantly along the edges of the articular surfaces of vertebrae (Figure 10B) and on the dorsal and plantar edges of the proximal articular surfaces of pedal phalanges as well as on the medial and lateral edges of their distal articular faces.

Fractures- Fractures are present on the majority of the hadrosaurid specimens preserved in the JBB (61.9% of NPSP, n = 135). Transverse fractures are the most abundant type of fracture, being present on 56.0% of NPSP (n = 122), predominantly on long bones. Spiral fractures are rare in the assemblage, having been observed on only 6.0% of NPSP (13 bones), mainly on the shafts of long bones. Post-burial compression fractures (sensu Ryan et al., 2001), exemplified as broken steps and concentric cracks on the bone surface, are present on 16.1 % of NPSP (35 bones), mostly on long bones and pelvic elements.

Wet rot- Removal of external layers of the bone (cortical bone) has been observed on all sides of the epiphyses of nearly all long bones (n = 30), on some ribs (n = 6), pectoral and pelvic elements (n = 8), and neural spines (n = 7), as well as on the symphysis of a few dentaries (n = 3) (Figure 10C). This feature has been interpreted as wet rot rather than weathering due to the pristine nature of the shafts of the affected specimens and their unabraded, well-defined edges (see Behrensmeyer, 1978; Scherzer and Varricchio, 2010).

Tooth marks- Theropod tooth marks are present on very few specimens in the bonebed (n = 3, 1.3% of NPSP) (Figure 10C). Two puncture marks (sensu Hone and Watabe, 2010) and one drag mark (sensu Hone and Watabe, 2010) are present on the lateral side of the proximal end of an ulna (TMP 1988.151.9). Four parallel drag marks are present on the medial side of the deltopectoral crest of a humerus (TMP 1988.151.20). Two parallel drag marks are present on the cranial side of a rib head (TMP 1988.151.38).

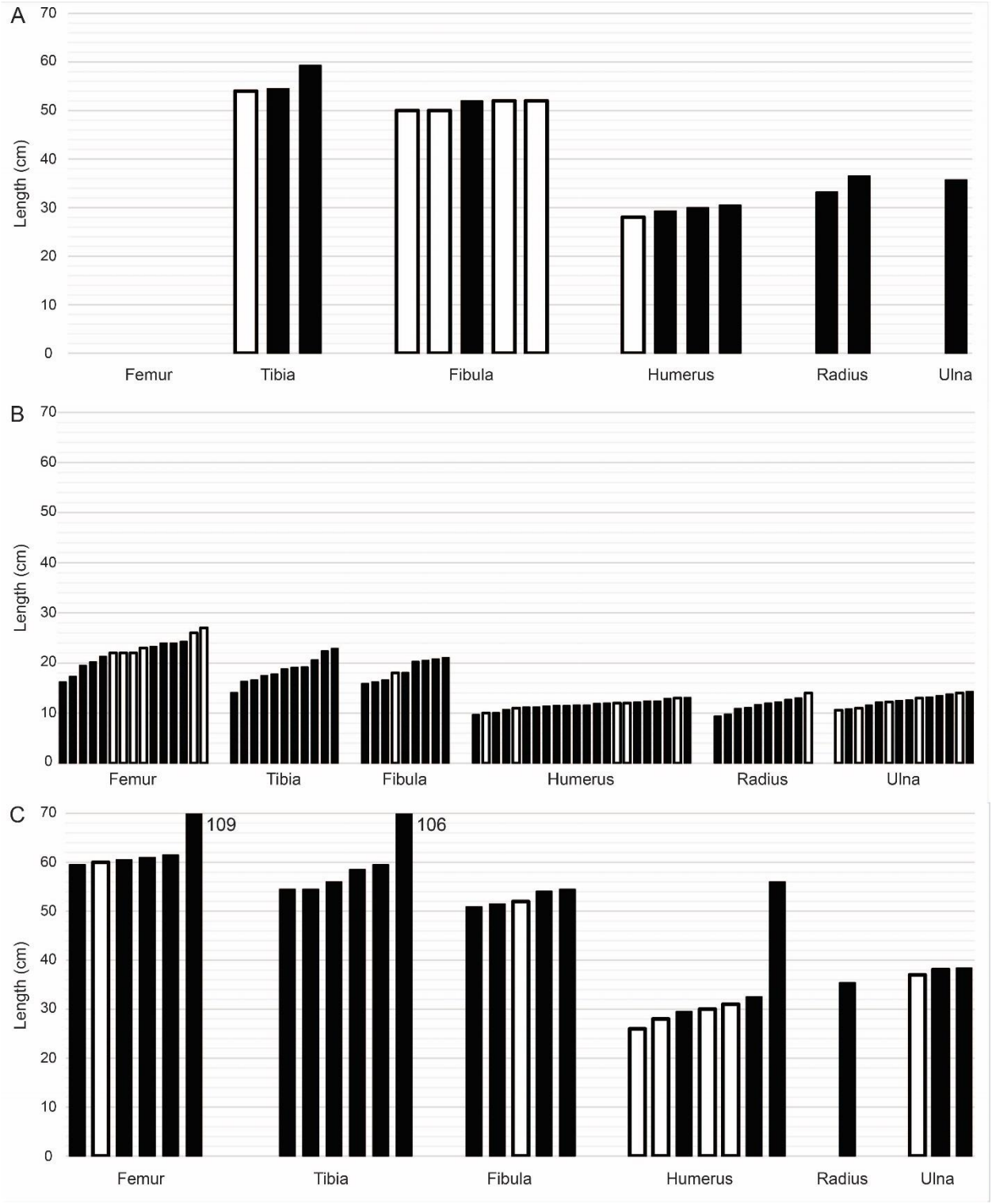
A
B
C
Length (cm)
0
10
20
30
40
50
60
70
Femur
Tibia
Fibula
Humerus
Radius
Ulna
109
106

Figure 8. Size distribution of hadrosaurid long bones in the three bonebeds. **A**, Devil's Coulee juvenile hadrosaur bonebed; **B**, Blacktail Creek North; **C**, Lambeosite. Black bars represent complete bones. White bars represent length estimates from broken bones.

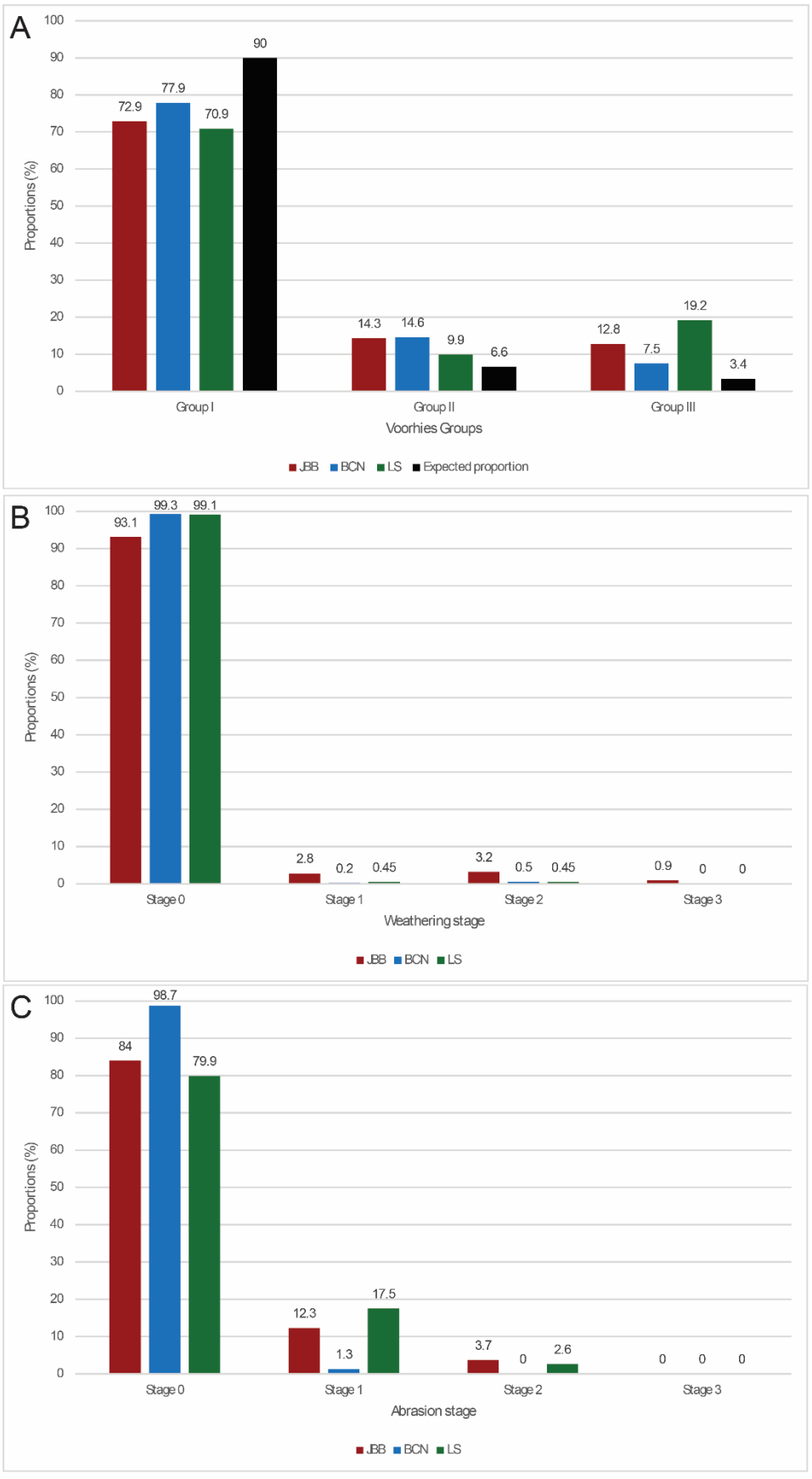
A
Proportions (%)
Group I
Group II
Group III
Voorhies Groups
JBB
BCN
LS
Expected proportion
B
Weathering stage
Stage 0
Stage 1
Stage 2
Stage 3
C
Abrasion stage

Figure 9. Taphonomic data for the Devil's Coulee juvenile hadrosaur bonebed (JBB), the Blacktail Creek North bonebed (BCN), and the Lambeosite bonebed (LS). **A**, Representation of each Voorhies group (Voorhies, 1969) in the bonebeds (expected proportions based on Holland et al. [2021]); **B**, proportions of hadrosaurid skeletal elements at each weathering stage (sensu Fiorillo, 1988) in the bonebeds; **C**, proportions of hadrosaurid skeletal elements at each abrasion stage (sensu Fiorillo, 1988) in the bonebeds.

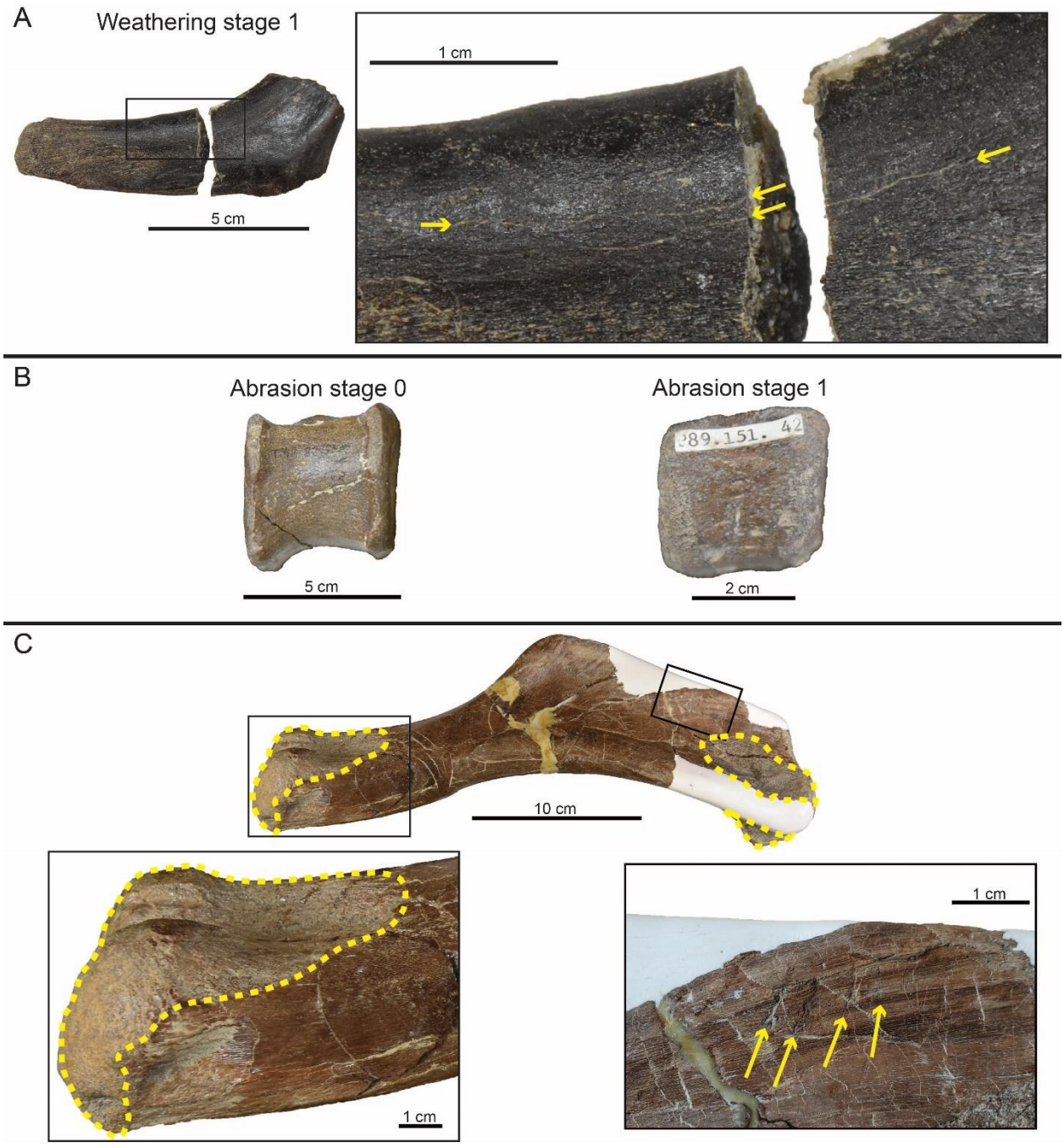

Figure 10. Bone modification features present in the Devil's Coulee juvenile hadrosaur bonebed (JBB). **A**, Rib head (TMP 1988.151.71) showing longitudinal cracking (weathering stage 1, sensu Fiorillo [1988]) indicated by yellow arrows; **B**, Left: caudal vertebra (TMP 1988.151.182) showing no alteration (abrasion stage 0, sensu Fiorillo [1988]), Right: caudal vertebra (TMP

1989.151.42) showing rounding of the edges of the articular surfaces (abrasion stage 1, sensu Fiorillo [1988]); **C**, Right humerus (TMP 1988.151.20). Yellow arrows point to tooth marks (drag marks, sensu Hone and Watabe [2010]). Areas affected by wet rot are outlined by yellow dashed lines.

3.2.4 Histologic description and age interpretation of fibulae from JBB

TMP 1988.151.4- The fibular cross-section of TMP 1988.151.4 is complete, well-preserved and undistorted, and measures 27.6 mm in maximum diameter (Figure 11). No true LAGs are present in this cross-section. The medullary cavity measures 10.3 mm in maximum diameter and contains cancellous bone. It is surrounded by an up to 3.5-mm-thick layer of woven bone that transitions into an up to 2.9-µm-thick layer of fibro-lamellar bone, characterized by a reticular vascularization pattern. These layers form the first zone observed on this specimen. Primary osteons are visible throughout the first zone. Resorption cavities are present towards the core of the section, suggesting that remodeling of the bone occurred. The first zone is surrounded by an up to 0.8-mm-thick layer of lamellar bone characterized by a laminar vascularization pattern. This layer forms the first annulus on this cross-section. The first zone and first annulus were formed during the first year of bone growth. The first annulus is surrounded by an up to 3.1-mm-thick layer of fibrolamellar bone that transitions from a reticular vascularization pattern (inwards) to a plexiform vascularization pattern (outwards), forming the second zone. An up to 0.9-mm-thick layer of lamellar bone with a laminar vascularization pattern surrounds the second zone and constitutes the second annulus. The pair composed of the second zone and the second annulus represent a second yearly growth cycle. The second annulus is surrounded by a 1.0-mm-thick layer of fibrolamellar bone characterized by a plexiform vascularization pattern, which forms the outermost layer of the cross-section. The presence of two annuli in the fibula indicates that TMP 1988.151.4 represents an individual that was at least two years old at the time of death. However, despite the fibulae preserving two annuli, the individual was likely three years old at death. Growth curves of *Hypacrosaurus stebingeri* have shown that femora from individuals similar in size to those from the JBB should present three growth cycles, indicating that they

would be three years old, unless bone remodeling occurred (Cooper et al., 2008). It has also been shown that fibulae tend to preserve fewer growth rings than other weight-bearing limb bones such as tibiae or femora due to increased bone remodeling (Horner et al., 1999). Evidence of bone remodeling is present in this specimen, which explains the discrepancy between the expected number of growth cycles based on its size and the observed number of annuli in the cross-section.

TMP 1988.151.23- The fibular cross-section of TMP 1988.151.4 is mostly complete, with minimal damage on one side, and measures 24.4 mm in maximum diameter (Figure 12). It is well-preserved and shows no sign of deformation. No true LAGs are present on this cross-section. The medullary cavity measures 10.1 mm in maximum diameter and contains cancellous bone. It is surrounded by an up to 8.2-mm-thick region of woven bone and Haversian tissue, suggesting remodeling of the primary bone. An up to 0.8-mm-thick layer of fibrolamellar bone characterized by a plexiform vascularization pattern surrounds the region of Haversian tissue, forming a zone. This zone is surrounded by a 0.9 mm-thick layer of lamellar bone characterized by a laminar vascularization pattern forming an annulus, which extends almost to the outermost layer of the bone. The zone and annulus represent a yearly growth cycle. The presence of one annulus in the cross-section indicates that this individual was at least one year old at the time of death. Based on the similar diameter of the TMP 1988.151.23 and TMP 1988.151.4 (described above) cross-sections, it is possible that the additional yearly growth cycle seen in TMP 1988.151.4 was present in TMP 1988.151.23 and was obscured by the remodelling, as evidenced by the presence of Haversian tissue, and that the specimen also represents a three-year-old individual that lost an additional annulus to remodelling.

TMP 1988.151.45- The fibular cross-section of TMP 1988.151.45 is severely crushed (Figure 13), making a histological analysis challenging. Nonetheless, a few features can still be identified. The medullary cavity contains cancellous bone. A 2.2-mm-thick layer of fibrolamellar bone characterized by a reticular vascularization pattern surrounds the medullary cavity. Primary osteons and a few resorption cavities are present in this layer. Towards the periosteal surface, a 0.8-mm-thick layer of lamellar bone with a laminar vascularization pattern is present. This layer could represent an annulus, although deformation to the cross-section makes this difficult to ascertain. This specimen is also similar in size to TMP 1988.151.4 and shows evidence of remodelling and heavy deformation, which suggests that it could also represent a three-year-old individual that lost two yearly growth cycles to remodeling, or that deformation rendered them unrecognizable.

TMP 1988.151.81- The fibular cross-section of TMP 1988.151.81 is complete and measures 29.7 mm in maximum diameter (Figure 14). It is well-preserved and shows no sign of deformation. No true LAGs are present in this cross-section. The medullary cavity measures 13.8 mm in maximum diameter and contains cancellous bone. It is surrounded by an up to 7.0-mm-thick layer of woven bone that transitions into an up to 6.1-mm-thick layer of fibro-lamellar bone, both characterized by a reticular vascularization pattern. Secondary osteons are abundant towards the medullary cavity, but their abundance decreases towards the margin of the cross-section. Externally, a 2.0-mm-thick layer of fibrolamellar bone with a plexiform vascularization pattern is present and, along with the previous fibrolamellar layer, forms a zone. The zone is surrounded by a 1.2-mm-thick layer of lamellar bone characterized by a laminar vascularization pattern forming an annulus that extends to the edge of the cross-section. The zone and annulus represent an annual growth cycle. Similar to TMP 1988.151.23, a single yearly growth cycle is

visible on the cross-section of TMP 1988.151.81. However, the presence of secondary osteons in proximity to the medullary cavity suggests remodeling of the bone, which could obscure signs of annual growth cycles. As such, based on the size of the cross-section and the presence of two yearly growth cycles in TMP 1988.151.4, it is estimated that a second yearly growth cycle composed of a zone and an annulus (as seen in TMP 1988.151.4) may have been lost to remodelling, as well as potentially an additional yearly growth cycle not seen in any of the four cross-sections from the JBB. Thus, TMP 1988.151.81 also represents a three-year-old individual.

Among the specimens from the JBB, LAGs are absent, while annuli are present on every cross-section. This indicates that growth never actually paused, but merely slowed for part of each year. One fibula (TMP 1988.151.4) preserves two annuli, whereas the rest preserve only one annulus. All specimens show signs of bone remodeling (e.g., resorption cavities, secondary osteons, Haversian tissue), which could have resulted in the loss of annuli. Given the similar size of all four cross-sections, it is highly likely that they each possessed at least two annuli prior to remodeling, which would indicate that they were at least two years old, and potentially a third yearly growth cycle based on its expected presence in a femur from a similar-sized individual (MOR 355: see Cooper et al., 2008), in which case the individuals would be three years old.

The histological features of the four fibulae from the JBB are consistent with a late juvenile ontogenetic stage. Horner et al. (2000) noted that histological cross-sections from juvenile individuals are characterized by the absence of an external fundamental system (EFS) which would indicate that the individuals had yet to reach somatic maturity, the presence of Haversian tissue and secondary osteons (particularly deep in the cortex), the presence of laminar, plexiform, and reticular vascularization patterns, and the presence of bony trabeculae in the medullary cavity. All of these criteria apply to the four fibulae examined. Thus, a late juvenile status for the

individuals preserved in the JBB is supported by both histologic features and the size of the bones relative to fully-grown adults.

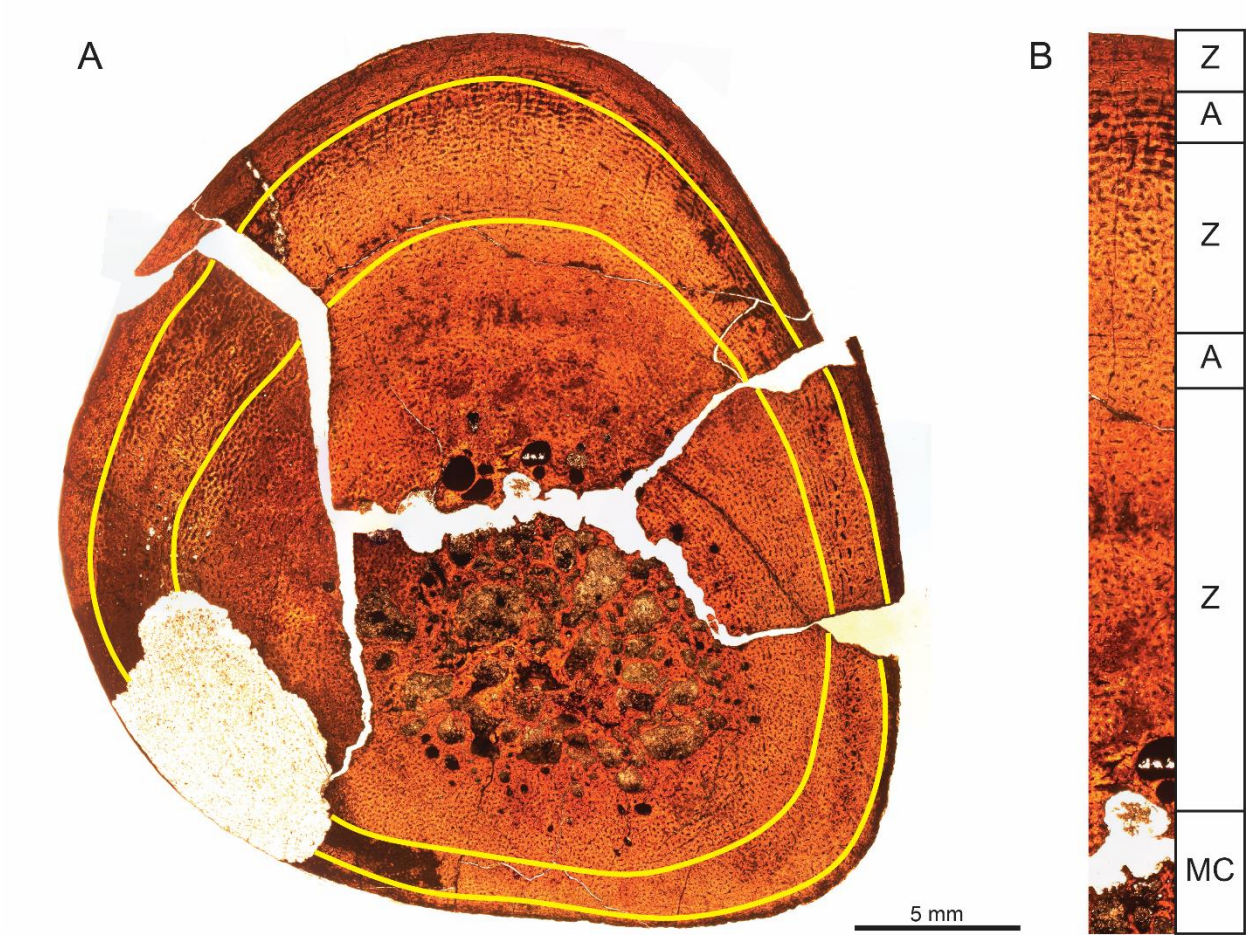

Figure 11. Histology of TMP 1988.151.4 (left fibula). **A**, Cross-section of TMP 1988.151.4 at mid-diaphysis; **B**, Close-up of the cross-section from the medullary cavity to the outer edge. Yellow lines represent yearly growth marks (annuli). **Abbreviations**: **A**, annulus; **MC**, medullary cavity; **Z**, zone.

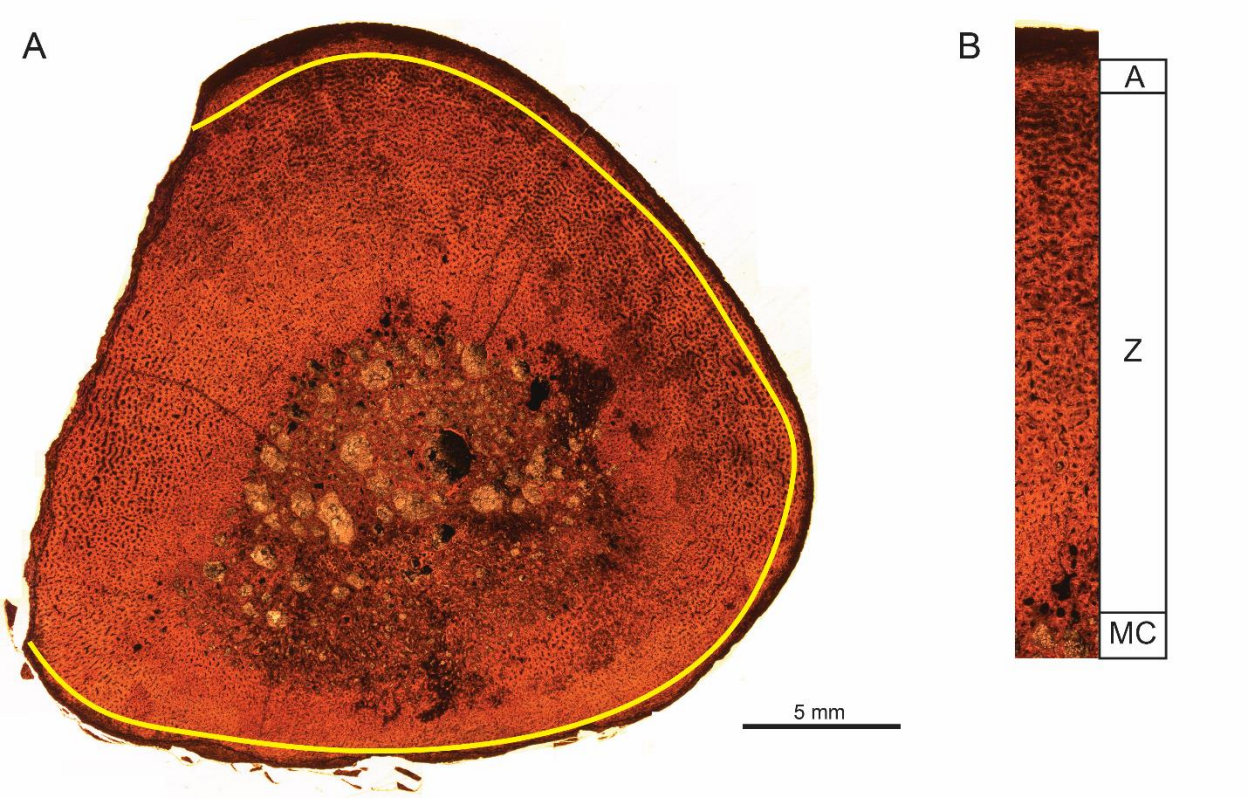

Figure 12. Histology of TMP 1988.151.23 (left fibula). **A**, Cross-section of TMP 1988.151.23 at mid-diaphysis; **B**, Close-up of the cross-section from the medullary cavity to the outer edge. Yellow line represents yearly growth mark (annulus). **Abbreviations**: **A**, annulus; **MC**, medullary cavity; **Z**, zone.

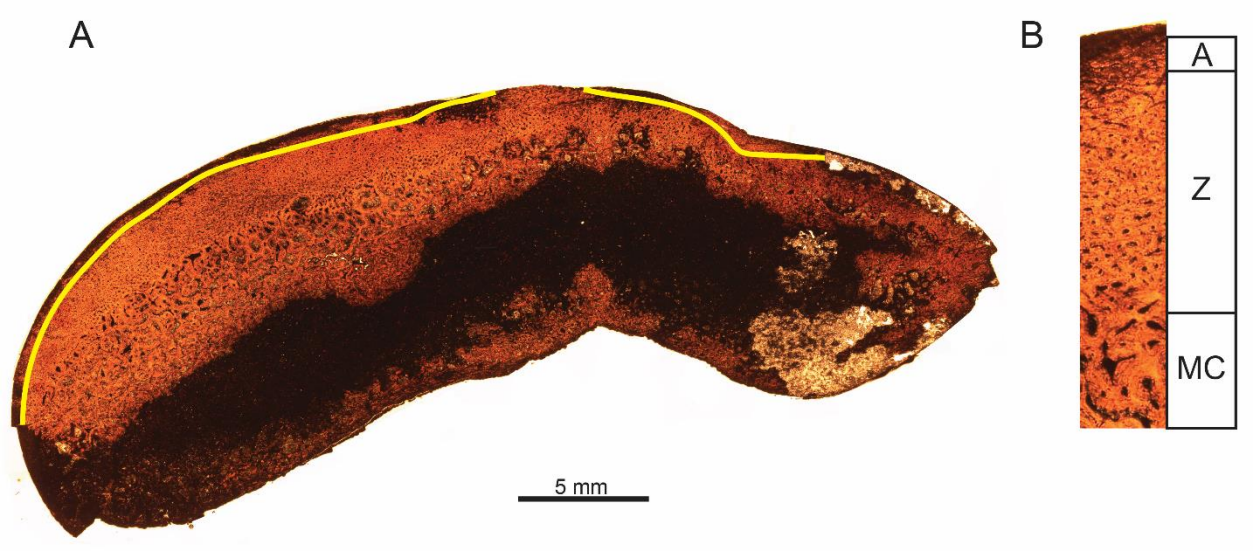

Figure 13. Histology of TMP 1988.151.45 (left fibula). **A**, Cross-section of TMP 1988.151.45 at mid-diaphysis; **B**, Close-up of the cross-section from the medullary cavity to the outer edge. Yellow line represents yearly growth mark (annulus). **Abbreviations**: **A**, annulus; **MC**, medullary cavity; **Z**, zone.

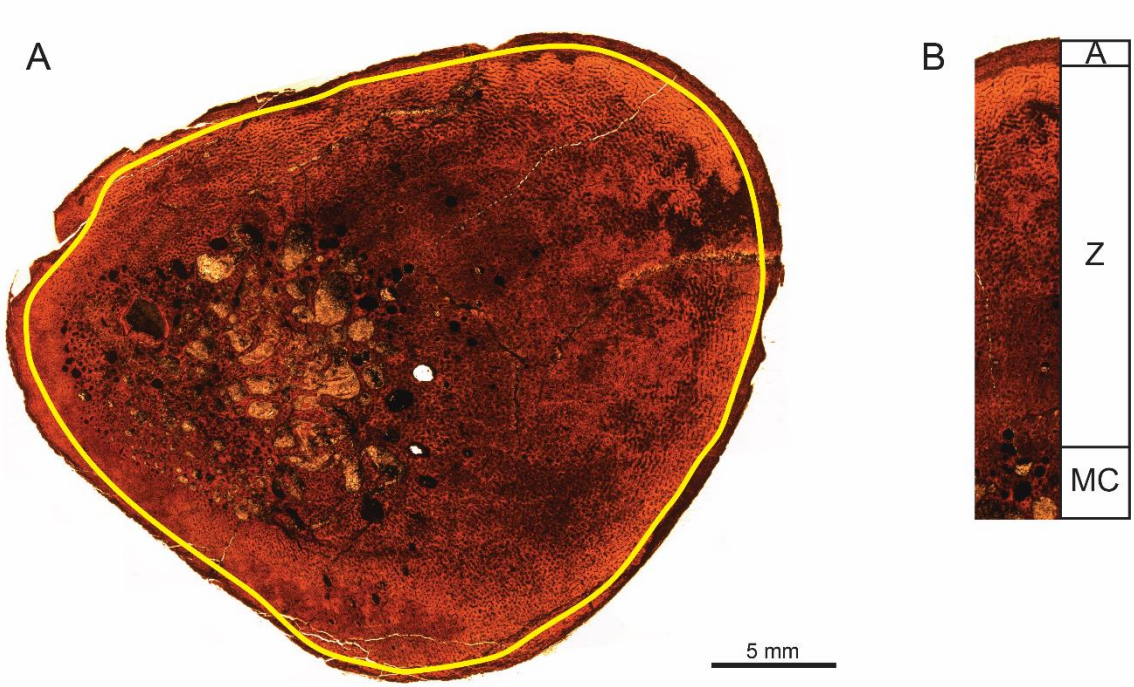

Figure 14. Histology of TMP 1988.151.81 (left fibula). **A**, Cross-section of TMP 1988.151.81 at mid-diaphysis; **B**, Close-up of the cross-section from the medullary cavity to the outer edge. Yellow line represents yearly growth mark (annulus). **Abbreviations**: **A**, annulus; **MC**, medullary cavity; **Z**, zone.

3.2.5 Faunal composition of the Blacktail Creek North bonebed (Montana)

The Blacktail Creek North bonebed preserves a total of 1348 identifiable prepared hadrosaurid specimens (NISP = 1348) and an additional 1111 small bone fragments (Appendix B). These fragments are not included in the analyses since they are often unidentifiable or too small to be assigned as distinct skeletal elements, and they may have been produced during collection or preparation of the specimens. The number of skeletal elements preserved in the assemblage is 1309 because in some cases multiple specimens may be fragments of a single skeletal element (Table 3; see Materials & Methods). The MNI is estimated at 23 based on the number of distinct right dentaries (Figure 7B).

	Category	Element	Count	Total	Observed Proportion (%)
Group I	Light Cranial Elements		208	1020	77.9
	Digital Elements	Pedal Phalanges	18		
		Manual Phalanges	40		
	Ribs		111		
	Vertebral Elements	With Centra	527		
		Other Processes	101		
	Pelvic Elements	Ischia	15		
Group II	Pectoral Elements	Sternal Plate	10	191	14.6
		Coracoid	14		
		Scapulae	36		
	Dense Cranial Elements	Maxillae	28		
		Dentaries	45		
	Metapodials	Metacarpals	28		
		Metatarsals	6		
		Calcaneum	9		
		Astragalus	7		
	Pelvic Elements	Pubes	8		
Group III	Limb Bones	Humeri	24	98	7.5
		Radii	10		
		Ulnae	14		
		Femora	17		
		Tibiae	11		
		Fibulae	8		
	Pelvic Elements	Ilia	14		

Table 3. Hadrosaurid elements preserved in the Blacktail Creek North bonebed. Categorization of the skeletal elements to Voorhies groups is based on Holland et al. (2021).

3.2.6 Taphonomic features of the Blacktail Creek North bonebed (Montana)

Size distribution- All hadrosaurid skeletal elements retrieved from the Blacktail Creek North bonebed belong to individuals referred to as "nestlings" by Horner [1994] and Horner and Currie [1994], likely due to their small size and their proximity to nesting sites, although their size slightly exceeds the upper limit for this ontogenetic stage as established by Horner et al. (2000). The femur length of the individuals from this bonebed ranges from 16.2 cm to 24.3 cm (Figure 8B) (15.4% to 23.1% of adult femur: MOR 549, femur length = 105 cm [Horner and Currie, 1994]), which falls in the early juvenile range based on femur length alone (Horner et al., 2000).

Sorting- Similar to the JBB, light skeletal elements (Voorhies group I) are under-represented in the bonebed (observed proportions of 77.9% vs expected proportions of 90.0%: $\chi^2 = 212.17$, $df = 2$, $p < 0.001$), whereas heavier skeletal elements (Voorhies groups II and III) are over-represented (observed proportions of 14.6% and 7.5% vs expected proportions of 6.6% and 3.4%, respectively) (Figure 9A; Table 3). The significant difference between the observed proportions and the expected proportions of elements from each Voorhies group indicates that preferential removal of light skeletal elements over heavier skeletal elements occurred.

Weathering and abrasion- Weathering and abrasion features are rare in the Blacktail Creek North assemblage (Figure 9B, C). Most specimens (99.3% of NISP, n = 1339) exhibit no sign of weathering. Although rare, signs of early stages of weathering (stages 1 and 2) are most common on cranial and forelimb elements. Only three specimens (0.2% of NISP) exhibit small longitudinal cracks (stage 1), whereas flaking of the bone surface (stage 2) is visible on seven specimens (0.5% of NISP). Signs of abrasion are present only on the articular surface of a small proportion of the vertebrae (1.3% of NISP, n = 18) in the form of slight rounding of the edges of the articular surfaces (abrasion stage 1).

Bone orientation- Based on the unprepared field jacket exposed at the MOR, the orientation of the bones in the Blacktail Creek North bonebed follows a uniform distribution (Figure 15). The results of the Rao's spacing test of uniformity (test statistic = 138.67, critical value [at α = 0.05] = 146.29) could not allow rejection of the null hypothesis (i.e., that the orientation of the elements is uniformly distributed), thus suggesting that there is no significant preferential alignment of the bones in the assemblage. The assemblage also presents a high circular variance of 0.97.

A

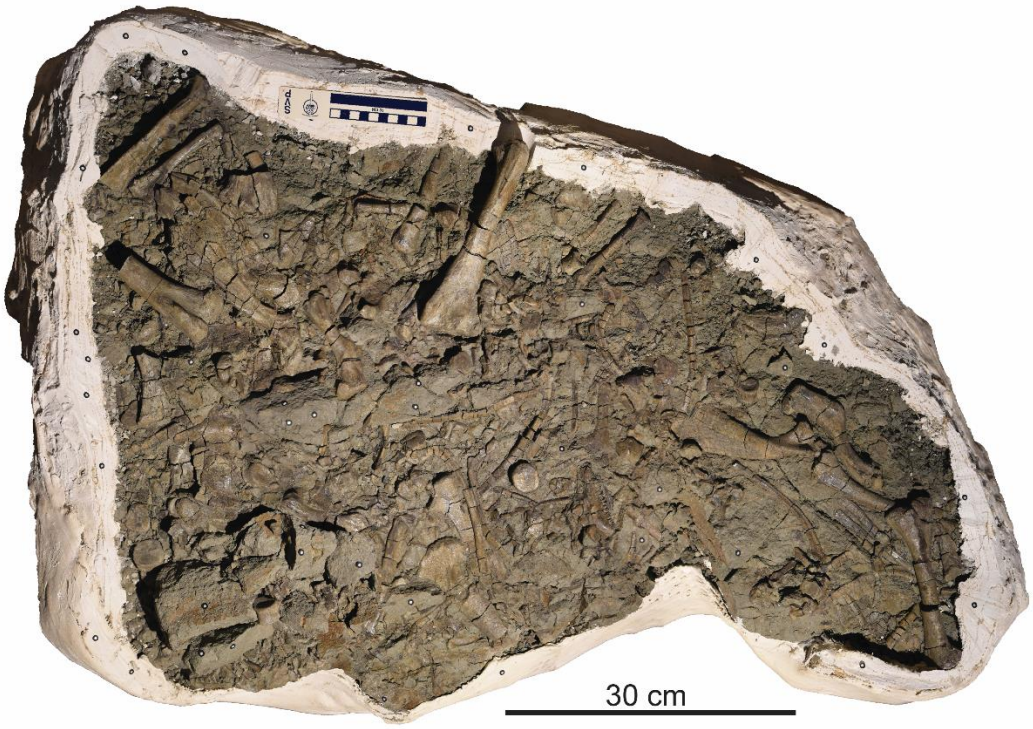

B

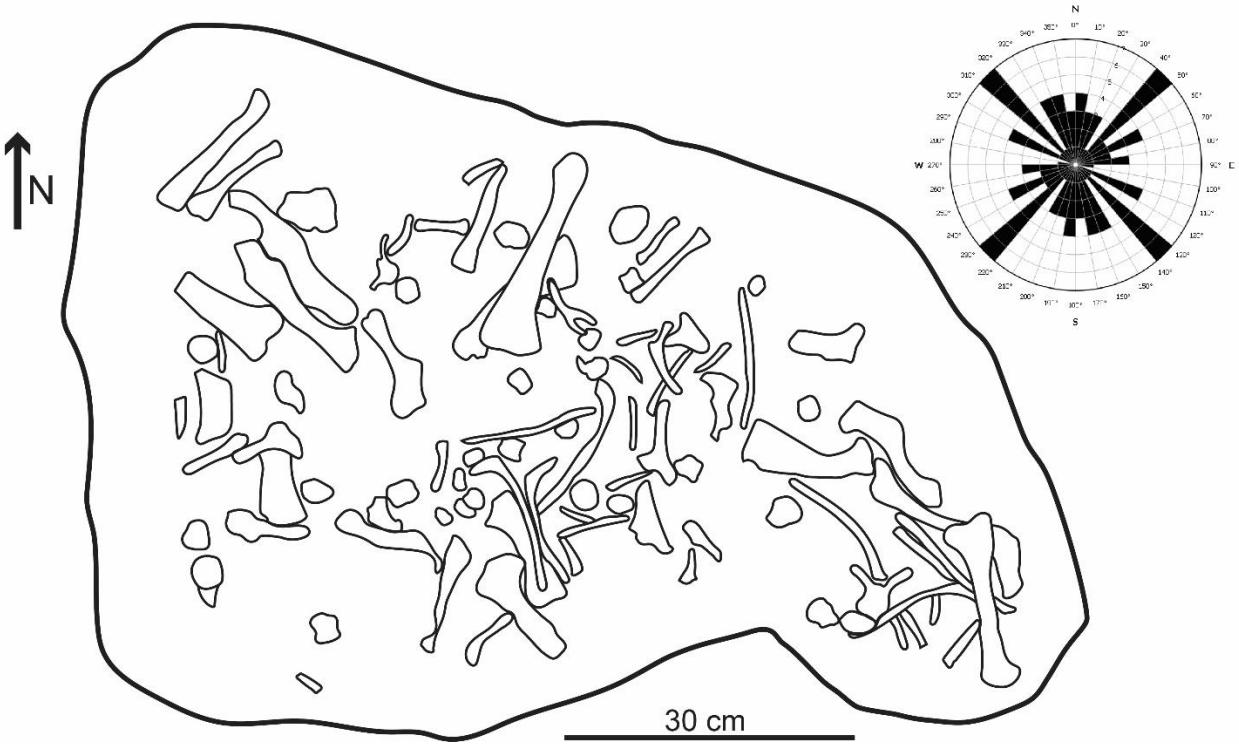

Figure 15. Field jacket from the Blacktail Creek North bonebed (MOR 548). **A**, Photograph of the field jacket; **B**, interpretative drawing of the field jacket with North arrow (based on Horner, 1994: figure 8.4) and rose diagram illustrating the orientation of long bones (Rao's spacing test of uniformity: test statistic = 138.67, critical value [at $\alpha = 0.05$] = 146.29).

3.2.7 Histologic description and age interpretation of a fibula from BCN

The fibular cross-section examined from the Blacktail Creek North bonebed (Figure 16) is complete and measures 10.6 mm in maximum diameter. It is well-preserved and shows no sign of deformation. No LAG or annulus is present in this cross-section. The medullary cavity measures 3.8 mm in maximum diameter and contains cancellous bone. The entire cortex of the fibular cross-section is composed of woven bone characterized by a reticular vascularization pattern, indicative of rapid growth. This cross-section is interpreted as representing an individual that had yet to reach one year of life, based on the absence of complete yearly growth cycles.

Figure 16. Histology of MOR 548 (fibula). Cross-section produced at mid-diaphysis.

3.2.8 Faunal composition of the Lambeosite bonebed (Montana)

The Lambeosite bonebed preserves a total of 234 identifiable hadrosaurid specimens (NISP = 234) and an additional 217 small bone fragments (Appendix C). Similar to the Blacktail Creek North bonebed, these fragments are not included in the analyses since they are often unidentifiable or too small to be assigned as distinct skeletal elements, and they may have been produced during collection or preparation of the specimens. The number of skeletal elements preserved in the assemblage is 182 due to the overlapping parts of some specimens (Table 4; see Materials & Methods). The MNI is five based on the presence of five left scapula, as well as four distinct juvenile right humeri and one adult left humerus.

	Category	Element	Count	Total	Observed Proportion (%)
Group I	Light Cranial Elements		5	129	70.9
	Digital Elements	Pedal Phalanges	5		
		Manual Phalanges	9		
	Ribs		14		
	Vertebral Elements	With Centra	66		
		Other Processes	26		
	Pelvic Elements	Ischia	4		
Group II	Pectoral Elements	Sternal Plate	0	18	9.9
		Coracoid	1		
		Scapulae	8		
	Dense Cranial Elements	Maxillae	2		
		Dentaries	1		
	Metapodials	Metacarpals	2		
		Metatarsals	4		
		Calcaneum	0		
		Astragalus	0		
	Pelvic Elements	Pubes	0		
Group III	Limb Bones	Humeri	8	35	19.2
		Radii	1		
		Ulnae	3		
		Femora	6		
		Tibiae	6		
		Fibulae	5		
	Pelvic Elements	Ilia	6		

Table 4. Hadrosaurid elements preserved in the Lambeosite bonebed. Categorization of the skeletal elements to Voorhies groups is based on Holland et al. (2021).

3.2.9 Taphonomic features of the Lambeosite bonebed (Montana)

Size distribution- The Lambeosite bonebed preserves individuals from two distinct ontogenetic stages: at least four juvenile individuals of similar size and at least one adult (Figure 8C). The femora of the juvenile individuals range from 59.5 cm (MOR 355 8-29-5-5) to 62.5 cm in length (MOR 355 7-20-6-2), which corresponds to 56.7% to 59.5% of a fully grown individual (MOR 549, femur length = 105 cm, see Horner and Currie [1994]: table 21.1), falling into the range of late juveniles (Horner et al., 2000; Ullmann et al., 2017). The femur of the adult individual preserved in the Lambeosite bonebed is slightly longer than the femur of the holotype (femur length of 109 cm vs 105 cm for the holotype [MOR 549]), which suggests that it reached somatic maturity.

Sorting- Similar to the two bonebeds described above, an under-representation of light skeletal elements (Voorhies group I) can be seen in the bonebed (observed proportions of 70.9% vs expected proportions of 90.0%: $\chi^2 = 144.53$, df = 2, $p < 0.001$), while heavier skeletal elements (Voorhies groups II and III) are over-represented (observed proportions of 9.9% and 19.2% vs expected proportions of 6.6% and 3.4%, respectively) (Figure 9A). The significant difference between the observed proportions of each Voorhies group and their expected proportions suggests a preferential removal of light skeletal elements.

Weathering and abrasion- Weathering features are rare in the assemblage. Nearly all specimens (99.1% of NISP, n = 232) exhibit no sign of weathering (Figure 9B). Only two specimens (0.9% of NISP) are affected by weathering: one exhibits features characteristic of weathering stage 1, while the other shows signs of weathering stage 2. Signs of weathering stage 3 are absent from the assemblage.

Throughout the assemblage, 187 specimens (79.9% of NISP) are unaffected by abrasion. Slight rounding of the edges (abrasion stage 1) is visible on 41 specimens (17.5% of NISP) and 6 specimens (2.6% of NISP) have developed a slight polish (abrasion stage 2) (Figure 9C). Most of the abraded specimens (roughly 94%) are light skeletal elements (e.g., phalanges, vertebrae, light cranial elements).

3.2.10 Histologic description and age interpretation of a tibia from Lambeosite

The thin section produced from the tibia of a late juvenile individual from the Lambeosite bonebed (MOR 355) consists of a wedge from a larger specimen, with only a portion from the medullary cavity to the periosteal surface represented (Figure 17). No true LAGs are present in this specimen, although an annulus may be present. The section measures 16.2 mm in maximum thickness (measured from the outer edge of the medullary cavity to the periosteal surface). A 14.5-mm-thick region composed of fibrolamellar bone characterized by a reticular vascularization pattern surrounds the medullary cavity. Signs of bone remodeling such as resorption cavities and secondary osteons are present in this layer. Surrounding this region, a 0.9-mm-thick layer of lamellar bone characterized by lenticular vascularization is present. This layer potentially represents an annulus, although this is difficult to ascertain as the layer cannot be traced throughout the whole section. A 1.3 mm-thick layer of lamellar bone characterized by a plexiform vascularization pattern forms the outermost portion of the section.

Although this specimen preserves at most one annulus, it is interpreted as representing a three-year-old individual based on its size and the presence of signs of remodeling which could have resulted in the loss of LAGs and annuli. Another specimen from the same bonebed (MOR

355: see Cooper et al., 2008) that preserves a single LAG is thought to represent an individual that lost two LAGs to bone remodeling (Cooper et al., 2008). As evidence of bone remodeling is also present in the specimen examined here, and all late juvenile individuals from this bonebed are of similar size (Figure 8C), these individuals are interpreted as being three-year-old late juvenile individuals.

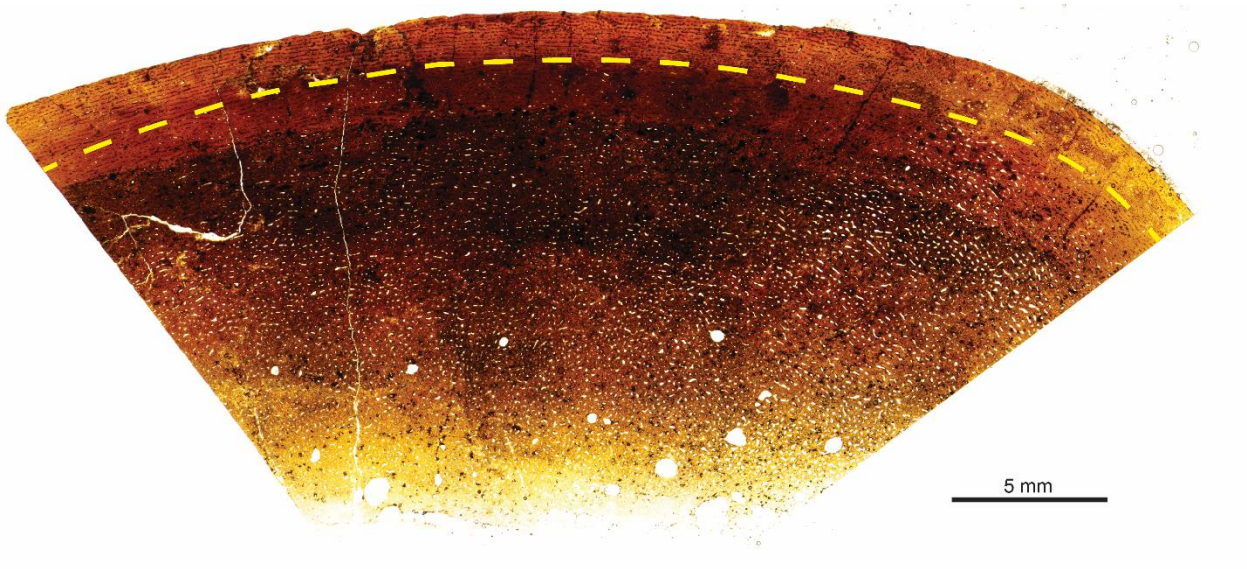

Figure 17. Histology of MOR 355 (tibia). Cross-section produced at mid-diaphysis. Yellow dashed line represents the inferred position of an annulus.

3.3 DISCUSSION

The three bonebeds examined as part of this study are monodominant assemblages that preserve multiple individuals of *Hypacrosaurus stebingeri* at different growth stages. Comparing the modes of formation and preservation of these bonebeds allows us to better understand the context that led to the preservation of these individuals and the life strategies employed by these dinosaurs throughout their life. To properly infer the paleoecological implications of these assemblages, an understanding of their taphonomic history is required. Two of the three bonebeds examined as part of this study (Blacktail Creek North and Lambeosite) were briefly described over 30 years ago (see Varricchio and Horner [1993]), whereas the taphonomy of the JBB has never been studied. Thus, a detailed interpretation of the preservation of the JBB assemblage and its taphonomic history, along with an updated taphonomic profile of the Blacktail Creek North and Lambeosite bonebeds, are discussed here.

3.3.1 Preservation of the JBB (Alberta)

Overall, the bones from the JBB show little pre-burial damage. The abundance of unweathered (Stage 0) and lightly weathered (Stages 1 and 2, to a lesser extent) bones in the assemblage suggests that most of the bones were exposed at the surface for only a short period of time prior to burial (less than a year for Stage 0, less than 3 years for Stage 1, 2 to 6 years for Stage 2; Behrensmeyer, 1978). The predominance of abrasion features on bones with high susceptibility to hydraulic transport (phalanges and vertebrae) suggests that the discrepancy between the observed and expected proportion of each Voorhies group in the bonebed is a result of hydraulic winnowing: light skeletal elements (Voorhies group I) have been preferentially removed from the assemblage relative to heavier skeletal elements (Voorhies groups II and III).

The presence of spiral fractures on some skeletal elements indicates that breakage of the bones started shortly after decomposition of the carcass, while the bone was still fresh, perhaps due to trampling (Myers et al., 1980; Haynes, 1983; Eberth and Getty, 2005; Karr and Outram, 2012; Scott et al., 2022a). Due to the limited transport of the bones as evidenced by the rarity of abrasion features on the bones and the over-representation of skeletal elements with low susceptibility to hydraulic transport (Voorhies groups II and III), transport likely played a minor role in the breakage of the bones. The presence of compression fractures on the surface of the bones are indicative of post-burial bone deformation during sediment compaction (Ryan et al., 2001; Ullmann et al., 2017). The presence of wet rot throughout the assemblage is consistent with the depositional environment inferred from the sedimentological data (i.e., burial in or on the shore of a river channel in a wetland), as wet rot occurs under humid conditions (e.g., on submerged bones) or on bones buried in waterlogged sediments (Andrews and Ersoy, 1990; Scherzer and Varricchio, 2010). The rarity of tooth-marked bones in the assemblage indicates either that the carcasses were exposed for a short time, thus limiting scavenging opportunities, or that there was an excessive number of carcasses, limiting scavenging on any one of them (e.g., Eberth and Getty, 2005). The comparatively small number of carcasses represented by the JBB assemblage suggests that the scarcity of scavenging traces is related to limited exposure time.

3.3.2 Taphonomic history of the JBB (Alberta)

The size of the individuals preserved, the monodominant nature of the bonebed, and the similarities in the taphonomic signatures throughout the assemblage indicate that the JBB represents a mass death assemblage. The absence of remains belonging to very young and very old individuals (with the exception of a single adult pedal phalanx) in the bonebed, age groups

with the highest mortality rates (Varricchio and Horner, 1993; Lyman, 1994; see supp. data of Erickson et al., 2006; Erickson et al., 2010; Lauters et al., 2008), does not reflect the expected age profile of an attritional assemblage. Furthermore, the uniformity of taphonomic signatures (i.e., predominance of early weathering and abrasion stages, uniform type of fractures throughout the assemblage, presence of wet rot on nearly all long bones) suggests that the bones do not represent a time-averaged, attritional assemblage, in which a wide variety of taphonomic signatures would be present (Behrensmeyer, 1978; Varricchio and Horner, 1993; Ryan et al., 2001; Chiba et al., 2015). As such, the JBB is interpreted as a mass death assemblage resulting from a catastrophic event.

Although the cause of death of the juvenile hadrosaurids preserved in the JBB cannot be determined with certainty, a few possibilities can be considered. The abundance of gley colorations in the paleosols, the absence of caliches at the bonebed level, and the presence of wet rot on most long bones in the assemblage suggest the bones accumulated in a poorly-drained, waterlogged setting (Leckie et al., 1989; Andrews and Ersoy, 1990; Therrien and Fastovsky, 2000; Scherzer and Varricchio, 2010), raising the possibility of a flooding-induced death assemblage. However, thick sandstone deposits, commonly associated with flooding-induced mass death assemblages preserved in paleochannels (Eberth and Getty, 2005), are absent in the stratigraphic interval hosting the JBB. As such, the death of the individuals preserved in the JBB cannot be confidently associated with a flooding event. The JBB could also represent a drought-induced death assemblage. The depositional environment in which the carcasses of the juvenile hadrosaurids were buried represents localized, seasonal wetlands in an otherwise arid to semi-arid environment, as evidence by the absence of gleyed paleosols above the bonebed level, indicating a shift towards better-drained settings. The presence of seasonal wetlands is consistent

with an overall semi-arid environment (Therrien and Fastovsky, 2000; Therrien et al., 2009), in which drought-induced mass death assemblages are common (e.g., Rogers, 1990; Varricchio and Horner, 1993; Gates, 2005).

Based on the lines of evidence presented above, the JBB is interpreted to have formed as a result of the following events: 1) a group of at least four, similar-sized three-year-old late juvenile *Hypacrosaurus stebingeri* individuals died from an undetermined cause, 2) theropod dinosaurs scavenged the hadrosaurid carcasses, leaving tooth marks on a few bones, 3) the hadrosaurid carcasses decomposed and disarticulated, 4) the hadrosaurid bones remained exposed for a short period of time, resulting in limited subaerial weathering of a minority of the bones, 5) the hadrosaurid bones were transported by a river over a short distance, resulting in only slight abrasion of a minority of bones, preferential removal of light skeletal elements, and wet rot on the epiphyses of nearly all long bones, 6) the bones were stranded and buried within a channel and/or on the margin of a channel in a seasonal wetland, where wet rot would continue to form. The presence of spiral fractures on some bones indicates that the bones were broken while they were still fresh, perhaps due to trampling, or during transport, to a lesser extent (see above). Trampling of the bones could have occurred either prior to transport, or after transport, once the bones settled in their burial location, as the short period of time between death of the individuals and burial of the bones would still allow for spiral fractures to form (i.e., the bones would still be relatively fresh) (Myers et al., 1980; Haynes, 1983). The presence of compression fractures on some bones is indicative of post-burial deformation due to sediment compaction (Ryan et al., 2001). As such, the JBB is interpreted as a parautochthonous mass mortality assemblage resulting from the fluvial accumulation of the bones of a group of late juvenile *Hypacrosaurus stebingeri* individuals.

3.3.3 Taphonomic information regarding the Blacktail Creek North and Lambeosite bonebeds (Montana)

While the Blacktail Creek North and Lambeosite bonebeds have previously been briefly described (see Varricchio and Horner, 1993; Horner, 1994), these descriptions require updating due to access to additional material and new methods. With our analyses, the MNI for both Montana bonebeds has been raised: the minimum number of individuals preserved in the Blacktail Creek North bonebed has changed from 12 (Horner, 1994; Horner and Currie, 1994) or 18 (Varricchio and Horner, 1993) to 23, based on the number of right dentaries, whereas the minimum number of individuals preserved in the Lambeosite bonebed has changed from four (Varricchio and Horner, 1993) to five, based on the number of scapulae and humeri in the assemblage. Furthermore, our chi-square test for skeletal representation in the Blacktail Creek North bonebed shows an under-representation of light skeletal elements (and consequently an over-representation of heavy skeletal elements), whereas the original description reported a proportional representation of each group. This discrepancy between our results and the original description could be explained either by the additional material that was accessible to us, which would change the relative proportions of each group and imply a greater effect of hydraulic sorting on the assemblage, or by the different methodology used to assess hydraulic sorting, as we based our analysis on the groupings proposed by Holland et al. (2021) adapted for juvenile lambeosaurines. Furthermore, Varricchio and Horner (1993) reported a weak alignment for the bones preserved in the Blacktail Creek North bonebed. This observation was not supported by our directional analysis, which revealed a uniform distribution of the orientation of the bones (i.e., no preferential alignment). However, it is important to note that our analysis is based on a

very small sample size (orientation of 54 skeletal elements) highly localized in a small field jacket (approximately 1 m^2) and may not represent the typical pattern of orientation of the skeletal elements throughout the entirety of the bonebed.

3.3.4 Taphonomic comparison among the three *Hypacrosaurus stebingeri* bonebeds

The three monodominant *Hypacrosaurus stebingeri* bonebeds described as part of this study share many similarities in their taphonomic signatures, but also present some considerable differences (Table 5). The Blacktail Creek North bonebed preserves a minimum of 23 small juvenile individuals ("nestlings") (contra Horner [1994], Horner and Currie [1994], and Varricchio and Horner [1993], who reported a MNI of 12 or 18) buried in a silty mudstone interpreted as channel and crevasse splay deposits (Varricchio and Horner, 1993). The JBB preserves at least four large juvenile individuals buried in channel and channel-margin deposits, whereas the Lambeosite bonebed preserves at least five individuals (four larger juveniles than the ones from JBB and one adult) buried in a silty mudstone interpreted as lacustrine deposits (Varricchio and Horner, 1993). The preservation style of the bones from the three bonebeds is similar: the material is mostly disarticulated, the bones show very little evidence of weathering and abrasion, and tooth marks are rare (Varricchio and Horner, 1993; Horner, 1994). Although skeletal elements from the three bonebeds are preserved in fine-grained sediments, the depositional environments differ: the bone assemblages from the JBB and Blacktail Creek North bonebed are interpreted as fluvial accumulations, whereas the Lambeosite bonebed is interpreted as resulting from the congregation of individuals at a waterhole during a drought (Varricchio and Horner, 1993; Horner, 1994; Horner and Currie, 1994). Despite the differences between the depositional environments of the JBB and the Lambeosite bonebed (channel and channel-margin

deposits vs lacustrine deposits, respectively), both sites formed under seasonally wet conditions (fluvial streams in wetland environments vs. lakes, respectively) in an otherwise arid to semi-arid environment (Varricchio, 1993; Varricchio and Horner, 1993). As such, it is possible that these bone accumulations are the result of similar behavior (i.e., the congregation of *H. stebingeri* individuals near a water source) during a similar catastrophic event (i.e., drought), although the cause of death of the individuals preserved in the JBB cannot be determined confidently (see above).

	Devil's Coulee juvenile hadrosaur bonebed (JBB, Alberta)	Blacktail Creek North bonebed (Montana)	Lambeosite bonebed (Montana)
Faunal component	Monodominant (*Hypacrosaurus stebingeri*)	Monodominant (*Hypacrosaurus stebingeri*)	Monodominant (*Hypacrosaurus stebingeri*)
Type of assemblage	Mass mortality	Mass mortality*	Mass mortality*
Depositional environments	Channel and channel-margin deposits	Crevasse splay*	Lacustrine*
Skeletal representation	Group I under-represented	Group I under-represented	Group I under-represented
Weathering	Limited (<7%)	Limited to absent	Limited to absent
Abrasion	Limited (16%, mostly light skeletal elements)	Limited to absent	Limited (~20%, mostly light skeletal elements)
Tooth marks	Rare (1.3%)	Absent	Absent
MNI	4 (late juveniles)	23 ('nestlings')	5 (4 late juveniles + 1 adult)
Biological age (years)	3	<1	3 (late juveniles)

Table 5. Summary of taphonomic signatures from the Devil's Coulee juvenile hadrosaur bonebed (JBB), the Blacktail Creek North bonebed, and the Lambeosite bonebed. *From Varricchio and Horner (1993).

3.3.5 Taphonomic comparison with other hadrosaurid bonebeds

Monodominant hadrosaurid bonebeds have been documented from multiple countries, including Canada (Eberth et al., 2014; Evans et al., 2015; Holland et al., 2021; Thompson et al., 2021; Scott et al., 2022a), the U.S.A. (Rogers, 1990; Varricchio and Horner, 1993; LaRock, 2000; Colson et al., 2004; Gangloff and Fiorillo, 2010; Scherzer and Varricchio, 2010; Schmitt et al., 2014; Ullmann et al., 2017; Snyder et al., 2020), Spain (Gaete Harzenetter, 2020), Russia (Lauters et al., 2008), Mongolia (Bell et al., 2018), and China (Godefroit et al., 2008; Hone et al., 2014b). Despite their wide geographical distribution and the diverse depositional environments, most of these bonebeds present uniform taphonomic signatures, a characteristic also seen in the JBB from Devil's Coulee and the Blacktail Creek North and Lambeosite bonebeds from Montana, along with an age profile biased towards the preservation of certain ontogenetic stages over others (Appendix D). Like the three bonebeds described in this study, most of these monodominant hadrosaurid bonebeds have been interpreted as representing mass mortality assemblages, in part due to the uniformity of taphonomic signatures throughout the assemblages. The three *Hypacrosaurus stebingeri* bonebeds described in this study present some striking taphonomic similarities with other hadrosaurid bonebeds from Alberta (e.g., Princess Bonebed, Bleriot Ferry, Fox Coulee, Prehistoric Park, Wendy's Bonebed: Appendix D) and the U.S.A. (e.g., West Hadrosaur Bonebed, Westside Quarry, Sun River Bonebed, Standing Rock Hadrosaur Site, Hanson Ranch Bonebed: Appendix D), in which weathering tends to be limited (typically more than 90% of the bones showing no sign of weathering), and tooth marks are rare (typically absent or present on very few bones). Abrasion and breakage of the bones are much more varied from one bonebed to another, ranging from mostly complete and unabraded (e.g., West Hadrosaur Bonebed, Westside Quarry, Standing Rock Hadrosaur Site: Appendix D) to high

degrees of abrasion and/or mostly incomplete bones (e.g., Princess Bonebed, Willow Creek Anticline Bonebed, Bleriot Ferry, Fox Coulee, Prehistoric Park, Wendy's Bonebed: Appendix D), depending on the depositional context. The JBB is one of the only hadrosaurid bonebeds for which wet rot has been reported, along with the Sun River Bonebed from the Two Medicine Formation of Montana, U.S.A. (Scherzer and Varricchio, 2010). The JBB and the Lambeosite are also among the monodominant hadrosaurid bonebeds with the smallest estimated MNI, with an MNI of four and five, respectively, whereas the Blacktail Creek North bonebed is one of the monodominant hadrosaurid bonebeds with the highest estimated MNI (MNI = 23).

3.3.6 Taphonomic comparison with ceratopsian bonebeds of North America

The three *Hypacrosaurus stebingeri* bonebeds described in this study share many taphonomic similarities with previously described monodominant ceratopsian bonebeds from the upper Campanian Dinosaur Park and Oldman Formations of Alberta, although ceratopsian bonebeds often preserve juvenile individuals along with subadult and adult individuals (e.g., Rogers, 1990; Ryan et al., 2001; Chiba et al., 2015). These ceratopsian bonebeds are typically characterized by minimal weathering, minimal abrasion, and evidence of rot or decomposition of the bones (Ryan et al., 2001; Eberth and Getty, 2005), characteristics also seen in the *Hypacrosaurus stebingeri* bonebeds. In addition to sharing similar taphonomic characteristics with the three *Hypacrosaurus stebingeri* bonebeds, the sedimentology of a *Centrosaurus apertus* bonebed from the upper Oldman Formation of southeastern Alberta (Manyberries area) represents the same kind of paleoenvironment as the JBB and the Blacktail Creek North bonebed, being hosted in fine-grained overbank deposits laid down on a seasonally humid, poorly-drained floodplain in an otherwise arid to semi-arid environment, promoting the development of similar taphonomic

signals such as wet rot (Chiba et al., 2015). Based on the taphonomic similarities between *Centrosaurus apertus* bonebeds from the Dinosaur Park Formation and the time-equivalent upper Oldman Formation of southernmost Alberta, it has been proposed that severe storm-induced flooding events likely affected the coastal lowlands in which the Dinosaur Park Formation and the Oldman Formation were deposited, and produced drowning-related mass mortality events (Eberth and Getty, 2005; Chiba et al., 2015). However, it is unknown whether such a scenario applies to the JBB and the Blacktail Creek North bonebeds, both of which could have been produced as the result of a flooding event.

The three *Hypacrosaurus stebingeri* bonebeds studied here are also comparable to ceratopsian bonebeds from the Two Medicine Formation of Montana. Two monodominant *Einiosaurus procurvicornis* bonebeds (Canyon Bonebed and Dino Ridge Quarry: see Rogers, 1990), originally referred to as *Styracosaurus* sp. (Rogers, 1990), are characterized by little weathering and an under-representation of light skeletal elements indicative of winnowing, a seemingly common phenomenon for bonebeds from the upper Campanian of North America. These two assemblages are preserved in lake deposits, similar to the Lambeosite bonebed. Similarly, sedimentological information from these bonebeds also indicates a drought as the likely cause of death (Rogers, 1990).

3.3.7 Paleoecological implications

The three monodominant *Hypacrosaurus stebingeri* bonebeds described here provide insight into the social behavior of juvenile individuals. The exclusive preservation of less than one-year-old ‘nestling’ (or early juvenile, see above) individuals in the Blacktail Creek North bonebed

suggests that the assemblage represents an isolated group of young individuals segregated from other *Hypacrosaurus stebingeri* individuals. The exclusive preservation of remains of similar-sized, three-year-old, late juvenile *Hypacrosaurus stebingeri* individuals in the JBB, without remains from smaller juvenile or adult individuals, further supports this interpretation and suggests that *Hypacrosaurus stebingeri* individuals remained segregated at least until they reached approximately 50% of a fully-grown adult's body size. The presence of a fully-grown adult individual with larger, three-year-old, late juvenile individuals in the Lambeosite mass-mortality assemblage suggests that young *Hypacrosaurus stebingeri* individuals rejoined multigenerational herds during their fourth year of life, when they approached 60% of the average body size of a fully-grown adult. A similar scenario has been hypothesized for *Amurosaurus riabinini*, in which segregated young individuals would join a multigenerational herd once they reached approximately half of the size of fully-grown adults (late juvenile stage) (Lauters et al., 2008).

The number of individuals preserved in the bonebeds appears to change with the ontogenetic stage of those individuals. Interestingly, the number of segregated "nestling" individuals (MNI = 23) preserved in the Blacktail Creek North bonebed approximates the number of eggs in a lambeosaurine nest/clutch, which consists of approximately 22 eggs (Horner, 1999), potentially indicating the hatchlings remained together after hatching. The size of the segregated groups appears to decrease at later ontogenetic stages, as evidenced by the MNI of four in the JBB and the preservation of four late juvenile individuals in the Lambeosite bonebed. Furthermore, the Sun River Bonebed, another lambeosaurine bonebed from the Two Medicine Formation that preserves late juvenile individuals potentially referable to *Hypacrosaurus stebingeri* (based on their lambeosaurine affinity and the biostratigraphy of the Two Medicine Formation), has a MNI

of eight, further indicating a low individual count with later ontogenetic stages (Scherzer and Varricchio, 2010). This pattern may be explained either by a high mortality rate in very young individuals such as nestlings (Varricchio and Horner, 1993; Lyman, 1994; see supp. data of Erickson et al., 2006; Erickson et al., 2010; Lauters et al., 2008), or by a splitting up of the large groups of “nestling” individuals. Reduction in group size, also known as group fission, is a phenomenon documented in modern animals that occurs when remaining in large groups becomes no longer advantageous for individual group members (e.g., Griesser et al., 2011; Gupte et al., 2019; Stredulinsky et al., 2021; Sueur and Maire, 2014).

Several hadrosaurid bonebeds that either preserve juvenile individuals exclusively (e.g., Varricchio and Horner, 1993; Scherzer and Varricchio, 2010; Holland et al., 2021; Scott et al., 2022a) or that lack juvenile individuals entirely (e.g., Lauters et al., 2008, Hone et al., 2014b; Evans et al., 2015; Ullmann et al., 2017) have been interpreted as evidence of age segregation among hadrosaurid dinosaurs. Age segregation has also been proposed to explain the absence or exclusive presence of juvenile individuals in a variety of other dinosaur bonebeds, including sauropodomorphs (Myers and Storrs, 2007; Myers and Fiorillo, 2009; Pol et al., 2021), ankylosaurs (Currie, 1989; Jerzykiewicz et al., 1993; Currie et al., 2011; Botfalvai et al., 2021), ceratopsians (Qi et al., 2007; Hone et al., 2014a), and non-hadrosaurid ornithopods (Forster, 1990). As such, it may have been a widespread life strategy employed by many different dinosaur taxa.

CHAPTER 4: CONCLUSION

The three monodominant *Hypacrosaurus stebingeri* bonebeds studied here are interpreted as mass mortality assemblages based on the uniformity of taphonomic signatures throughout the assemblages and sedimentological data. The Devil's Coulee juvenile hadrosaur bonebed (JBB), examined here for the first time in the context of a detailed taphonomic study, preserves the remains of a group of at least four, similar-sized, late juvenile individuals preserved in fine-grained units representing channel and channel-margin deposits in seasonal poorly-drained wetlands. Our re-examination of the Blacktail Creek North and Lambeosite bonebeds from Montana revealed a greater minimum number of individuals preserved in these bonebeds than originally recognized. While the Blacktail Creek North bonebed preserves a minimum of 23 small-sized individuals, the minimum number of individuals preserved in the Lambeosite bonebeds is estimated at one adult and four late juvenile individuals. The reduction in the minimum number of individuals with increasing ontogenetic stages may be due to a high mortality rate in young individuals or to splitting of a group of segregated juvenile individuals.

The age profile of the three *Hypacrosaurus stebingeri* bonebeds studied here are data points that can be used to make inferences into the social dynamics of this species. The exclusive preservation of similar-sized young individuals ("nestlings") in the Blacktail Creek North bonebed, as well as the exclusive preservation of similar-sized late juvenile individuals in the JBB provide strong evidence that young *Hypacrosaurus stebingeri* individuals formed segregated groups of their own. The presence of an adult individual among the Lambeosite mass-mortality assemblage, which also preserves larger late juvenile individuals, indicates that segregated *Hypacrosaurus stebingeri* individuals would rejoin a multigenerational herd during

their fourth year of life, when they reached approximately 60% of the size of a fully-grown individual. As such, this detailed taphonomic comparison of the three monodominant *Hypacrosaurus stebingeri* significantly improves our understanding of social dynamics in this species.

REFERENCES

Andrews, P., & Ersoy, A. (1990). Taphonomy of the Miocene bone accumulations at Paşalar, Turkey. *Journal of Human Evolution, 19*(4-5), 379-396.

Behrensmeyer, A. K. (1978). Taphonomic and ecologic information from bone weathering. *Paleobiology*, *4*(2), 150-162.

Behrensmeyer, A. K. (1982). Time resolution in fluvial vertebrate assemblages. *Paleobiology*, *8*(3), 211-227.

Behrensmeyer, A. K. (1991). Terrestrial vertebrate accumulations. In P. A. Allison & D. E. G. Briggs (Eds.), *Taphonomy: Releasing the Data Locked in the Fossil Record* (pp. 291-335). Plenum Press.

Bell, P. R. (2012). Standardized terminology and potential taxonomic utility for hadrosaurid skin impressions: a case study for *Saurolophus* from Canada and Mongolia. *PLoS ONE*, *7*(2), e31295.

Bell, P. R. (2014). A review of hadrosaurid skin impressions. In D. A. Eberth & D. C. Evans (Eds.), *Hadrosaurs* (pp. 572-590). Indiana University Press.

Bell, P. R., & Campione, N. E. (2014). Taphonomy of the Danek Bonebed: a monodominant *Edmontosaurus* (Hadrosauridae) bonebed from the Horseshoe Canyon Formation, Alberta. *Canadian Journal of Earth Sciences*, *51*(11), 992-1006.

Bell, P. R., Evans, D. C., Eberth, D. A., Fanti, F., Tsogtbaatar, K., & Ryan, M. J. (2018). Sedimentological and taphonomic observations on the “Dragon's Tomb” *Saurolophus* (Hadrosauridae) bonebed, Nemegt Formation (Upper Cretaceous), Mongolia. *Palaeogeography, Palaeoclimatology, Palaeoecology*, *494*, 75-90.

Blob, R. W., Espinoza, I. Z., & Iijima, M. (2023). Anatomy informs geology: Hydrodynamic dispersal of alligator bones, with implications for taphonomic interpretations of fossil deposits of crocodylians, dinosaurs, and other morphologically novel taxa. *The Anatomical Record*, *306*(7), 1618-1630.

Botfalvai, G., Prondvai, E., & Ősi, A. (2021). Living alone or moving in herds? A holistic approach highlights complexity in the social lifestyle of Cretaceous ankylosaurs. *Cretaceous Research*, *118*, 104633.

Brink, K. S. (2009). Cranial ontogeny and evolution of the lambeosaurine dinosaur *Hypacrosaurus stebingeri* (Ornithischia: Hadrosauridae). (Master's thesis, University of Calgary).

Brink, K. S., Zelenitsky, D. K., Evans, D. C., Horner, J. R., & Therrien, F. (2014). Cranial morphology and variation in *Hypacrosaurus stebingeri* (Ornithischia: Hadrosauridae). In D. A. Eberth & D. C. Evans (Eds.), *Hadrosaurs* (pp. 245-260). Indiana University Press.

Brink, K. S., Zelenitsky, D. K., Evans, D. C., Therrien, F., & Horner, J. R. (2011). A sub-adult skull of *Hypacrosaurus stebingeri* (Ornithischia: Lambeosaurinae): anatomy and comparison. *Historical Biology, 23*(01), 63-72.

Brinkman, D. B., Russell, A. P., Eberth, D. A., & Peng, J. (2004). Vertebrate palaeocommunities of the lower Judith River Group (Campanian) of southeastern Alberta, Canada, as interpreted from vertebrate microfossil assemblages. *Palaeogeography, Palaeoclimatology, Palaeoecology, 213*(3-4), 295-313.

Brown, B. (1913). A new trachodont dinosaur, *Hypacrosaurus,* from the Edmonton Cretaceous of Alberta. Bulletin of the AMNH; v. 32, article 20.

Brown, B. (1914). *Corythosaurus casuarius*, a new crested dinosaur from the Belly River Cretaceous; with Provisional classification of the family Trachodontidae. Bulletin of the AMNH; v. 33, article 35.

Brown, C. M., Currie, P. J., & Therrien, F. (2022). Intraspecific facial bite marks in tyrannosaurids provide insight into sexual maturity and evolution of bird-like intersexual display. *Paleobiology*, *48*(1), 12-43.

Brown, C. M., Tanke, D. H., & Hone, D. W. (2021). Rare evidence for 'gnawing-like' behavior in a small-bodied theropod dinosaur. *PeerJ*, *9*, e11557.

Carpenter, K. (1992). Behavior of hadrosaurs as interpreted from footprints in the" Mesaverde" Group (Campanian) of Colorado, Utah, and Wyoming. *Rocky Mountain Geology*, *29*(2), 81-96.

Chiba, K., Ryan, M. J., Braman, D. R., Eberth, D. A., Scott, E. E., Brown, C. M., Kobayashi, Y., & Evans, D. C. (2015). Taphonomy of a monodominant *Centrosaurus apertus* (Dinosauria: Ceratopsia) bonebed from the upper Oldman Formation of southeastern Alberta. *Palaios*, *30*(9), 655-667.

Chinsamy-Turan, A. (2005). *The microstructure of dinosaur bone*. John Hopkins University Press.

Colson, M. C., Colson, R. O., & Nellermoe, R. (2004). Stratigraphy and depositional environments of the upper Fox Hills and lower Hell Creek Formations at the Concordia Hadrosaur Site in northwestern South Dakota. *Rocky Mountain Geology*, *39*(2), 93-111.

Cooper, L. N., Lee, A. H., Taper, M. L., & Horner, J. R. (2008). Relative growth rates of predator and prey dinosaurs reflect effects of predation. *Proceedings of the Royal Society B: Biological Sciences*, *275*(1651), 2609-2615.

Cruzado-Caballero, P., Pereda-Suberbiola, X., & Ruiz-Omeñaca, J. I. (2010). *Blasisaurus canudoi* gen. et sp. nov., a new lambeosaurine dinosaur (Hadrosauridae) from the latest Cretaceous of Arén (Huesca, Spain). *Canadian Journal of Earth Sciences*, *47*(12), 1507-1517.

Currie, P. J. (1989). Long-distance dinosaurs: annual migrations may haven taken some dinosaurs to the Arctic-and beyond. *Natural History*, *6/89*, 60-65.

Currie, P. J., Badamgarav, D., Koppelhus, E. B., Sissons, R., & Vickaryous, M. K. (2011). Hands, feet, and behaviour in *Pinacosaurus* (Dinosauria: Ankylosauridae). *Acta Palaeontologica Polonica*, *56*(3), 489-504.

Driese, S. G., & Ober, E. G. (2005). Paleopedologic and paleohydrologic records of precipitation seasonality from Early Pennsylvanian" underclay" paleosols, USA. *Journal of Sedimentary Research*, *75*(6), 997-1010.

Drumheller, S. K., Boyd, C. A., Barnes, B. M., & Householder, M. L. (2022). Biostratinomic alterations of an *Edmontosaurus* “mummy” reveal a pathway for soft tissue preservation without invoking “exceptional conditions”. *PLoS ONE*, *17*(10), e0275240.

Eberth, D. A. (1996). Origin and significance of mud-filled incised valleys (Upper Cretaceous) in southern Alberta, Canada. *Sedimentology*, *43*(3), 459-477.

Eberth, D. A. (2005). The Geology. In P. J. Currie & E. B. Koppelhus (Eds.), *Dinosaur Provincial Park: A Spectacular Ancient Ecosystem Revealed* (pp. 54-82). Indiana University Press.

Eberth, D. A. (2024). Stratigraphic architecture of the Belly River Group (Campanian, Cretaceous) in the plains of southern Alberta: Revisions and updates to an existing model and implications for correlating dinosaur-rich strata. *PLoS ONE*, *19*(1), e0292318.

Eberth, D. A., & Bergman, K. M. (1997). Sequences and Correlation of the Judith River Group (Campanian) in Southern Alberta and Saskatchewan. Abstract (Canadian Society of Petroleum Geologists).

Eberth, D. A., & Currie, P. J. (2010). Stratigraphy, sedimentology, and taphonomy of the *Albertosaurus* bonebed (upper Horseshoe Canyon Formation; Maastrichtian), southern Alberta, Canada. *Canadian Journal of Earth Sciences*, *47*(9), 1119-1143.

Eberth, D. A., & Hamblin, A. P. (1993). Tectonic, stratigraphic, and sedimentologic significance of a regional discontinuity in the upper Judith River Group (Belly River wedge) of southern Alberta, Saskatchewan, and northern Montana. *Canadian Journal of Earth Sciences*, *30*(1), 174-200.

Eberth, D. A., & Getty, M. A. (2005). Ceratopsian bonebeds: occurrence, origins, and significance. In P. J. Currie & E. B. Koppelhus (Eds.), *Dinosaur Provincial Park: A Spectacular Ancient Ecosystem Revealed* (pp. 501-536). Indiana University Press.

Eberth, D. A., Shannon, M., & Noland, B. G. (2007). A bonebed database: classification, biases, and patterns of occurrence. In R. R. Rogers, D. A. Eberth, & A. R. Fiorillo (Eds.), *Bonebeds: genesis, analysis, and paleobiological significance* (pp. 103-219). Chicago Press.

Eberth, D. A., Evans, D. C., & Lloyd, D. W. H. (2014). Occurrence and taphonomy of the first documented hadrosaurid bonebed from the Dinosaur Park Formation (Belly River Group, Campanian) at Dinosaur Provincial Park, Alberta, Canada. In D. A. Eberth & D. C. Evans (Eds.), *Hadrosaurs* (pp. 502-523). Indiana University Press.

Erickson, G. M., Currie, P. J., Inouye, B. D., & Winn, A. A. (2006). Tyrannosaur life tables: an example of nonavian dinosaur population biology. *Science*, *313*(5784), 213-217.

Erickson, G. M., Currie, P. J., Inouye, B. D., & Winn, A. A. (2010). A revised life table and survivorship curve for *Albertosaurus sarcophagus* based on the Dry Island mass death assemblage. *Canadian Journal of Earth Sciences, 47*(9), 1269-1275.

Erickson, G. M., Curry Rogers, K., Varricchio, D. J., Norell, M. A., & Xu, X. (2007). Growth patterns in brooding dinosaurs reveals the timing of sexual maturity in non-avian dinosaurs and genesis of the avian condition. *Biology Letters, 3*(5), 558-561.

Evans, D. C. (2010). Cranial anatomy and systematics of *Hypacrosaurus altispinus*, and a comparative analysis of skull growth in lambeosaurine hadrosaurids (Dinosauria: Ornithischia). *Zoological Journal of the Linnean Society, 159*(2), 398-434.

Evans, D. C., Eberth, D. A., & Ryan, M. J. (2015). Hadrosaurid (*Edmontosaurus*) bonebeds from the Horseshoe Canyon Formation (Horsethief Member) at Drumheller, Alberta, Canada: geology, preliminary taphonomy, and significance. *Canadian Journal of Earth Sciences, 52*(8), 642-654.

Evans, D. C., & Reisz, R. R. (2007). Anatomy and relationships of *Lambeosaurus magnicristatus*, a crested hadrosaurid dinosaur (Ornithischia) from the Dinosaur Park Formation, Alberta. *Journal of Vertebrate Paleontology, 27*(2), 373-393.

Fiorillo, A. R. (1988). Taphonomy of Hazard Homestead Quarry (Ogallala Group), Hitchcock County, Nebraska. *Rocky Mountain Geology, 26*(2), 57-97.

Fiorillo, A. R. (1991). Taphonomy and depositional setting of Careless Creek Quarry (Judith River Formation), Wheatland County, Montana, USA. *Palaeogeography, Palaeoclimatology, Palaeoecology, 81*(3-4), 281-311.

Fiorillo, A. R., Hasiotis, S. T., & Kobayashi, Y. (2014). Herd structure in Late Cretaceous polar dinosaurs: A remarkable new dinosaur tracksite, Denali National Park, Alaska, USA. *Geology*, *42*(8), 719-722.

Forster, C. A. (1990). Evidence for juvenile groups in the ornithopod dinosaur *Tenontosaurus tilletti* Ostrom. *Journal of Paleontology*, *64*(1), 164-165.

Gaete Harzenetter, R. (2021). Estudio paleontológico (Sistemática, tafonomía, paleobiología) del yacimiento de Basturs Poble (Maastrichtiense, Isona i Conca Dellà, Pallars Jussà). (PhD thesis, Universitat Autònoma de Barcelona). [In Spanish]

Gangloff, R. A., & Fiorillo, A. R. (2010). Taphonomy and paleoecology of a bonebed from the Prince Creek Formation, North Slope, Alaska. Palaios, *25*(5), 299-317.

Gates, T. A. (2005). The Late Jurassic Cleveland-Lloyd dinosaur quarry as a drought-induced assemblage. *Palaios*, *20*(4), 363-375.

Gates, T. A., Sampson, S. D., De Jesús, C. R. D., Zanno, L. E., Eberth, D., Hernandez-Rivera, R., Martinez, M. C. A., & Kirkland, J. I. (2007). *Velafrons coahuilensis*, a new lambeosaurine hadrosaurid (Dinosauria: Ornithopoda) from the late Campanian Cerro del Pueblo Formation, Coahuila, Mexico. *Journal of Vertebrate Paleontology*, *27*(4), 917-930.

Godefroit, P., Bolotsky, Y., & Alifanov, V. (2003). A remarkable hollow-crested hadrosaur from Russia: an Asian origin for lambeosaurines. *Comptes Rendus Palevol*, *2*(2), 143-151.

Godefroit, P., Bolotsky, Y. L., & Van Itterbeeck, J. (2004). The lambeosaurine dinosaur *Amurosaurus riabinini*, from the Maastrichtian of Far Eastern Russia. *Acta Palaeontologica Polonica*, *49*(4).

Godefroit, P., Shulin, H., Tingxiang, Y., & Lauters, P. (2008). New hadrosaurid dinosaurs from the uppermost Cretaceous of northeastern China. *Acta Palaeontologica Polonica*, *53*(1), 47-74.

Gordon, J. (2000). Stratigraphy and sedimentology of the Foremost Formation in southeastern Alberta and southwestern Saskatchewan. (Master's thesis, University of Regina).

Griebeler, E. M., Klein, N., & Sander, P. M. (2013). Aging, maturation and growth of sauropodomorph dinosaurs as deduced from growth curves using long bone histological data: an assessment of methodological constraints and solutions. *PLoS ONE*, *8*(6), e67012.

Griesser, M., Ma, Q., Webber, S., Bowgen, K., & Sumpter, D. J. (2011). Understanding animal group-size distributions. *PLoS ONE*, *6*(8), e23438.

Griffith, S. J., Thompson, C. E. L., Thompson, T. J. U., & Gowland, R. L. (2016). Experimental abrasion of water submerged bone: the influence of bombardment by different sediment classes on microabrasion rate. *Journal of archaeological science: reports*, *10*, 15-29.

Gupte, P. R., Koffijberg, K., Müskens, G. J., Wikelski, M., & Kölzsch, A. (2019). Family size dynamics in wintering geese. *Journal of Ornithology*, *160*, 363-375.

Hamblin, A. P. (1997). Stratigraphic architecture of the Oldman Formation, Belly River Group, surface and subsurface of southern Alberta. *Bulletin of Canadian Petroleum Geology*, *45*(2), 155-177.

Haynes, G. (1983). Frequencies of spiral and green-bone fractures on ungulate limb bones in modern surface assemblages. *American Antiquity*, *48*(1), 102-114.

Holland, B., Bell, P. R., Fanti, F., Hamilton, S. M., Larson, D. W., Sissons, R., Sullivan, C., Vavrek, M. J., Wang, Y., & Campione, N. E. (2021). Taphonomy and taxonomy of a

juvenile lambeosaurine (Ornithischia: Hadrosauridae) bonebed from the late Campanian Wapiti Formation of northwestern Alberta, Canada. *PeerJ*, *9*, e11290.

Hone, D. W., Farke, A. A., Watabe, M., Shigeru, S., & Tsogtbaatar, K. (2014a). A new mass mortality of juvenile *Protoceratops* and size-segregated aggregation behaviour in juvenile non-avian dinosaurs. *PLoS ONE*, *9*(11), e113306.

Hone, D. W., & Rauhut, O. W. (2010). Feeding behaviour and bone utilization by theropod dinosaurs. *Lethaia*, *43*(2), 232-244.

Hone, D. W., Sullivan, C., Zhao, Q., Wang, K., & Xu, X. (2014b). Body size distribution in a death assemblage of a colossal hadrosaurid from the Upper Cretaceous of Zhucheng, Shandong Province, China. In D. A. Eberth & D. C. Evans (Eds.), *Hadrosaurs* (pp. 524-531). Indiana University Press.

Hone, D. W., & Watabe, M. (2010). New information on scavenging and selective feeding behaviour of tyrannosaurids. *Acta Palaeontologica Polonica*, *55*(4), 627-634.

Horner, J. R. (1994). Comparative taphonomy of some dinosaur and extant bird colonial nesting grounds. In K. Carpenter, K. F. Hirsch, & J. R. Horner (Eds.), *Dinosaur eggs and babies* (pp. 116-123). Cambridge University Press.

Horner, J. R. (1999). Egg clutches and embryos of two hadrosaurian dinosaurs. *Journal of Vertebrate Paleontology*, *19*(4), 607-611.

Horner, J. R., & Currie, P. J. (1994). Embryonic and neonatal morphology and ontogeny of a new species of *Hypacrosaurus* (Ornithischia, Lambeosauridae) from Montana and Alberta. In K. Carpenter, K. F. Hirsch, & J. R. Horner (Eds.), *Dinosaur eggs and babies* (pp. 312-336). Cambridge University Press.

Horner, J. R., de Ricqlès, A., & Padian, K. (1999). Variation in dinosaur skeletochronology indicators: implications for age assessment and physiology. *Paleobiology*, *25*(3), 295-304.

Horner, J. R., De Ricqlès, A., & Padian, K. (2000). Long bone histology of the hadrosaurid dinosaur *Maiasaura peeblesorum*: growth dynamics and physiology based on an ontogenetic series of skeletal elements. *Journal of Vertebrate Paleontology*, *20*(1), 115-129.

Horner, J. R., & Makela, R. (1979). Nest of juveniles provides evidence of family structure among dinosaurs. *Nature*, *282*(5736), 296-298.

Horner, J. R., & Weishampel, D. B. (1988). A comparative embryological study of two ornithischian dinosaurs. *Nature*, *332*(6161), 256-257.

Jerzykiewicz, T., Currie, P. J., Eberth, D. A., Johnston, P. A., Koster, E. H., & Zheng, J. J. (1993). Djadokhta Formation correlative strata in Chinese Inner Mongolia: an overview of the stratigraphy, sedimentary geology, and paleontology and comparisons with the type locality in the pre-Altai Gobi. *Canadian Journal of Earth Sciences*, *30*(10), 2180-2195.

Joubarne, T., Therrien, F., & Zelenitsky, D. K. (2022). Integumentary impressions on hadrosaurid specimens from the Upper Cretaceous (upper Campanian) Dinosaur Park Formation, Alberta, Canada: implications for integument patterns and hand morphology. *Journal of Vertebrate Paleontology*, *42*(6), e2213287.

Karr, L. P., & Outram, A. K. (2012). Tracking changes in bone fracture morphology over time: environment, taphonomy, and the archaeological record. *Journal of Archaeological Science*, *39*(2), 555-559.

LaRock, J. W. (2000). Sedimentology and taphonomy of a dinosaur bonebed from the Upper Cretaceous (Campanian) Judith River Formation of north central Montana (Master's thesis, Montana State University).

Lauters, P., Bolotsky, Y. L., Van Itterbeeck, J., & Godefroit, P. (2008). Taphonomy and age profile of a latest Cretaceous dinosaur bone bed in far eastern Russia. *Palaios*, *23*(3), 153-162.

Leckie, D., Fox, C., & Tarnocai, C. (1989). Multiple paleosols of the late Albian Boulder Creek Formation, British Columbia, Canada. *Sedimentology*, *36*(2), 307-323.

Libke, C., Bell, P. R., Somers, C. M., & McKellar, R. C. (2022). New scale type from a small-bodied hadrosaur in the Frenchman Formation of southern Saskatchewan: Potential implications for integumentary diversity in *Edmontosaurus annectens*. *Cretaceous Research*, *136*, 105215.

Lorenz, J. C. (1981). Sedimentary and tectonic history of the Two Medicine Formation, late Cretaceous (Campanian), northwestern Montana. (PhD thesis, Princeton University).

Lyman, R. L. (1994). Vertebrate Taphonomy. Cambridge University Press. 550 p.

Mallon, J. C., Evans, D. C., Ryan, M. J., & Anderson, J. S. (2012). Megaherbivorous dinosaur turnover in the Dinosaur Park formation (upper Campanian) of Alberta, Canada. *Palaeogeography, Palaeoclimatology, Palaeoecology*, *350*, 124-138.

Munsell Color. (2000). Munsell Soil Color Charts (Year 2000 Revised Washable Edition). New Windsor, New York, GratgMacbeth.

Myers, T. S., & Fiorillo, A. R. (2009). Evidence for gregarious behavior and age segregation in sauropod dinosaurs. *Palaeogeography, Palaeoclimatology, Palaeoecology*, *274*(1-2), 96-104.

Myers, T. S., & Storrs, G. W. (2007). Taphonomy of the Mother's Day Quarry, Upper Jurassic Morrison Formation, south-central Montana, USA. *Palaios*, *22*(6), 651-666.

Myers, T. P., Voorhies, M. R., & Corner, R. G. (1980). Spiral fractures and bone pseudotools at paleontological sites. *American Antiquity*, *45*(3), 483-490.

Ogunyomi, O., & Hills, L. V. (1977). Depositional environments, Foremost Formation (Late Cretaceous), Milk River area, southern Alberta. *Bulletin of Canadian Petroleum Geology*, *25*(5), 929-968.

Parks, W. A. (1922). *Parasaurolophus walkeri*: a new genus and species of crested trachodont dinosaur. *Toronto The University Library*, 13, 1-32.

Pereda-Suberbiola, X., Canudo, J. I., Cruzado-Caballero, P., Barco, J. L., López-Martínez, N., Oms, O., & Ruiz-Omenaca, J. I. (2009). The last hadrosaurid dinosaurs of Europe: a new lambeosaurine from the uppermost Cretaceous of Arén (Huesca, Spain). *Comptes Rendus Palevol*, *8*(6), 559-572.

Pol, D., Mancuso, A. C., Smith, R. M., Marsicano, C. A., Ramezani, J., Cerda, I. A., Otero, A., & Fernandez, V. (2021). Earliest evidence of herd-living and age segregation amongst dinosaurs. *Scientific Reports*, *11*(1), 1-9.

Qi, Z., Barrett, P. M., & Eberth, D. A. (2007). Social behaviour and mass mortality in the basal ceratopsian dinosaur *Psittacosaurus* (Early Cretaceous, People's Republic of China). *Palaeontology*, *50*(5), 1023-1029.

Ramezani, J., Beveridge, T. L., Rogers, R. R., Eberth, D. A., & Roberts, E. M. (2022). Calibrating the zenith of dinosaur diversity in the Campanian of the Western Interior Basin by CA-ID-TIMS U–Pb geochronology. *Scientific Reports*, *12*(1), 16026.

Retallack, G. J. (2019). Soils of the Past: An Introduction to Paleopedology [Third Edition]. Wiley Blackwell, 534 p.

Rice, D. D. (1980). Coastal and deltaic sedimentation of Upper Cretaceous Eagle Sandstone: relation to shallow gas accumulations, north-central Montana. *AAPG Bulletin, 64*(3), 316-338.

Rogers, R. R. (1990). Taphonomy of three dinosaur bone beds in the Upper Cretaceous Two Medicine Formation of northwestern Montana: evidence for drought-related mortality. *Palaios*, *5*(5), 394-413.

Rogers, R. R. (1998). Sequence analysis of the Upper Cretaceous Two Medicine and Judith River formations, Montana; nonmarine response to the Claggett and Bearpaw marine cycles. *Journal of Sedimentary Research*, *68*(4), 615-631.

Rosenau, N. A., Tabor, N. J., Elrick, S. D., & Nelson, W. J. (2013). Polygenetic history of paleosols in middle–upper Pennsylvanian cyclothems of the Illinois basin, USA: Part I. Characterization of paleosol types and interpretation of pedogenic processes. *Journal of Sedimentary Research*, *83*(8), 606-636.

Ryan, M. J. & Evans, D. C. (2005). Ornithischian dinosaurs. In P. J. Currie & E. B. Koppelhus (Eds.), *Dinosaur Provincial Park: A Spectacular Ancient Ecosystem Revealed* (pp. 312-348). Indiana University Press.

Ryan, M. J., Russell, A. P., Eberth, D. A., & Currie, P. J. (2001). The taphonomy of a *Centrosaurus* (Ornithischia: Certopsidae) bone bed from the Dinosaur Park Formation (Upper Campanian), Alberta, Canada, with comments on cranial ontogeny. *Palaios*, *16*(5), 482-506.

Sander, P. M. (1992). The Norian *Plateosaurus* bonebeds of central Europe and their taphonomy. *Palaeogeography, Palaeoclimatology, Palaeoecology*, *93*(3-4), 255-299.

Scherzer, B. A., & Varricchio, D. J. (2010). Taphonomy of a juvenile lambeosaurine bonebed from the Two Medicine Formation (Campanian) of Montana, United States. *Palaios*, *25*(12), 780-795.

Schmitt, J. G., Jackson, F. D., & Hanna, R. R. (2014). Debris flow origin of an unusual Late Cretaceous hadrosaur bonebed in the Two Medicine Formation of Western Montana. In D. A. Eberth & D. C. Evans (Eds.), *Hadrosaurs* (pp. 486-501). Indiana University Press.

Scott, E. E., Chiba, K., Fanti, F., Saylor, B. Z., Evans, D. C., & Ryan, M. J. (2022a). Taphonomy of a monodominant *Gryposaurus* sp. bonebed from the Oldman Formation (Campanian) of Alberta, Canada. *Canadian Journal of Earth Sciences*, *59*(6), 389-405.

Scott, S. H., Ryan, M. J., & Evans, D. C. (2022b). Postcranial description of *Wendiceratops pinhornensis* and a taphonomic analysis of the oldest monodominant ceratopsid bonebed. *The Anatomical Record*, *306*(7), 1824-1841.

Snyder, K., McLain, M., Wood, J., & Chadwick, A. (2020). Over 13,000 elements from a single bonebed help elucidate disarticulation and transport of an *Edmontosaurus* thanatocoenosis. *PLoS ONE*, *15*(5), e0233182.

Sprecher, S. W. (2001). Basic concepts of soil science. In J. L. Richardson & M. J. Vepraskas (Eds.), *Wetland soils: genesis, hydrology, landscapes, and classification* (pp. 3-18). Lewis Publishers.

Storrs, G. W., Oser, S. E., & Aull, M. (2012). Further analysis of a Late Jurassic dinosaur bone-bed from the Morrison Formation of Montana, USA, with a computed three-dimensional

reconstruction. *Earth and Environmental Science Transactions of the Royal Society of Edinburgh*, *103*(3-4), 443-458.

Stredulinsky, E. H., Darimont, C. T., Barrett-Lennard, L., Ellis, G. M., & Ford, J. K. (2021). Family feud: permanent group splitting in a highly philopatric mammal, the killer whale (Orcinus orca). *Behavioral Ecology and Sociobiology*, *75*, 1-17.

Sueur, C., & Maire, A. (2014). Modelling animal group fission using social network dynamics. *PLoS ONE*, *9*(5), e97813.

Therrien, F., & Fastovsky, D. E. (2000). Paleoenvironments of early theropods, Chinle Formation (Late Triassic), Petrified Forest National Park, Arizona. *Palaios*, *15*(3), 194-211.

Therrien, F., Zelenitsky, D. K., Quinney, A., & Tanaka, K. (2015). Dinosaur trackways from the Upper Cretaceous Oldman and Dinosaur Park formations (Belly River Group) of southern Alberta, Canada, reveal novel ichnofossil preservation style. *Canadian Journal of Earth Sciences*, *52*(8), 630-641.

Therrien, F., Zelenitsky, D. K., Tanaka, K., Sloboda, W. J. (2014). First hadrosaur trackway from the Upper Cretaceous (late Campanian) Oldman Formation, southeastern Alberta. In D. A. Eberth & D. C. Evans (Eds.), *Hadrosaurs* (pp. 532-539). Indiana University Press.

Therrien, F., Zelenitsky, D. K., & Weishampel, D. B. (2009). Palaeoenvironmental reconstruction of the Late Cretaceous Sânpetru Formation (Haţeg Basin, Romania) using paleosols and implications for the “disappearance” of dinosaurs. *Palaeogeography, Palaeoclimatology, Palaeoecology*, *272*(1-2), 37-52.

Thompson, C. E., Ball, S., Thompson, T. J., & Gowland, R. (2011). The abrasion of modern and archaeological bones by mobile sediments: the importance of transport modes. *Journal of Archaeological Science*, *38*(4), 784-793.

Thompson, M. G., Bedek, F. V., Schröder-Adams, C., Evans, D. C., & Ryan, M. J. (2021). The oldest occurrence of brachylophosaurin hadrosaurids in Canada. *Canadian Journal of Earth Sciences*, *58*(10), 993-1004.

Thompson, M. G., Ryan, M. J., & Schröder-Adams, C. J. (2020). The first record of the hadrosaur *Probrachylophosaurus* in the Foremost Formation, representing the oldest occurrence of a brachylophosaurin in Alberta. In A. M. Murray, V. Arbour, & R. Holmes (Eds.), *CSVP Abstracts 2020: 8th annual meeting - fossilized* (pp. 58-59).

Trexler, D. (2001). Two Medicine Formation, Montana: geology and fauna. In D. H. Tanke & K. Carpenter (Eds.), *Mesozoic Vertebrate Life*, (pp. 298-309). Indiana University Press.

Ullmann, P. V., Shaw, A., Nellermoe, R., & Lacovara, K. J. (2017). Taphonomy of the Standing Rock Hadrosaur Site, Corson County, South Dakota. *Palaios*, *32*(12), 779-796.

Varricchio, D. (1993). Montana climatic changes associated with the Cretaceous Claggett and Bearpaw transgressions. Montana Geological Society, 1993 Field Conference Guidebook.

Varricchio, D. J. (1995). Taphonomy of Jack's Birthday Site, a diverse dinosaur bonebed from the Upper Cretaceous Two Medicine Formation of Montana. *Palaeogeography, Palaeoclimatology, Palaeoecology*, *114*(2-4), 297-323.

Varricchio, D. J., & Horner, J. R. (1993). Hadrosaurid and lambeosaurid bone beds from the Upper Cretaceous Two Medicine Formation of Montana: taphonomic and biologic implications. *Canadian Journal of Earth Sciences, 30*(5), 997-1006.

Vepraskas, M. J. (2001). Morphological features of seasonally reduced soils. In J. L. Richardson & M. J. Vepraskas (Eds.), *Wetland soils: genesis, hydrology, landscapes, and classification* (pp. 163-182). Lewis Publishers.

Vepraskas, M. J., & Sprecher, S. W. (1997). Overview of aquic conditions and hydric soils. *Aquic conditions and hydric soils: The problem soils*, *50*, 1-22.

Voorhies, M. R. (1969). Taphonomy and population dynamics of an early Pliocene vertebrate fauna, Knox County, Nebraska. University of Wyoming Contributions to Geology, Special Paper 1, 1-69.

Wosik, M., & Evans, D. C. (2022). Osteohistological and taphonomic life-history assessment of *Edmontosaurus annectens* (Ornithischia: Hadrosauridae) from the Late Cretaceous (Maastrichtian) Ruth Mason dinosaur quarry, South Dakota, United States, with implication for ontogenetic segregation between juvenile and adult hadrosaurids. *Journal of Anatomy*, *241*(2), 272-296.

Young, C. C. (1958). The dinosaurian remains of Laiyang, Shantung. *Palaeontologia Sinica, New Series C, Whole Number 42*(16), 1-138.

APPENDIX A: TAPHONOMIC DATA FOR THE DEVIL'S COULEE JUVENILE HADROSAUR BONEBED (JBB)

Specimen number	Fossil ID	Side	W	A	Other marks	Notes
TMP 1988.151.80	Scapula	L	0	0	Wet rot	
TMP 1988.151.94	Scapula	L	0	0	Wet rot	
TMP 1988.151.92	Tibia	L	0	1	Wet rot	
TMP 1988.151.6	Tibia	R	0	0	Wet rot	
TMP 1989.151.149	Fibula	R	0	0	Wet rot	
TMP 1988.151.23	Fibula	L	0	0	Wet rot	
TMP 1988.151.81	Fibula	L	0	1	Wet rot	
TMP 1988.151.4	Fibula	L	0	0	Wet rot	
TMP 1988.151.12	Fibula	L	0	0	Wet rot	
TMP 1988.151.45	Fibula	L	0	0	Wet rot	
TMP 1988.151.3	Humerus	R	0	1	Wet rot	
TMP 1988.151.20	Humerus	R	0	0	Wet rot, Tooth marks	
TMP 1989.151.78	Humerus	L	0	0	Wet rot	
TMP 1988.151.9	Ulna	R	0	0	Wet rot, Tooth marks	
TMP 1988.151.95	Ulna	L	0	0	Wet rot	
TMP 1988.151.119	Ulna	L	0	0	Wet rot	
TMP 1988.151.1	Radius	R	0	0	Wet rot	
TMP 1988.151.21	Radius	R	0	0	Wet rot	
TMP 1989.151.89	Radius	L	0	0	Wet rot	
TMP 1988.151.125	Radius	L	0	0	Wet rot	
TMP 1989.151.142	Radius	L	0	0	Wet rot	
TMP 1989.151.141	Radius	L	0	0	Wet rot	
TMP 1989.151.92	Radius	R	0	0	Wet rot	
TMP 1989.151.112	Radius	L	0	0	Wet rot	
TMP 1988.151.49	Radius	L	0	0	---	
TMP 1989.151.96	Ischium	R	0	0	---	
TMP 1989.151.33	Ischium	R	0	0	---	
TMP 1988.151.126	Ischium	R	0	0	---	
TMP 1988.151.135	Pubis	L	0	0	---	
TMP 1988.151.136	Ischium	R	0	0	---	
TMP 1988.151.150	Pubis	L	0	0	Wet rot	
TMP 1988.151.124	Ischium	L	0	0	Wet rot	

Specimen number	Fossil ID	Side	W	A	Other marks	Notes
TMP 1988.151.43	Ischium	?	0	0	---	
TMP 1988.151.37	Ilium	R	0	0	Wet rot	
TMP 1988.151.93	Ilium	L	0	0	---	
TMP 1988.151.74	Pubis	L	0	0	Wet rot	
TMP 1988.151.26	Pubis	R	0	0	Wet rot	
TMP 1988.151.88	Dentary + Teeth	L	0	0	Wet rot	
TMP 1988.151.75	Dentary	R	0	0	Wet rot	
TMP 1994.666.80	Maxilla	R	0	0	---	
TMP 1988.151.5	Dentary	L	0	0	Wet rot	
TMP 1988.151.5	Dentary	R	0	0	Wet rot	
TMP 1988.151.120	Dentary	L	0	0	---	
TMP 1988.151.116	Dentary Coronoid Process	R	0	0	---	
TMP 1988.151.86	Angular	R	0	0	---	
TMP 1988.151.84	Maxilla + Fragm.	L	0	0	---	
TMP 1988.151.85	Predentary	---	0	0	---	
TMP 1988.151.53	Quadrate	R	0	0	---	
TMP 1988.151.56	Dentary Coronoid Process	R	0	0	---	
TMP 1988.151.101	Squamosal	L	0	0	---	
TMP 1989.151.59	Squamosal	L	0	0	---	
TMP 1988.151.183	Hadrosaur Tooth	---	---	---	---	
TMP 1989.151.25	Hadrosaur Teeth	---	---	---	---	
TMP 1989.151.69	Hadrosaur Tooth	---	---	---	---	
TMP 1988.151.159	Hadrosaur Teeth fragments	---	---	---	---	
TMP 1988.151.46	Hadrosaur Tooth	---	---	---	---	
TMP 1988.151.100	Hadrosaur Teeth	---	---	---	---	
TMP 1989.151.41	Hadrosaur Teeth	---	---	---	---	
TMP 1988.151.27	Hadrosaur Tooth	---	---	---	---	
TMP 1988.151.76	Rib	L	0	0	Wet rot	
TMP 1988.151.31	Rib	L	1	0	Wet rot	
TMP 1989.151.132	Rib	L	0	0	---	
TMP 1989.151.113	Rib	L	0	0	---	
TMP 1988.151.118	Rib	R	0	0	---	

Specimen number	Fossil ID	Side	W	A	Other marks	Notes
TMP 1989.151.98	Rib	R	0	0	---	
TMP 1988.151.128	Rib	R	2	0		
TMP 1989.151.87	Rib	L	0	0		
TMP 1988.151.98	Metacarpal II	R	2	0		
TMP 1988.151.185	Rib	R	0	0		
TMP 1988.151.127	Rib	?	0	0		
TMP 1988.151.122	Rib	L	0	0		
TMP 1988.151.129	Rib	?	0	0		
TMP 1988.151.169	Rib	R	0	0		
TMP 1988.151.131	Rib	R	0	0		
TMP 1988.151.71	Rib	L	1	0		
TMP 1988.151.151	Rib	R	0	0		
TMP 1988.151.138	Rib	?	0	0		
TMP 1988.151.61	Tendons	?	0	0		
TMP 1988.151.145	Tendons	?	0	0		
TMP 1988.151.153	Tendons	?	0	0		
TMP 1988.151.143	Rib	?	0	0		
TMP 1988.151.177	Rib?	?	0	0		
TMP 1989.151.158	Dentary	L	0	0		
TMP 1988.151.18	Metatarsal III	R	0	0		
TMP 1988.151.175	Cervical Vertebra	---	3	2		
TMP 1988.151.147	Zygapophysis	---	0	0		
TMP 1988.151.148	Zygapophysis	---	0	0		
TMP 1988.151.60	Prezygapophysis	---	0	0		
TMP 1988.151.132	Skull fragments	?	0	0		
TMP 1988.151.167	Assorted Bone Fragments	?	2	1		
TMP 1988.151.164	Neural Spine	---	0	0		
TMP 1988.151.152	Zygapophysis	---	0	0		
TMP 1988.151.123	Zygapophysis	---	0	1		
TMP 1988.151.181	Caudal Vertebra	---	0	0		
TMP 1988.151.41	Zygapophysis	---	0	0		
TMP 1989.151.156	Caudal Vertebra	---	0	0		

Specimen number	Fossil ID	Side	W	A	Other marks	Notes
TMP 1988.151.64	Caudal Vertebra	---	0	1		
TMP 1988.151.62	Caudal Vertebra	---	0	0		
TMP 1988.151.72	Caudal Vertebra	---	0	1		
TMP 1989.151.39	Caudal Vertebra	---	0	1-2		
TMP 1989.151.145	Caudal Vertebra	---	0	0		
TMP 1989.151.77	Caudal Vertebra	---	0	1		
TMP 1988.151.36	Caudal Vertebra	---	0	1		
TMP 1993.76.1	Manual Phalanx (V-3)	R	3	0		
TMP 1988.151.2	Metatarsal III	R	0	1		
TMP 1989.151.38	Manual Phalanx (V-3)	L	0	0		
TMP 1989.151.1	Pedal Ungual (Pedal Phalanx II-3)	R	0	0		
TMP 1988.151.24	Pedal Ungual (Pedal Phalanx IV-5)	L	0	0		
TMP 1988.151.34	Pedal Ungual (Pedal Phalanx III-4)	R	0	0		
TMP 1989.151.136	Manual Ungual (Manual Phalanx III-3)	L	0	0		
TMP 1989.151.4	Manual Ungual (Manual Phalanx III-3)	R	0	0		
TMP 1988.151.14	Manual Ungual (Manual Phalanx II-3)	R	0	0		
TMP 1993.76.15	Manual Phalanx (IV-1)	R	0	0		
TMP 1989.151.37	Manual Phalanx (II-1)	R	0	0		
TMP 1988.151.83	Manual Phalanx (V-2)	R	2	0		
TMP 1989.151.150	Pedal Phalanx (III-1)	R	0	1		
TMP 1989.151.9	Pedal Phalanx (III-3)	L	0	1		
TMP 1988.151.25	Pedal Phalanx (II-2)	R	0	0		
TMP 1989.151.152	Manual Phalanax (II-1)	R	0	0		
TMP 1989.151.10	Pedal phalanx (III-2)	R	0	0		
TMP 1989.151.155	Metacarpal V	L	0	0		
TMP 1988.151.19	Pedal Phalanx (IV-3)	L	0	1		
TMP 1988.151.78	Pedal Phalanx (II-1)	L	0	0		
TMP 1988.151.82	Manual Phalanx (IV-1)	R	0	0		
TMP 1988.151.96	Pedal Phalanx (II-1)	R	2	2		

Specimen number	Fossil ID	Side	W	A	Other marks	Notes
TMP 1988.151.98	Metacarpal V	L	0	1		
TMP 1988.151.55	Caudal Vertebra	---	0	0		
TMP 1989.151.67	Vertebra	---	0	0		
TMP 1989.151.79	Vertebra	---	2	1		
TMP 1989.151.97	Vertebra	---	0	0		
TMP 1988.151.13	Thoracic Vertebra	---	0	1		
TMP 1988.151.70	Neural Spine (Caudal)	---	0	0		
TMP 1989.151.42	Caudal Vertebra	---	0	1		
TMP 1988.151.186	Caudal Vertebra	---	0	1		
TMP 1989.151.139	Dorsal Vertebra	---	0	0		
TMP 1988.151.97	Vertebra + Zygapophysis	---	0	2		
TMP 1988.151.69	Thoracic Vertebra	---	0	1		
TMP 1988.151.90	Neural Spine	---	0	0		
TMP 1988.151.182	Caudal Vertebra	---	0	0		
TMP 1988.151.121	Zygapophysis	---	0	0		
TMP 1988.151.112	Vertebra	---	2	2		
TMP 1988.151.133	Zygapophysis	---	0	0		
TMP 1988.151.117	Vertebra	---	0	0		
TMP 1989.151.54	Atlas Neural Arch	---	0	0		
TMP 1988.151.11	Vertebra	---	0	0		
TMP 1988.151.87	Neural Arch + Neural Spine	---	0	1		
TMP 1988.151.59	Caudal Vertebra	---	0	0		
TMP 1988.151.16	Thoracic Vertebra	---	0	1		
TMP 1988.151.15	Caudal Vertebra	---	0	0		
TMP 1988.151.51	Caudal Vertebra	---	0	2		
TMP 1988.151.114	Neural Spine	---	0	0	Wet rot	
TMP 1988.151.178	Neural Arch Fragments	---	0	1		
TMP 1988.151.180	Vertebra	---	0	2		
TMP 1988.151.22	Sacral Vertebra	---	0	2		
TMP 1989.151.124	Caudal Vertebra	---	0	0		
TMP 1988.151.58	Caudal Vertebra	---	0	0		
TMP 1988.151.32	Caudal Vertebra	---	0	2		

Specimen number	Fossil ID	Side	W	A	Other marks	Notes
TMP 1988.151.8	Neural Arch + Spine Fragments	---	0	0	Wet rot	
TMP 1988.151.54	Caudal Vertebra	---	0	0		
TMP 1988.151.17	Sacral Vertebra	---	0	0		
TMP 1988.151.77	Cervical Vertebra	---	0	0		
TMP 1989.151.151	Vertebra	---	0	0		
TMP 1988.151.168	Skull Bone Fragments	?	0	0		
TMP 1988.151.134	Exoccipital	L	0	1		
TMP 1988.151.42	Quadratojugal	?	0	0		
TMP 1988.151.165	Parietal	R	0	0		
TMP 1989.151.115	Scapula	R	0	0		
TMP 1988.151.0003	Humerus Fragments (condyle)	?	0	0		
TMP 1988.151.0065	Humerus	R	0	0		
TMP 1988.151.0115	Tibia	L	0	0		
TMP 1988.151.0093	Metatarsal II	R	0	0		
TMP 1988.151.0007	Femur	R	0	0	Wet rot	
TMP 1988.151.174	Frontal	?	0	0		
TMP 1988.151.149	Skull Fragments	?	0	0		
TMP 1988.151.111	Hadrosauridae Egg Shell	---	---	---		
TMP 1989.151.55	Ischium	R	0	0	Wet rot, Root etchings	
TMP 1989.151.56	Neural Arch + Neural Spine	---	0	0	Wet rot	
TMP 1989.151.121	Humerus	R	0	0	Wet rot	
TMP 1989.151.46	Neural Spine	R	0	0	---	
TMP 1989.151.46	Haemal Arch (Chevron)	---	0	0	---	
TMP 1989.151.102	Rib	R	0	0	---	
TMP 1989.151.74	Rib	R	0	0	Wet rot	
TMP 1989.151.122	Rib	R	0	0	---	
TMP 1989.151.53	Caudal Vertebra	---	0	0	---	
TMP 1989.151.49	Caudal Vertebra	---	0	1	---	
TMP 1989.151.45	Vertebra	---	0	0	---	
TMP 1989.151.57	Caudal Vertebra	---	0	1	---	
TMP 1989.151.48	Radius	L	0	0	Wet rot	
TMP 1989.151.100	Rib	R	1	0	Wet rot	

Specimen number	Fossil ID	Side	W	A	Other marks	Notes
TMP 1989.151.61	Neural Arch + Spine	---	0	0	---	
TMP 1989.151.35	Transverse Process	---	0	0	---	
TMP 1989.151.36	Transverse Process	---	0	0	---	
TMP 1989.151.58	Neural Arch	---	0	0	Wet rot	
TMP 1989.151.99	Neural Arch + Spine	---	0	0	Wet rot	
TMP 1989.151.43	Maxilla	L	0	0	---	
TMP 1989.151.51	Ulna	L	0	0	---	
TMP 1989.151.60	Metatarsal IV	L	0	0	Wet rot	
TMP 1989.151.154	Rib	R	0	0	---	
TMP 1989.151.144	Neural Arch	---	0	0	---	
TMP 1989.151.120	Sacral Rib (?)	?	?	?	---	
TMP 1989.151.106	Postorbital	L	0	0	---	
TMP 1989.151.90	Transverse Process	---	0	0	---	
TMP 1989.151.63	Metacarpal III	R	0	0	---	
TMP 1989.151.83	Metatarsal IV	R?	0	0	Wet rot	
TMP 1989.151.86	Sternal Plate	R	0	0	---	
TMP 1989.151.91	Rib	L	1	0	---	
TMP 1989.151.131	Rib	R	0	0	---	
TMP 1989.151.153	Neural Arch Fragment	---	0	0	---	Fragm.
TMP 1989.151.94	Cervical Vertebra	---	?	?	---	
TMP 1989.151.143	Skull Bone Fragment	?	3	0	---	
TMP 1989.151.104	Caudal Vertebra	---	0	0	---	
TMP 1989.151.108	Dorsal Vertebra	---	0	0	---	
TMP 1989.151.76	Vertebra	---	0	1	---	
TMP 1989.151.70	Rib	L	1	0	---	Fragm.
TMP 1989.151.73	Neural Arch	---	0	0	---	
TMP 1989.151.118	Cervical Zygapophysis	---	0	0	---	
TMP 1989.151.75	Cervical Rib	?	0	0	---	
TMP 1989.151.64	Vertebra	---	?	?	---	
TMP 1989.151.81	Rib	?	?	?	---	
TMP 1989.151.71	Skull Element	?	0	0	---	
TMP 1989.151.88	Caudal Vertebra	---	0	0	---	

Specimen number	Fossil ID	Side	W	A	Other marks	Notes
TMP 1989.151.107	Rib	R	0	0	---	
TMP 1989.151.101	Rib	?	1	0	---	Fragm.
TMP 2022.014.1	Ischium	?	0	0	---	Fragm.
TMP 2022.014.2	Rib	?	0	0	---	Fragm.
TMP 1989.151.50	Hadrosaur Tooth	---	---	---	---	
TMP 1989.151.146	Tyrannosauridae Tooth	---	---	---	---	
TMP 1989.151.82	Crocodylidae Scute (Osteoderm)	---	0	0	---	
TMP 1989.151.148	Astragalus	R	2?	0	---	
TMP 1988.151.5	Maxilla	R	0	0	---	
TMP 1988.151.139	Fish Scales	---	---	---	---	
TMP 1988.151.47	Ankylosaur Scute	---	3?	2?	---	
TMP 1988.151.40	Tyrannosauridae Tooth	---	---	---	---	
TMP 1989.151.7	Tyrannosauridae Tooth	---	---	---	---	
TMP 1988.151.28	Ankylosauridae Tooth	---	---	---	---	
TMP 1989.151.15	Crocodile Scute	---	0	0	---	
TMP 1988.151.35	Theropod Tooth	---	---	---	---	
TMP 1989.151.5	Crocodile Vertebra	---	0	1	---	
TMP 1988.151.137	Tyrannosauridae Phalanx	?	0	1	---	
TMP 1989.151.3	Tyrannosauridae Tooth	---	---	---	---	
TMP 1989.151.6	Tyrannosauridae Phalanx	?	0	0	---	
TMP 1988.151.113	Theropod Caudal Vertebra	---	0	1	---	
TMP 1989.151.12	Turtle Shell	---	0	0	---	
TMP 1988.151.102	Tyrannosauridae Tooth	---	---	---	---	
TMP 1988.151.109	Osteichthyes Jaw. Tooth	---	---	---	---	
TMP 1989.151.16	Dermal Ossicle (Ankylo. Osteoderm)	---	0	0	---	
TMP 1989.151.22	Turtle (Trionychidae) Phalanx	?	0	0	---	
TMP 1988.151.176	Champsosaur Bone (unidentified)	?	0	2	---	
TMP 1988.151.161	Crocodylidae Scute	---	0	1?	---	
TMP 1988.151.146	Lepisosteus Scale	---	---	---	---	
TMP 1988.151.173	Amphibia Neural Arch	---	0	0	---	
TMP 1988.151.172	Champsosaurus Neural Arch	---	0	2	---	

Specimen number	Fossil ID	Side	W	A	Other marks	Notes
TMP 1988.151.156	Theropod Tooth	---	---	---	---	
TMP 1988.151.144	Crocodylidae Tooth	---	---	---	---	
TMP 1988.151.163	Vertebrata Tooth	---	---	---	---	
TMP 1988.151.157	Saurornitholestes Tooth	---	---	---	---	
TMP 1988.151.160	Ankylosaur Tooth	---	---	---	---	
TMP 1988.151.141	Ankylosaur Tooth	---	---	---	---	
TMP 1988.151.158	Crocodylidae Tooth	---	---	---	---	
TMP 1988.151.155	Vertebrate Scale	---	---	---	---	
TMP 1993.77.1	Crocodylidae Vertebra	---	0?	2?	---	
TMP 1993.77.2	Lepisosteus Scale	---	---	---	---	
TMP 1988.151.140	Saurornitholestes Tooth	---	---	---	---	
TMP 1988.151.108	Champsosaurus Vertebra	---	0	2?	---	
TMP 1988.151.106	Crocodylidae Tooth	---	---	---	---	
TMP 1988.151.104	Lepisosteus Scale	---	---	---	---	
TMP 1988.151.110	Osteichthyes Rib	?	0	0	---	
TMP 1992.110.6	Tyrannosauridae Tooth	---	---	---	---	
TMP 1992.110.8	Archosaur Rib (?)	?	0	1?	---	
TMP 1993.77.3	Crocodylidae Tooth	---	---	---	---	
TMP 1989.151.17	Ankylosaur Tooth	---	---	---	---	
TMP 1989.151.18	Ankylosaur Tooth	---	---	---	---	
TMP 1989.151.21	Ankylosaur Tooth	---	---	---	---	
TMP 1989.151.19	Turtle Phalanx	?	0	0	---	
TMP 1988.151.130	Theropod Long Bone Fragment (unidentified)	?	0	0	---	
TMP 1989.151.159	Hadrosauridae Ilium	R	0	0	---	
TMP 1988.151.30	Tyrannosauridae Vertebral Element (Transverse Process)	---	2	0	---	
TMP 1988.151.35	Tyrannosauridae Tooth	---	---	---	---	
TMP 1988.151.38	Rib	R	0	0	---	
TMP 1988.151.105	Turtle (Chelydridae) Shell	---	0	1?	---	
TMP 1988.151.107	Ankylosaur Tooth	---	---	---	---	
TMP 1989.151.20	Osteichthyes Skull Element	?	0	0	---	

Specimen number	Fossil ID	Side	W	A	Other marks	Notes
TMP 1989.151.44	Osteichthyes Skull Element	?	0	0	---	
TMP 1988.151.142	Actinopterygii Scale	---	---	---	---	
TMP 1988.151.162	Chelydridae (Turtle) Shell (Peripheral)	---	1	0	---	
TMP 1988.151.170	Squamata (Lacertilia) Skull Bone Fragment	?	0	2	---	
TMP 1988.151.171	Squamata Ulna	?	0	0	---	
TMP 1989.151.110	Varanidae Tibia	?	0	0	---	
TMP 1988.151.187	Vertebrata - Mixed Bone Fragments	---	0	0	---	
TMP 1989.151.2	Lepisosteus Scale	---	---	---	---	
TMP 1989.151.8	Ornithomimid Pedal Ungual	?	0	0	---	
TMP 1989.151.11	Amiidae (Kindleia) Vertebra	---	0	0	---	
TMP 1989.151.13	Troodon Premaxillary Tooth	---	---	---	---	
TMP 1989.151.14	Ankylosaur Tooth	---	---	---	---	
TMP 1989.151.24	Plant (Anthophyta) Seed	---	---	---	---	
TMP 1988.151.39	Plant - Amber	---	---	---	---	
TMP 1988.151.73	Plant - Amber	---	---	---	---	
TMP 1989.151.26	Gastropoda	---	---	---	---	
TMP 1989.151.27	Gastropoda	---	---	---	---	
TMP 1988.151.103	Gastropod Operculum	---	---	---	---	

APPENDIX B: TAPHONOMIC DATA FOR THE BLACKTAIL CREEK NORTH BONEBED

Bone	Side	Measurements (cm)	W	A	Notes
Humerus	L	Length 11.5, A-P Crest 2.9, Circumf. 5.5	0	0	
Humerus	R	Length 12.9, A-P Crest 3.5, Circumf. 5.8	0	0	
Humerus	R	Length 11.4, A-P Crest 2.8, Circumf. 5.2	0	0	
Humerus	R	Length 12.4, A-P Crest 3.2, Circumf. 5.3	0	0	
Humerus	R	Length 11.6, A-P Crest 3.2, Circumf. 5.5	0	0	
Humerus	R	Length 12.0, A-P Crest 3.1, Circumf. 5.1	0	0	
Humerus	R	Length 11.9, A-P Crest 2.8, Circumf. 5.2	0	0	
Humerus	R	Length 10.1, A-P Crest >2.1, Circumf. 4.6	0	0	
Humerus	L	Length >9.5, A-P Crest 3.1, Circumf. 4.9	0	0	
Humerus	L	Length 10.7, A-P Crest 2.8, Circumf. 4.7	0	0	
Humerus	R	Length 11.2, A-P Crest 2.8, Circumf. 5.0	0	0	
Humerus	L	Length 11.6, A-P Crest 3.0, Circumf. 5.2	0	0	
Humerus	L	Length 9.7, A-P Crest 2.4, Circumf. 4.4	0	0	
Humerus	L	Length 11.5, A-P Crest 3.1, Circumf. 5.4	0	0	
Humerus	L	Length 11.2, A-P Crest 3.1, Circumf. 5.1	0	0	
Humerus	L	Length 13.1, A-P Crest >3.2, Circumf. 5.7	0	0	
Humerus	L	Length >5.6, A-P Crest 2.3, Circumf. 4.1	0	0	
Humerus	L	Length >3.9, A-P Crest 3.2, Circumf. 5.2	0	0	
Humerus	L	Length >4.2	0	0	
Humerus	L?	---	0	0	
Humerus	R	Length >2.9	0	0	
Humerus	R	Length >7.2, Circumf. 4.8	0	0	
Humerus	R	Length >7.1, A-P Crest 2.7, Circumf. 4.7	0	0	
Humerus	R	Length >4.0	0	0	
Humerus	R?	Length >2.4	0	0	
Humerus	R	Length >3.8	0	0	
Humerus	R	Length >3.2, A-P Crest 2.5	2	0	
Humerus	R	Length >2.7	0	0	
Humerus	R	Length >3.8	0	0	
Humerus	L	Length 12.2, A-P Crest 3.1, Circumf. 5.2	0	0	
Humerus	L	Length 12.4, A-P Crest 3.3, Circumf. 5.7	?	?	
Ulna	L	Length 13.8, Cicumf. 4.4	0	0	

Bone	Side	Measurements (cm)	W	A	Notes
Ulna	L	Length 12.2, Circumf. 3.8	0	0	
Ulna	L	Length 11.6, Circumf. 3.4	0	0	
Ulna	L	Length 10.8, Circumf. 3.2	0	0	
Ulna	L	Length 12.5, Circumf. 3.9	0	0	
Ulna	R	Length 14.3, Circumf. 4.4	0	0	
Ulna	R	Length 13.5, Circumf. 4.3	0	0	
Ulna	R	Length >8.0, Circumf. 3.4	0	0	
Ulna	R	Length >10.6, Circumf. 3.2	0	0	
Ulna	R	Length >12.2, Circumf. 3.5	0	0	
Ulna	R	Length 12.6, Circumf. 3.9	0	0	
Ulna	R	Length 13.2, Circumf. around 4.0	0	0	
Ulna	R	Length >5.0, Circumf. max 4.0	0	0	
Ulna	L?	Length >2.7, Circumf. max 4.2	2	0	
Radius	R	Length 11.7, Circumf. 3.6	0	0	
Radius	R	Length 12.0, Circumf. around 3.5	0	0	
Radius	R	Length 12.2, Circumf. 3.4	0	0	
Radius	R	Length >9.7, Circumf. 3.5	0	0	
Radius	R	Length 9.8, Circumf. 2.9	0	0	
Radius	R	Length 11.1, Circumf. 2.8	0	0	
Radius	L	Length 12.7, Circumf. 3.4	0	0	
Radius	L	Length 10.9, Circumf. 3.4	0	0	
Radius	L	Length 9.4, Circumf. 2.6	0	0	
Radius	L	Length 13.0, Circumf. 3.8	0	0	
Bone fragment		Length >3.9, Circumf. 3.1	2	0	
Bone fragment		Length >4.3, Cirumf. 3.9	2	0	
Bone fragment		Length >1.9	3	0	
Bone fragment		Length >4.2, Circumf. 3.6	0	0	
Bone fragment		Length >4.4, Circumf. 3.9	2	0	
Bone fragment		Length >3.4, Circumf. 3.5	0	0	
Bone fragment		Length >3.0, Circumf. 3.3	3	0	
Bone fragment		Length >3.3, Circumf. max 3.6	2	0	
Bone fragment		Length >2.3, Circumf. 2.7	0	0	

Bone	Side	Measurements (cm)	W	A	Notes
Bone fragment		Length >2.0	2	0	
Bone fragment		Length >2.4	0	0	
Bone fragment		Length >1.3	0	0	
Bone fragment		Length >2.0	0	0	
Bone fragment		Length >1.9	0	0	
Bone fragment		Length >1.7	0	0	
Bone fragment		Length >1.6, Circumf. 3.0	0	0	
Bone fragment		Length >1.8	0	0	
Bone fragment		Length >1.6	0	0	
Metacarpal IV	R?	Length 4.4	0	0	
Metacarpal IV	L?	Length 4.2	0	0	
Metacarpal IV	R?	Length 5.9	0	0	
Metacarpal IV	R?	Length 6.2	0	0	
Metacarpal		Length 4.8	0	0	
Metacarpal		Length 4.5	0	0	
Metacarpal		Length 5.2	0	0	
Metacarpal		Length 5.9	0	0	
Metacarpal		Length >5.1	0	0	
Metacarpal		Length 5.0	0	0	
Metacarpal		Length 3.7	2	0	
Metacarpal V?		Length 1.8	0	0	
Metacarpal V?		Length 2.2	0	0	
Metacarpal V?		Length 2.2	0	0	
Metacarpal		Length 6.3	0	0	
Metacarpal		Length 4.2	0	0	
Metacarpal		Length 5.0	0	0	
Metacarpal		Length 4.7	0	0	
Metacarpal V?		Length 1.7	0	0	
Metacarpal IV	R?	Length 4.8	0	0	
Metacarpal		Length 4.2	0	0	
Metacarpal		Length 5.1	0	0	
Metacarpal		Length >4.9	0	0	

Bone	Side	Measurements (cm)	W	A	Notes
Metacarpal		Length >3.7	0	0	
Metacarpal II	R	Length 4.8	0	0	
Metacarpal III	R	Length 5.6	0	0	
Metacarpal IV	R	Length 5.3	0	0	
Metacarpal V	R	Length 2.0	0	0	
Manual Phalanx		Length 1.7	0	0	
Manual Phalanx		Length 1.0	0	0	
Manual Phalanx?		Length 3.1	0	0	
Manual Phalanx		Length 0.4	0	0	
Manual Phalanx Ungual		Length >1.1	0	0	
Manual Phalanx		Length 0.4	0	0	
Manual Phalanx		Length 0.5	0	0	
Manual Phalanx		Length 1.9	0	0	
Manual Phalanx		Length 1.3	0	0	
Manual Phalanx		Length 1.0	0	0	
Manual Phalanx		Length 1.5	0	0	
Manual Phalanx		Length 1.1	0	0	
Manual Phalanx Ungual		Length 0.9	0	0	
Manual Phalanx Ungual		Length 1.2	0	0	
Manual Phalanx		Length 0.5	0	0	
Manual Phalanx?		Length 0.3	0	0	
Manual Phalanx		Length 1.3	0	0	
Manus Phalanx		Length 1.3	0	0	
Manus Phalanx		Length 1.6	0	0	
Manus Phalanx		Length 1.6	0	0	
Manus Phalanx		Length 1.4	0	0	
Manux Phalanx		Length 1.0	0	0	
Manus Phalanx		Length 1.1	0	0	
Manus Phalanx		Length 1.0	0	0	
Manus Phalanx		Length 0.6	0	0	
Manus Phalanx		Length 1.6	0	0	
Manus Phalanx Ungual		Length >1.1	0	0	

Bone	Side	Measurements (cm)	W	A	Notes
Manus Phalanx Ungual		Length 1.4	0	0	
Manus Phalanx Ungual		Length 1.3	0	0	
Manus Phalanx Ungual		Length 1.2	0	0	
Manus Phalanx Ungual		Length 1.6	0	0	
Manus Phalanx II-1	R	Length >1.0	0	0	
Manus Phalanx II-2	R	Length 0.6	0	0	
Manus Phalanx II-3	R	Length 1.2	0	0	
Manus Phalanx III-1	R	Length 1.3	0	0	
Manus Phalanx III-3	R	Length 1.5	0	0	
Manus Phalanx IV-1	R	Length 1.4	0	0	
Manus Phalanx V-1	R	Length 1.4	0	0	
Manus Phalanx V-2	R	Length 1.0	0	0	
Manus Phalanx V-3	R	Length 0.9	0	0	
Scapula	R	Length >16.8, Pinch 2.2	0	0	
Scapula	R	Length >16.6, Pinch 2.2	0	0	
Scapula	R	Length >18.9, Pinch 2.5	0	0	
Scapula	R	Length >15.7, Pinch 2.7	0	0	
Scapula	R	Length >11.8, Pinch 2.0	0	0	
Scapula	R	Length >18.9, Pinch 2.8	0	0	
Scapula	R	Length >14.3, Pinch 2.3	0	0	
Scapula	R	Length >17.9, Pinch 2.5	0	0	
Scapula	R	Length >20.2, Pinch 2.6	0	0	
Scapula	R	Length >13.9, Pinch 1.9	0	0	
Scapula	R	Length >9.5, Pinch 2.4	0	0	
Scapula	R	Length >12.0, Pinch 2.6	0	0	
Scapula	R	Length >9.9, Pinch 2.5	0	0	
Scapula	R	Length >16.4, Pinch 2.4	0	0	
Scapula	R	Length >8.0, Pinch 2.3	0	0	
Scapula	R	Length >8.9, Pinch 1.9	0	0	
Scapula	R	Length >7.1, Pinch 2.3	0	0	
Scapula	L	Length >10.4, Pinch 2.2	0	0	
Scapula	L	Length >14.9, Pinch 2.3	0	0	

Bone	Side	Measurements (cm)	W	A	Notes
Scapula	L	Length >9.2, Pinch 2.1	0	0	
Scapula	L	Length >18.9, Pinch 2.9	0	0	
Scapula	L	Length >18.5, Pinch 2.2	0	0	
Scapula	L	Length >12.0, Pinch 2.0	0	0	
Scapula	L	Length >15.0, Pinch 2.1	0	0	
Scapula	L	Length >17.4, Pinch 2.1	0	0	
Scapula	L	Length >15.8, Pinch 2.1	0	0	
Scapula	L	Length >14.9, Pinch 2.0	0	0	
Scapula	L	Length >17.6, Pinch 2.1	0	0	
Scapula	L	Length >22.3, Pinch 2.6	0	0	
Scapula	L	Length >17.3, Pinch 2.4	0	0	
Scapula	L	Length >13.2, Pinch 2.3	0	0	
Scapula	L	Length >12.2, Pinch 2.4	0	0	
Scapula	L	Length >7.4, Pinch 2.4	0	0	
Scapula	R	Length >6.9, Pinch 2.1	0	0	
Scapula	L	Length >4.0, Pinch 2.1	0	0	
Scapula	R	Length >5.7, Pinch >1.9	0	0	
Scapula Fragments (15)		---	0	0	
Scapula	R	Length >13.3, Pinch 2.2	0	0	
Scapula	L	Length >7.8, Pinch 2.1	?	?	
Scapula	L	Length >13.8, Pinch 2.8	?	?	
Scapula	R	Length >17.7, Pinch 2.4	?	?	
Sternal Plate	R	Length 8.7, Width 5.9	0	0	
Sternal Plate	R	Length 9.9, Width 6.7	0	0	
Sternal Plate	L	Length 8.8, Width 4.7	0	0	
Sternal Plate	L	Length 9.2, Width >5.9	0	0	
Sternal Plate	R	Length >7.7, Width >3.4	0	0	
Sternal Plate	R	Length >5.9, Width >2.2	0	0	
Sternal Plate	R	Length >5.7, Width >2.2	0	0	
Sternal Plate	L	Length >3.3, Width 2.7	0	0	
Sternal Plate	R	Length 9.0, Width 5.7	0	0	
Sternal Plate	R?	Length >3.7, Width 4.2	0	0	

Bone	Side	Measurements (cm)	W	A	Notes
Coracoid	?	Length 4.6, Width 2.6	0	0	
Coracoid	?	Length 4.0, Width 3.2	0	0	
Coracoid	?	Length 4.0, Width 2.7	0	0	
Coracoid	?	Length 3.8, Width 3.0	0	0	
Coracoid	?	Length >3.6, Width 2.7	0	0	
Coracoid	?	Length 3.6, Width 2.5	0	0	
Coracoid	?	Length 3.6, Width 2.6	0	0	
Coracoid	?	Length 3.4, Width 2.7	0	0	
Coracoid	?	Length 4.2, Width 1.8	0	0	
Coracoid	?	Length 3.9, Width 2.2	0	0	
Coracoid	?	Length >2.3, Width >1.5	0	0	
Coracoid	?	Length 3.7, Width >1.8	0	0	
Coracoid	?	Length >2.3, Width 2.4	0	0	
Coracoid	?	Length >2.2, Width 2.5	2?	0	
Dentary	L	Length 10.6, Coron 6.9	0	0	
Dentary	L	Length >9.8, Coron 5.7	0	0	
Dentary	R	Length 10.6, Coron 6.6	0	0	
Dentary	R	Length 9.9, Coron 5.4	0	0	
Dentary	R	Length 9.2, Coron 5.1	0	0	
Dentary	R	Length 10.7, Coron >5.6	0	0	
Dentary	L	Length >7.9, Coron 6.0	0	0	
Dentary	L	Length 9.6, Coron 5.8	0	0	
Dentary	L	Length 10.2, Coron >4.0	0	0	
Dentary	R	Length 11.1, Coron 6.4	0	0	
Dentary	R	Length >9.6, Coron >5.7	0	0	
Dentary	R	Length 10.8, Coron 6.0	0	0	
Dentary	R	Length >9.7	0	0	
Dentary	R	Length >7.7, Coron >5.0	0	0	
Dentary	R	Length >7.0	0	0	
Dentary	R	Length >8.8	0	0	
Dentary	L	Length >8.8	0	0	
Dentary	L	Length >8.2	0	0	

Bone	Side	Measurements (cm)	W	A	Notes
Dentary	L	Length >9.8	0	0	
Dentary	L	Length >5.7	0	0	
Dentary	R	Length >4.5	0	0	
Dentary	L	Length >6.6, Coron >3.2	0	0	
Dentary	L	Length >6.4, Coron >3.5	0	0	
Dentary	L	Length >6.0	0	0	
Dentary	L	Length >5.2	0	0	
Dentary	L	Length >5.8	0	0	
Dentary	R	Length >6.6	0	0	
Dentary	R	Length >41.4	0	0	
Dentary	R	Length >5.1	0	0	
Dentary	L	Length >5.4	0	0	
Dentary	R	Length >6.2, Coron >4.5	0	0	
Dentary	L	Length >3.8	0	0	
Dentary	L	Length >4.6	0	0	
Dentary	R	Length >3.7	1?	0	
Dentary	R	Length >4.0	0	0	
Dentary	L	Length >4.0	0	0	
Dentary Fragments		---	0-1-2	0	29 fragm.
Dentary	L	Length >9.4, Coron 6.1	0	0	
Dentary	R	Length >10.0, Coron 6.2	0	0	
Dentary	R	Length 9.7, Coron 5.6	0	0	
Dentary	R	Length >12.0, Coron 7.5	0	0	
Dentary	L	Length 12.8, Coron 7.0	0	0	
Dentary	R	Length >6.7, Coron >5.9	0?	0?	
Dentary	L	Length >9.0, Coron 5.5	0?	0?	
Dentary	R	Length 10.1, Coron 5.9	0	0	
Dentary	L	Length 10.7, Coron 5.7	0	0	
Unknown Cranial Elements	---	---	0-1	0	
Unknown Cranial Elements	---	---	0	0	
Maxilla	L	Length 8.2, Height >3.9	0	0	
Maxilla	L	Length >6.5, Height >3.2	0	0	

Bone	Side	Measurements (cm)	W	A	Notes
Maxilla	L	Length 9.6, Height >4.2	0	0	
Maxilla	R	Length 9.7, Height >4.3	0	0	
Maxilla	L	Length >7.1, Height 3.8	0	0	
Maxilla	L	Length 8.8, Height 3.7	0	0	
Maxilla	L	Length 8.2, Height 3.7	0	0	
Maxilla	L	Length 8.5, Height >2.9	0	0	
Maxilla	L	Length >8.0, Height >3.2	0	0	
Maxilla	L	Length >8.0, Height >3.5	0	0	
Maxilla	R	Length >7.9, Height >3.0	0	0	
Maxilla	L	Length 8.3, Height >2.5	0	0	
Maxilla	L	Length >6.9, Height 3.3	0	0	
Maxilla	L	Length >6.3, Height >2.1	0	0	
Maxilla	L	Length >7.8, Height 3.2	0	0	
Maxilla	R	Length 7.9, Height 3.0	0	0	
Maxilla	R	Length 8.5, Height 3.7	0	0	
Maxilla	L	Length 8.2, Height 3.7	0	0	
Maxilla	R	Length >7.9, Height 3.8	0	0	
Maxilla	R	Length 8.2, Height >2.4	0	0	
Maxilla	R	Length 9.3, Height 3.9	0	0	
Maxilla	R	Length >6.4, Height >3.3	0	0	
Maxilla	R	Length >6.0, Height >3.0	0	0	
Maxilla	L	Length >8.1, Height >1.9	0	0	
Maxilla Fragments		---	0	0	19 fragm.
Maxilla	R	Length >7.9, Height >4.0	0?	0?	
Maxilla	L	Length >7.0, Height >3.3	0?	0?	
Maxilla	R	Length 8.9, Height 4.3	0	0	
Maxilla	L	Length 7.9, Height >4.1	0	0	
Jugal	L	Length 8.0, Pinch 1.5, Height 5.2	0	0	
Jugal	L	Length >4.5, Pinch 1.4, Height >3.0	0	0	
Jugal	R	Length >7.8, Pinch 1.6, Height 5.3	0	0	
Jugal	R	Length 7.8, Pinch 1.4, Height 4.6	0	0	
Jugal	R	Length >7.4, Pinch 1.7, Height 5.1	0	0	

Bone	Side	Measurements (cm)	W	A	Notes
Jugal	L	Length >6.4, Pinch 1.2, Height >3.7	0	0	
Jugal	R	Length >6.8, Pinch 1.3, Height >3.5	0	0	
Jugal	L	Length >7.7, Pinch 1.6, Height >2.8	0	0	
Jugal	R	Length >7.3, Pinch 1.4, Height >3.8	0	0	
Jugal	L	Length >7.7, Pinch 1.4, Height >2.3	0	0	
Jugal	L	Length >6.6, Pinch 1.4, Height >2.3	0	0	
Jugal	R	Length >6.1, Pinch 1.4, Height >2.0	0	0	
Jugal	R	Length >6.2, Pinch 1.3, Height >3.9	0	0	
Jugal	L	Length >6.7, Pinch 1.0, Height 4.1	0	0	
Jugal	R	Length >5.7, Pinch 1.2, Height >3.3	0	0	
Jugal	R	Length 8.1, Pinch 1.4, Height 4.3	0	0	
Jugal	L	Length 7.5, Pinch 1.3, Height >2.1	0	0	
Premaxilla	R	Length >5.4, Pinch 1.5	0	0	
Premaxilla	L	Length >6.6	0	0	
Premaxilla	R	Length >9.2, Pinch 2.9	0	0	
Premaxilla	L	Length >7.9, Pinch 2.0	0	0	
Premaxilla	L	Length >8.3, Pinch 2.4	0	0	
Premaxilla	R	Length >10.4, Pinch 1.4	0	0	
Premaxilla	R	Length >9.1	0	0	
Premaxilla	R	Length >8.0, Pinch 1.9	0	0	
Premaxilla	L	Length >5.7, Pinch 2.2	0	0	
Premaxilla	R	Length 10.3, Pinch 2.5	0	0	
Premaxilla	L	Length 10.5, Pinch 2.3	0	0	
Quadrate	R	Length 8.5	0	0	
Quadrate	L	Length 8.5	0	0	
Quadrate	R	Length 8.5	0	0	
Quadrate	L	Length >7.9	0	0	
Quadrate	R	Length 8.2	0	0	
Quadrate	L	Length 10.0	0	0	
Quadrate	L	Length 9.3	0	0	
Quadrate	L	Length 8.6	0	0	
Quadrate	L	Length >6.1	0	0	

Bone	Side	Measurements (cm)	W	A	Notes
Quadrate	R	Length 8.3	0	0	
Quadrate	R	Length >6.2	0	0	
Quadrate	R	Length 9.1	0	0	
Quadrate	R	Length 8.1	0	0	
Quadrate	L	Length 7.9	0	0	
Quadrate	L	Length >6.5	0	0	
Quadrate	R	Length 8.4	0	0	
Quadrate	L	Length 8.2	0	0	
Quadrate	R	Length 9.1	0	0	
Quadrate	L	Length 9.8	0	0	
Quadratojugal	?	Length 2.2	0	0	
Quadratojugal	?	Length 1.7	0	0	
Quadratojugal	?	Length 2.1	0	0	
Quadratojugal	?	Length >2.1	0	0	
Prefrontal	L	Length >3.1	0	0	
Prefrontal	L	Length 3.7	0	0	
Prefrontal	L	Length3.7	0	0	
Prefrontal	L	Length 5.0	0	0	
Prefrontal	R	Length >4.5	0	0	
Prefrontal	L	Length >3.7	0	0	
Prefrontal	L	Length >5.0	0	0	
Prefrontal	L	Length >3.7	0	0	
Prefrontal	R	Length 4.5	0	0	
Prefrontal	L	Length 4.8	0	0	
Prefrontal	R	Length 5.0	0	0	
Prefrontal	R	Length 5.4	0	0	
Prefrontal	L	Length 4.4	0	0	
Postorbital	R	Length >2.8, Height >2.0	0	0	
Postorbital	L	Length >2.3, Height >1.6	0	0	
Postorbital	L	Length >5.0, Height >2.7	0	0	
Postorbital	L	Length >4.2, Height >2.8	0	0	
Postorbital	L	Length >3.8, Height >2.2	0	0	

Bone	Side	Measurements (cm)	W	A	Notes
Postorbital	L	Length >4.9, Height 3.9	0	0	
Postorbital	R	Length >5.0, Height >3.4	0	0	
Postorbital	L	Length >5.2, Height >3.9	0	0	
Postorbital	L	Length >3.7, Height 3.6	0	0	
Postorbital	R	Length >4.5, Height >2.9	0	0	
Postorbital	R	Length >4.5, Height >2.3	0	0	
Postorbital	L	Length 5.0, Height 3.6	0	0	
Postorbital	L	Length >3.7, Height >3.0	0	0	
Postorbital	R	Length 5.8, Height 4.2	0	0	
Postorbital	L	Length 6.4, Height 4.0	0	0	
Parietal	---	Length >2.3, Width >2.4	2	0	
Parietal	---	Length 2.2, Width 2.8	0	0	
Parietal	---	Length >4.1, Width >3.5	0	0	
Parietal	---	Length >3.4, Width >3.3	0	0	
Parietal	---	Length 4.5, Width 3.6	0	0	
Parietal	---	Length 3.6, Width 3.4	0	0	
Parietal	---	Length >2.7, Width >3.5	0	0	
Parietal	---	Length 4.8, Width 3.7	0	0	
Parietal	---	Length 4.9, Width >3.3	0	0	
Parietal	---	Length 4.4, Width 3.2	0	0	
Parietal	---	Length 4.2, Width 3.3	0	0	
Parietal	---	Length 4.3, Width 3.8	0	0	
Lacrimal	R	Length >1.7	0	0	
Lacrimal	R	Length 3.1	0	0	
Lacrimal	R	Length 2.5	0	0	
Lacrimal	L	Length 2.3	0	0	
Nasal	R	Length >3.1	0	0	
Nasal	R	Length >3.5	0	0	
Nasal	R	Length >5.6	0	0	
Nasal	L	Length 3.3	0	0	
Frontal	R?	Length >1.5	2	0	
Frontal	L	Length 4.4, Width 3.1	0	0	

Bone	Side	Measurements (cm)	W	A	Notes
Frontal	R	Length 4.7, Width 3.0	0	0	
Frontal	R	Length 4.1, Width 2.9	0	0	
Frontal	L	Length 4.5, Width 2.7	0	0	
Frontal	L	Length 4.3, Width 2.8	0	0	
Frontal	L	Length 3.7, Width 2.7	0	0	
Frontal	R	Length 4.2, Width 2.7	0	0	
Frontal	R	Length 4.4, Width 2.7	0	0	
Frontal	R	Length 4.1, Width 2.8	0	0	
Frontal	R	Length 4.1, Width >2.4	0	0	
Frontal	L	Length 4.8, Width 2.5	0	0	
Frontal	R	Length >4.0, Width 2.5	0	0	
Frontal	L	Length 4.5, Width 2.5	0	0	
Frontal	R	Length >4.0, Width 2.7	0	0	
Frontal	R	Length 4.1, Width 2.6	0	0	
Frontal	L	Length >3.8, Width 2.6	0	0	
Frontal	L	Length 4.5, Width 2.7	0	0	
Frontal	L	Length 4.2, Width 2.7	0	0	
Frontal	L	Length 4.8, Width 2.8	0	0	
Frontal	R	Length 4.8, Width 2.5	0	0	
Frontal	R	Length 4.1, Width2.5	0	0	
Frontal	R	Length 4.0, Width 2.4	0	0	
Frontal	R	Length 4.7, Width 2.8	0	0	
Frontal	R	Length 4.1, Width 2.8	0	0	
Frontal	L	Length 4.3, Width 2.5	0	0	
Palatine	?	Length >1.9	0	0	
Palatine	?	Length >3.1	0	0	
Palatine	?	Length >2.9	0	0	
Palatine	?	Length >2.6	0	0	
Palatine	?	Length >2.6	0	0	
Palatine	?	Length >3.7	0	0	
Palatine	?	Length 4.8	0	0	
Orbitosphenoid	R	Length >2.3	0	0	

Bone	Side	Measurements (cm)	W	A	Notes
Orbitosphenoid	R	Length >2.3	0	0	
Orbitosphenoid	?	Length >2.3	0	0	
Laterosphenoid	L	Length >3.1	0	0	
Laterosphenoid	L	Length 3.0	0	0	
Basisphenoid	---	Length 2.1	0	0	
Basisphenoid	---	Length 4.4	0	0	
Laterosphenoid	L	Length 3.2	0	0	
Laterosphenoid	L	Length 4.3	0	0	
Laterosphenoid	R	Length 3.4	0	0	
Laterosphenoid	R	Length 3.4	0	0	
Laterosphenoid	R	Length 3.7	0	0	
Laterosphenoid	L	Length 3.5	0	0	
Basisphenoid	---	Length 2.9	0	0	
Laterosphenoid	L	Length 3.8	0	0	
Laterosphenoid	L	Length 3.7	0	0	
Laterosphenoid	R	Length 3.0	0	0	
Laterosphenoid	L	Length 2.8	0	0	
Supraoccipital	---	Width 3.2	---	---	Cast
Supraoccipital	---	Width 2.7	0	0	
Supraoccipital	---	Width 2.5	0	0	
Exoccipital	?	---	1	0	
Basioccipital	?	Length 2.4	0	0	
Basioccipital	?	Length 2.1	0	0	
Basioccipital	?	Length 2.1	0	0	
Basioccipital	?	Length 2.6	0	0	
Basioccipital	?	Length >1.9	0	0	
Basioccipital	?	Length 2.6	0	0	
Basioccipital	?	Length 2.4	0	0	
Basioccipital	?	Length 2.3	0	0	
Prootic	L	Length 3.2	0	0	
Supraoccipital	---	Width 2.5	0	0	
Basioccipital	?	Length 2.4	0	0	

Bone	Side	Measurements (cm)	W	A	Notes
Exoccipital	L	Length 3.1	0	0	
Exoccipital	L	Length 3.3	0	0	
Exoccipital	L	Length 2.7	0	0	
Exoccipital	?	Length 2.5	0	0	
Exoccipital	R	Length 3.0	0	0	
Supraoccipital	---	Width 4.0	0	0	
Prootic	R	Width 2.5	0	0	
Prootic	L	Width 2.4	0	0	
Supraoccipital	---	Width 3.1	0	0	
Exoccipital	R	Length 3.5	0	0	
Exoccipital	L	Length 3.7	0	0	
Basioccipital	---	Length 2.6	0	0	
Squamosal	L	Length 5.9	0	0	
Squamosal	L	Length >4.5	0	0	
Squamosal	L	Length >4.3	0	0	
Squamosal	L	Length >4.4	0	0	
Squamosal	L	Length >4.8	0	0	
Squamosal	L	Length >3.7	0	0	
Squamosal	L	Length 6.2	0	0	
Squamosal	L	Length >4.3	0	0	
Squamosal	L	Length >3.4	0	0	
Squamosal	R	Length >5.2	0	0	
Squamosal	L	Length 6.2	0	0	
Squamosal	R	Length >4.3	0	0	
Squamosal	R	Length >4.8	0	0	
Squamosal	R	Length >4.1	0	0	
Squamosal	L	Length >4.0	0	0	
Surangular	L	Length >6.2	0	0	
Surangular	L	Length >5.3	0	0	
Surangular	R	Length >5.3	0	0	
Surangular	L	Length >4.0	0	0	
Surangular	L	Length >4.7	0	0	

Bone	Side	Measurements (cm)	W	A	Notes
Surangular	L	Length >4.5	0	0	
Surangular	L	Length >4.2	0	0	
Surangular	R	Length >4.9	0	0	
Surangular	L	Length >5.6	0	0	
Surangular	R	Length >4.5	0	0	
Surangular	L	Length >3.8	0	0	
Surangular	R	Length >5.3	0	0	
Surangular?	L?	Length >4.2	0	0	
Surangular	R	Length 5.3	0	0	
Surangular	L	Length 4.7	0	0	
Predentary	---	Width >4.8	0	0	
Predentary	---	Width 5.1	0	0	
Predentary	---	Width 4.9	0	0	
Predentary	---	Width 5.0	0	0	
Articular	---	Length >4.7	0	0	
Vertebra	---	Length 2.1, Width 2.2	0	0	
Vertebra	---	Length 2.2, Width 2.8	0	0	
Vertebra	---	Length 2.2, Width 2.5	0	0	
Vertebra	---	Length 1.1, Width 1.8	0	0	
Vertebra	---	Length 1.2, Width 1.6	0	0	
Vertebra	---	Length 1.1, Width 1.6	0	0	
Vertebra	---	Length 1.2, Width 1.7	0	0	
Vertebra	---	Length 1.1, Width 1.5	0	0	
Vertebra	---	Length 1.1, Width 1.5	0	0	
Vertebra	---	Length 1.1, Width 1.8	0	0	
Vertebra	---	Length 1.1, Width 1.6	0	0	
Vertebra	---	Length 1.1, Width 1.5	0	0	
Vertebra	---	Length 1.1, Width 1.7	0	0	
Vertebra	---	Length 1.2, Width 1.6	0	0	
Vertebra	---	Length 1.2, Width 1.9	0	0	
Vertebra	---	Length 1.0, Width 2.3	0	0	
Vertebra	---	Length 1.2, Width 2.5	0	0	

Bone	Side	Measurements (cm)	W	A	Notes
Vertebra	---	Length 1.2, Width 2.4	0	0	
Vertebra	---	Length 1.2, Width 2.3	0	0	
Sacral vertebra	---	Length 1.9, Width 3.0	0	0	
Sacral vertebra	---	Length 1.7, Width 3.0	0	0	
Sacral vertebra	---	Length 2.0, Width 2.9	0	0	
Sacral vertebra	---	Length 2.1, Width 2.3	0	0	
Sacral vertebra	---	Length 1.9, Width 2.3	0	0	
Vertebra	---	Length 1.9, Width 3.5	0	0	
Vertebra	---	Length 2.6, Width 3.9	0	0	
Vertebra	---	Length 1.5, Width 1.7	0	0	
Vertebra	---	Length 1.5, Width 1.5	0	0	
Vertebra	---	Length 1.5, Width 2.2	0	0	
Vertebra	---	Length 1.5, Width 2.2	0	0	
Vertebra	---	Length 1.3, Width 2.9	0	1	
Vertebra	---	Length 1.1, Width 3.1	0	0	
Vertebra	---	Length 1.5, Width 2.3	0	0	
Vertebra	---	Length 1.1, Width 2.1	0	1	
Vertebra	---	Length 1.3, Width 3.0	0	1	
Vertebra	---	Length 1.1, Width 3.7	0	0	
Vertebra	---	Length 1.2, Width 3.0	0	0	
Vertebra	---	Length 1.1, Width 2.9	0	0	
Vertebra	---	Length 1.3, Width 1.7	3	0	
Vertebra	---	Length 1.6, Width 2.7	3	0	
Vertebra	---	Length 1.5, Width 2.7	0	0	
Vertebra	---	Length 1.1, Width 2.5	0	0	
Vertebra	---	Length 1.3, Width 3.2	0	0	
Vertebra	---	Length 1.3, Width 3.0	3	0	
Vertebra	---	Length 1.2, Width 2.9	0	1	
Vertebra	---	Length 1.3, Width 3.3	0	0	
Vertebra	---	Length 1.9, Width 3.4	0	0	
Vertebra	---	Length 1.8, Width 3.6	0	1	
Vertebra	---	Length 1.8, Width 2.8	0	0	

Bone	Side	Measurements (cm)	W	A	Notes
Vertebra	---	Length 1.3, Width 3.3	0	0	
Vertebra	---	Length 9.0, Width 3.3	0	0	
Vertebra	---	Length 1.3, Width 2.6	0	0	
Vertebra	---	Length 1.5, Width 3.0	3	0	
Vertebra	---	Length 1.2, Width 1.9	3	0	
Vertebra	---	Length 1.3, Width 2.4	0	0	
Vertebra	---	Length 1.2, Width 1.9	0	0	
Vertebra	---	Length 1.1, Width 1.9	3	0	
Vertebra	---	Length 1.1, Width 2.0	3	0	
Vertebra	---	Length 1.3, Width 2.1	0	0	
Vertebra	---	Length 1.1, Width 1.9	0	0	
Vertebra	---	Length 1.3, Width 2.1	0	0	
Vertebra	---	Length 1.1, Width 2.1	0	0	
Vertebra	---	Length 1.1, Width 2.4	0	0	
Vertebra	---	Length 1.4, Width 2.0	0	0	
Vertebra	---	Length 1.1, Width 2.6	0	0	
Vertebra	---	Length 1.2, Width >1.4	3	0	
Vertebra	---	Length 1.7, Width 3.0	0	0	
Vertebra	---	Length 1.5, Width 3.4	0	0	
Vertebra	---	Length 1.8, Width 3.9	0	0	
Vertebra	---	Length 1.7, Width 3.0	0	0	
Vertebra	---	Length 1.9, Width 3.8	0	1	
Vertebra	---	Length 2.5, Width 3.2	0	0	
Vertebra	---	Length 2.2, Width 3.4	2	0	
Vertebra	---	Length 1.6, Width 2.8	0	0	
Vertebra	---	Length 2.3, Width 2.7	0	0	
Vertebra	---	Length 1.7, Width 2.1	0	0	
Vertebra	---	Length 2.0, Width 2.9	2	0	
Vertebra	---	Length 2.2, Width 2.9	0	0	
Vertebra	---	Length 2.3, Width 2.3	0	0	
Vertebra	---	Length 2.0, Width 3.1	0	0	
Vertebra	---	Length 2.3, Width 3.3	0	0	

Bone	Side	Measurements (cm)	W	A	Notes
Vertebra	---	Length 2.3, Width 3.0	0	0	
Vertebra	---	Length 1.6, Width 2.5	3	0	
Vertebra	---	Length 2.1, Width 3.1	0	0	
Vertebra	---	Length 1.7, Width 2.6	0	0	
Vertebra	---	Length 2.4, Width 2.5	0	0	
Vertebra	---	Length 1.9, Width 3.0	0	0	
Vertebra	---	Length 2.1, Width 2.3	0	0	
Vertebra	---	Length 1.9, Width 2.0	0	0	
Vertebra	---	Length 1.9, Width 2.5	0	0	
Vertebra	---	Length 1.9, Width 2.3	0	0	
Vertebra	---	Length 1.8, Width 2.3	0	0	
Vertebra	---	Length 1.8, Width 2.8	3	0	
Vertebra	---	Length 1.6, Width 2.9	0	0	
Vertebra	---	Length 2.0, Width 3.5	0	0	
Vertebra	---	Length 2.2, Width 2.6	0	0	
Vertebra	---	Length 1.7, Width 2.9	0	0	
Vertebra	---	Length 1.9, Width 3.0	0	0	
Vertebra	---	Length 2.2, Width 2.7	0	0	
Vertebra	---	Length 2.3, Width 2.6	0	0	
Vertebra	---	Length 1.9, Width 2.5	0	0	
Vertebra	---	Length 1.9, Width 2.4	2	0	
Vertebra	---	Length 2.0, Width 3.1	0	0	
Vertebra	---	Length 2.0, Width 2.7	0	0	
Vertebra	---	Length 1.8, Width 3.6	2	0	
Vertebra	---	Length 1.9, Width 2.9	0	0	
Vertebra	---	Length 1.2, Width 2.6	0	0	
Vertebra	---	Length 2.0, Width 1.7	0	0	
Vertebra	---	Length 1.9, Width 3.9	0	0	
Vertebra	---	Length 2.0, Width 1.8	0	0	
Vertebra	---	Length 2.1, Width 1.9	0	0	
Vertebra	---	Length 1.9, Width 2.7	0	0	
Vertebra	---	Length 1.5, Width 3.5	0	0	

Bone	Side	Measurements (cm)	W	A	Notes
Vertebra	---	Length 2.0, Width 2.8	0	0	
Vertebra	---	Length 2.0, Width 1.7	2	0	
Vertebra	---	Length 2.2, Width 3.8	2	0	
Vertebra	---	Length 2.4, Width 2.8	0	1	
Vertebra	---	Length 1.6, Width 1.7	0	0	
Vertebra	---	Length 2.0, Width 2.7	2	0	
Vertebra	---	Length 2.0, Width 2.7	0	0	
Vertebra	---	Length 1.9, Width 2.0	0	0	
Vertebra	---	Length 2.1, Width 3.9	0	0	
Vertebra	---	Length 1.8, Width 3.2	0	0	
Vertebra	---	Length 2.0, Width 2.9	0	0	
Vertebra	---	Length 1.9, Width 2.6	0	0	
Vertebra	---	Length >0.6, Width 2.1	0	0	
Vertebra	---	Length 2.1, Width 2.5	0	0	
Vertebra	---	Length 1.4, Width 1.4	0	0	
Vertebra	---	Length 1.0, Width 1.3	0	0	
Vertebra	---	Length 1.0, Width 1.3	0	0	
Vertebra	---	Length 1.1, Width 1.4	0	0	
Vertebra	---	Length 0.6, Width 0.7	0	0	
Vertebra	---	Length 0.6, Width 0.8	0	0	
Vertebra	---	Length 0.5, Width 0.7	0	0	
Vertebra	---	Length 0.6, Width 0.5	0	0	
Vertebra	---	Length 0.5, Width 0.5	0	0	
Vertebra	---	Length 0.5, Width 0.6	0	0	
Vertebra	---	Length 0.5, Width 0.4	0	0	
Vertebra	---	Length 1.6, Width 2.3	0	0	
Neural arch	---	Width 2.2	0	0	
Neural arch	---	Width 2.1	0	0	
Vertebra	---	Length 1.2, Width 2.2	0	0	
Vertebra	---	Length 1.3, Width 2.3	0	0	
Vertebra	---	Length 2.1, Width 2.1	0	0	
Neural arch + spine	---	Width 3.6	0	0	

Bone	Side	Measurements (cm)	W	A	Notes
Neural arch + spine	---	Width 3.5	0	0	
Neural arch + spine	---	Width >3.0	0	0	
Neural arch + spine	---	Width 3.2	0	0	
Neural arch + spine	---	Width >3.0	0	0	
Neural spine	---	Length >4.2	0	0	
Vertebra	---	Length 1.0, Width 1.6	0	0	
Vertebra	---	Length 1.1, Width 1.7	0	0	
Vertebra	---	Length 1.6, Width 2.3	0	0	
Neural arch	---	Width 1.7	0	0	
Neural arch	---	Width 2.5	0	0	
Neural arch	---	Width 1.5	0	0	
Haemal arch	---	Width >1.2	0	0	
Neural arch	---	Width 1.6	0	0	
Haemal arch	---	Width 1.3	0	0	
Neural arch	---	Width 2.4	0	0	
Haemal arch	---	Width 2.4	0	0	
Haemal arch	---	Width 1.4	0	0	
Neural/Haemal arch fragm.	---	---	0	0	24 fragm.
Vertebrae (see notes)	---		0	0	22 centra, 1 neural arch
Vertebrae (see notes)	---		0	0	16 vertebrae
Vertebrae (see notes)	---		0	0	5 centra, 3 processes
Vertebrae (see notes)	---		0	0	21 centra, 2 processes
Vertebrae (see notes)	---		0	0	12 centra, 17 processes
Vertebrae (see notes)	---		0	0	48 centra, 2 neural arches
Vertebrae (see notes)	---		0	0	79 centra, 13 transv. processes
Vertebrae (see notes)	---		2	0	8 centra, 1 transv. process
Vertebrae (see notes)	---		0	0	15 centra, 34 neural arches
Vertebrae (see notes)	---		0	0	134 centra
Vertebra	---	Length 1.6, Width 2.4, Height 1.7	?	?	
Vertebra	---	Length 2.2, Width 2.2, Height 0.9	?	?	
Vertebra	---	Length 1.9, Width 2.4, Height 1.7	?	?	
Vertebra	---	Length 1.5, Width 2.2, Height 1.4	?	?	

Bone	Side	Measurements (cm)	W	A	Notes
Vertebra	---	Length 1.3, Width 1.8, Height 1.2	?	?	
Vertebra	---	Length 1.6, Width 2.4, Height 1.4	?	?	
Vertebra	---	Length 2.0, Width 2.9, Height 1.9	?	?	
Vertebrae (see notes)	---		0?	0?	2 centra, 2 neural arches
Vertebrae (see notes)	---		0?	0?	13 centra, 10 neural arches
Vertebrae (see notes)	---		0	0	9 neural arches
Vertebrae (see notes)	---		0?	0?	7 centra
Sacral ribs (58 fragm.)	---	---	0	0	58 frag.
Tibia	L	Length 16.6, Cicrumf 6.0, Cnem 5.8	0	0	
Tibia	L	Length 20.6, Circumf 8.3, Cnem 6.9	0	0	
Tibia	L	Length 19.1, Circumf 7.7, Cnem not measurable	0	0	
Tibia	L	Length 17.5, Circum 6.9, Cnem 6.7	0	0	
Tibia	R	Length 16.3, Circumf 6.0, Cnem 4.5	0	0	
Tibia	L	Length 18.8, Circumf 7.4, Cnem 5.5	0	0	
Tibia	R	Length 22.4, Circumf 8.7, Cnem 8.4	0	0	
Tibia	L	Length 22.9, Circumf 8.6, Cnem 6.6	0	0	
Tibia	R	Length 14.1, Circumf 5.5, Cnem 4.8	0	0	
Tibia	R	Length 17.8, Circumf 7.0, Cnem 5.1	0	0	
Tibia	R	Length 19.2, Circumf 7.0, Cnem 6.4	0	0	
Fibula	L	Length 16.2, Cranial peg 2.6	0	0	
Fibula	L	Length 16.6, Cranial peg 2.7	0	0	
Fibula	L	Length 20.5, Cranial peg 3.6	0	0	
Fibula	L	Length 21.1, Cranial peg 2.8	0	0	
Fibula	R	Length >11.4, Cranial peg 3.0	0	0	
Fibula	R	Length 20.3, Cranial peg 3.9	0	0	
Fibula	L	Length 18.1, Cranial peg 3.4	0	0	
Fibula	R	Length 20.8, Cranial peg 3.8	0	0	
Fibula	R	Length 15.9, Cranial peg 2.7	0?	0?	
Metatarsal	?	Length 9.1, Circumf 6.0	0	0	
Metatarsal	?	Length 8.9, Circumf 5.9	0	0	
Metatarsal	?	Length 7.8, Circumf 4.4	0	0	

Bone	Side	Measurements (cm)	W	A	Notes
Metatarsal	?	Length 6.4, Circumf 3.9	0	0	
Metatarsal	?	Length 6.5, Circumf 4.4	0	0	
Metatarsal	?	Length 6.1, Circumf 3.7	0	0	
Metatarsal Fragments (14)	?	---	0-2	0	
Pes Phalanx	?	Length 2.4	0	0	
Pes Phalanx	?	Length 0.5	0	0	
Pes Phalanx	?	Length 0.3	0	0	
Pes Phalanx	?	Length 0.8	0	0	
Pes Phalanx	?	Length 0.3	0	0	
Pes Phalanx	?	Length 0.7	0	0	
Pes Phalanx	?	Length 0.5	0	0	
Pes Phalanx	?	Length 0.5	0	0	
Pes Phalanx	?	Length 0.7	0	0	
Pes Phalanx - Ungual	?	Length 1.9, Width 1.5	0	0	
Pes Phalanx - Ungual	?	Length 1.9, Width 1.6	0	0	
Pes Phalanx - Ungual	?	Length 1.7, Width 1.8	0	0	
Pes Phalanx - Ungual	?	Length 2.0, Width 1.8	0	0	
Pes Phalanx - Ungual	?	Length 1.9, Width 2.0	0	0	
Pes Phalanx - Ungual	?	Length 1.7, Width 1.2	0	0	
Pes Phalanx - Ungual	?	Length 1.6, Width 1.6	0	0	
Pes Phalanx - Ungual	?	Length 1.9, Width 1.8	0	0	
Pes Phalanx - Ungual	?	Length >1.3, Width 1.1	0	0	
Calcaneum	?	Width 2.4	0	0	
Calcaneum	?	Width 1.8	0	0	
Calcaneum	?	Width 1.8	0	0	
Calcaneum	?	Width 1.8	0	0	
Calcaneum	?	Width 1.5	0	0	
Calcaneum	?	Width 1.9	0	0	
Calcaneum	?	Width 1.9	0	0	
Calcaneum	?	Width 1.7	0	0	
Calcaneum	?	Width 1.3	0	0	
Astragalus	?	Width 2.6	0	0	

Bone	Side	Measurements (cm)	W	A	Notes
Astragalus	?	Width 2.6	0	0	
Astragalus	?	Width 4.1	0	0	
Astragalus	?	Width 3.5	0	0	
Astragalus	?	Width 3.0	1	0	
Astragalus	?	Width 3.4	0	0	
Astragalus	?	Width 3.3	0	0	
Femur	L	Length 21.3, Circumf 8.5	0	0	
Femur	L	Length 20.2, Circumf 8.6	0	0	
Femur	L	Length 23.3, Circumf 9.2	0	0	
Femur	L	Length 24.0, Circumf 9.5	0	0	
Femur	R	Length 16.2, Circumf 6.4	0	0	
Femur	R	Length 24.3, Circumf 8.9	0	0	
Femur	L	Length 19.5, Circumf 8.1	0	0	
Femur	R	Length 24.0, Circumf 10.0	0	0	
Femur	L	Length 17.3, Circumf 6.2	0	0	
Femur	L	Length >16.5, Circumf 9.1	0	0	
Femur	L	Length >16.9, Circumf 7.7	0	0	
Femur	R	Length >15.7, Circumf 7.8	0	0	
Femur	R	Length >14.3, Circumf 7.9	0	0	
Femur	R	Length >9.9	0	0	
Femur	R	Length >13.7	0	0	
Femur	R	Length >16.9, Circumf 9.7	0	0	
Femur	L	Length >11.7	0	0	
Femur	L	Length >9.6, Circumf 7.8	0	0	
Femur	R	Length >7.6	0	0	
Femur Fragments	---	---	0	0	21 fragm.
Ischium	R	Length >18.0	0	0	
Ischium	R	Length 20.0	0	0	
Ischium	R	Length >12.2	0	0	
Ischium	L	Length 22.7	0	0	
Ischium	L	Length >17.9	0	0	
Ischium	R	Length >20.1	0?	0	

Bone	Side	Measurements (cm)	W	A	Notes
Ischium	R	Length >22.8	0	0	
Ischium	L	Length 20.6	0	0	
Ischium	L	Length >11.0	0	0	
Ischium	L	Length >11.0	0	0	
Ischium	L	Length >8.3	0	0	
Ischium	R	Length >13.4	0	0	
Ischium	R	Length >20.7	0	0	
Ischium	R	Length >16.9	0?	0?	
Ischium	R	Length >16.8	0	0?	
Pubis	R	Length >10.1, Constriction 2.2	0	0	
Pubis	L	Length >13.5, Constriction 2.5	0	0	
Pubis	L	Length >13.1, Constriction 2.4, Blade height 6.3	0	0	
Pubis	R	Length >8.3, Constriction 3.5	0	0	
Pubis	L	Length >6.1	0	0	
Pubis	L	Length >4.9	0	0	
Pubis	L	Length >3.9	0	0	
Pubis	R	Length >1.9	0	0	
Pubis	L	Length >1.6	0	0	
Ilium	R	Length 22.9, Height at acetab. 5.7	0	0	
Ilium	R	Length >18.9, Height at acetab. 5.0	0	0	
Ilium	R	Length 23.9, Height at acetab. 5.2	0	0	
Ilium	R	Length >17.8, Height at acetab. 4.6	0	0	
Ilium	R	Length >14.9, Height at acetab. 5.0	0	0	
Ilium	R	Length >11.4, Height at acetab. 5.8	0	0	
Ilium	R	Length >16.4, Height at acetab. 4.4	0	0	
Ilium	R	Length >19.2, Height at acetab. >4.3	0	0	
Ilium	R	Length >11.0, Height at acetab. roughly 4.8	0	0	
Ilium	R	Length >10.3	0	0	
Ilium	L	Length 22.2, Height at acetab. 5.5	0	0	
Ilium	L	Length 21.4, Height at acetab. 5.0	0	0	
Ilium	L	Length >12.7, Height at acetab. 5.6	0	0	

Bone	Side	Measurements (cm)	W	A	Notes
Ilium	L	Length >18.7, Height at acetab. 5.1	0	0	
Ilium	R	Length 16.8, Height at acetab. 4.6	0?	0?	
Ilium	R	Length >9.1	0?	0?	
Ilium	R	Length >11.2	0?	0?	
Ilium Fragments	---	---	0-3	0-1	21 fragm.
Ribs	L	Length >5.1, 9.0, 4.9	0	0	3 distinct ribs
Ribs	R	Length >6.0, 6.2, 5.0	0	0	3 distinct ribs
Ribs	L	Length from >3.4 to >22.3	0	0	8 distinct ribs
Ribs	R	Length from >6.9 to >22.6	0	0	12 distinct ribs
Rib fragments	---	Length from >4.7 to >14.3	0	0	8 fragm.
Ribs	L	Length from >7.5 to >14.8	0	0	8 distinct ribs
Ribs	R	Length from >4.6 to >16.7	0	0	20 distinct ribs
Ribs	---	Length from >1.8 to >16.5	0	0	10 fragm.
Ribs	L	Length from >7.0 to >21.0	0	0	4 distinct ribs
Ribs	R	Length from >7.2 to >16.9	0	0	6 distinct ribs
Ribs	---	Length from >2.9 to >12.6	0	0	13 fragm.
Ribs	L	Length from >3.6 to >15.1	0	0	9 distinct ribs
Ribs	R	Length from >4.7 to >14.3	0	0	12 distinct ribs
Ribs	---	Length from >0.7 to >12.5	0	0	100 fragm.
Ribs	L	Length from >9.1 to >11.6	0?	0?	2 distinct ribs
Ribs	R	Length from >4.1 to >13.4	0?	0?	4 fragm.
Ribs	---	Length from >3.9 to >11.0	0?	0?	5 fragm.
Ribs	L	Length from >2.5 to >7.8	0?	0?	12 distinct ribs
Ribs	R	Length from >3.6 to >5.1	0?	0?	8 distinct ribs
Ribs	---	Length from >0.6 to >8.7	0?	0?	242 fragm.
Ribs	---	Length from >0.5 to >5.1	0?	0?	
Bone Fragments	---		0-3	0-2	427 fragm.
Bone Fragments	---		0-3	0-2	85 fragm.
Bone Fragments	---	Length from >0.3 to >6.1	0?	0?	
Bone Fragments	---		0	0	
Bone Fragments	---		0?	0?	
Tooth	---	Length >1.0	---	---	Hadrosaur tooth

Bone	Side	Measurements (cm)	W	A	Notes
Teeth	---		---	---	15 *Troodon* teeth

APPENDIX C: TAPHONOMIC DATA FOR THE LAMBEOSITE BONEBED

Specimen number	Bone	Side	Measurements (cm)	W	A	Notes
MOR 355 (8-26-5-6)	Femur	R	Length 61.5, Circumf. 23.2	0	0	Juvenile
MOR 355 (8-29-5-5)	Femur	R	Length 59.5, Circumf. 22.4	0	0	Juvenile
MOR 355 (7-20-6-2)	Femur	L	Length >62.5, Circumf. 21.7	0	0	Juvenile
MOR 355 (8-22-5-11)	Femur	L	Length 60.5, Circumf. 20.8	0	0	Juvenile
MOR 355 (2022-C-648)	Femur	L	Length 61.0, Circumf. 22.1	0	0	Juvenile
MOR 355 (8-24-5-6)	Femur	L	Length 109.0, Circumf 40.8	0	0	Adult
MOR 355 (8-27-5-3)	Scapula	L	Length >40.2, Pinch 5.9	0	0	Juvenile
MOR 355 (8-22-5-4)	Scapula	R	Length >56.7, Pinch 11.2	0	0	Adult
MOR 355 (2022-C-651)	Scapula	R	Length >21.5, Pinch 6.6	0	0	Juvenile
MOR 355 (8-29-5-3)	Scapula	L	Length >10.2	0	0	Juvenile
MOR 355 (8-25-5-13)	Scapula	R	Length >43.3, Pinch 5.4	0	0	Juvenile
MOR 355 (8-25-5-4)	Scapula	L	Length >35.8, Pinch 5.8	0	1	Juvenile
MOR 355 (7-11-6-2)	Scapula	R	Length >41.2, Pinch 5.5	0	0	Juvenile
MOR 355 (8-28-5-12)	Scapula	R	Length 45.1, Pinch 5.6	0	0	Juvenile
MOR 355 (8-28-5-12)	Coracoid	R	Length 11.2	0	0	
MOR 355 (7-6-5-3)	Tibia	L	Length 59.5, Circumf. 17.9, Cnem >15.0	0	0	Juvenile
MOR 355 (G-22-6-1)	Tibia	R	Length 56.0, Circumf. 19.3, Cnem >12.8	0	0	Juvenile
MOR 355 (8-26-5-8)	Tibia	R	Length 58.5, Circumf. 17.9, Cnem 14.0	0	0	Juvenile
MOR 355 (7-7-1-1)	Tibia	L	Length 54.5, Circumf. 18.0, Cnem 17.3	0	0	Juvenile
MOR 355 (6-2-6-6)	Tibia	R	Length 54.5, Circumf. 17.5, Cnem 16.7	0	0	Juvenile
MOR 355 (8-24-5-4)	Tibia	L	Length 106.0, Circumf. 31.0, Cnem 34.3	0	0	Adult
MOR 355 (2022-C-649)	Fibula	L	Length 51.5, Circumf. 8.0, Cranial peg 8.2	0	0	Juvenile
MOR 355 (6-22-6-2)	Fibula	R	Length 54.5, Circumf. 9.1, Cranial peg >7.6	0	0	Juvenile
MOR 355 (8-25-5-5)	Fibula	L	Length 54.1, Circumf. 8.0, Cranial peg 9.3	0	0	Juvenile
MOR 355 (8-22-5-17)	Fibula	R	Length 50.9, Circumf 7.5, Cranial peg 5.8	0	0	Juvenile
MOR 355 (2022-C-716)	Fibula	L	Length >12.0, Cranial peg 8.6	1	0	Juvenile

Specimen number	Bone	Side	Measurements (cm)	W	A	Notes
MOR 355 (8-22-5-6)	Humerus	L	Length 56, A-P Crest 15.0, Circumf. 21.4	0	0	Adult
MOR 355 (2022-C-660)	Humerus	L	Length >21.9, A-P Crest 6.9, Circumf. 10.7	2	2	Juvenile
MOR 355 (8-27-5-2)	Humerus	R	Length >8.5, A-P Crest >8.6, Circumf. 12.8	0	0	Juvenile
MOR 355 (8-25-5-5)	Humerus	R	Length >10.0, A-P Crest >5.2, Circumf. 12.4	0	0	Juvenile
MOR 355 (7-5-6-1)	Humerus	L	Length 29.5, A-P Crest 8.7, Circumf. 12.7	0	0	Juvenile
MOR 355 (8-24-5-8)	Humerus	R	Length >22.9, A-P Crest 6.9, Circumf. 11.4	0	0	Juvenile
---	Humerus	R	Length >9.6	0	0	Juvenile
MOR 355 (8-29-5-7)	Humerus	L	Length 32.5, A-P Crest 7.7, Circumf. 12.9	0?	0	Juvenile
MOR 355 (8-22-5-1)	Vert. Element (Neural Arch + Spine)	---	Length 40.6, Spine A-P Length 6.3	0	0	Adult
MOR 355 (7-20-6-1)	Vert. Element (Centrum with Neural Arch and Spine)	---	Centrum Length 4.2, Centrum Width 6.9, Centrum Height 7.0, Spine Height 20.9, Spine A-P Length 4.0, Total Height 29.7	0	0	
MOR 355 (2022-C-650)	Vert. Element (Centrum only)	---	Length 8.5, Width 4.6, Height 7.6	0	2	
MOR 355 (8-26-5-4)	Vert. Element (Centrum only)	---	Length 5.8, Width 5.5, Height 3.0	0	0	
MOR 355 (8-22-5-14)	Vert. Element (Centrum only)	---	Length 8.9, Width 11.4, Height 7.0	0	1	Adult
MOR 355 (8-22-5-14)	Vert. Element (Centrum only)	---	Length 9.2, Width 14.2, Height 6.9	0	1	Adult
MOR 355 (8-22-5-1)	Vert. Element (Cerv., Centrum + Neural Arch)	---	Length 6.5, Width 5.9, Height 3.6	0	0	
MOR 355 (8-28-5-1)	Vert. Element (Centrum only)	---	Length 6.6, Width 6.0, Height 3.5	0	1	
MOR 355 (8-26-5-9)	Vert. Element (Centrum + Neural arch)	---	Length 3.5, Width 4.2, Height 3.7	0	1	
MOR 335 (7-17-6-1)	Vert. Element (Neural Arch + Spine)	---	Length 17.6, Spine A-P Length 5.0	0	0	

Specimen number	Bone	Side	Measurements (cm)	W	A	Notes
MOR 355 (8-28-5-3)	Vert. Element (Neural Arch + Spine)	---	Length 15.4, Spine A-P Length 4.5	0	0	
MOR 355 (8-25-5-11)	Vert. Element (Neural Arch + Base of Spine)	---	Length >7.6, Spine A-P Length 3.0	0	0	
MOR 355 (8-25-5-8)	Vert. Element (Centrum only)	---	Length 4.8, Width 6.6, Height 3.0	0	0	
MOR 355 (8-26-5-8)	Vert. Element (Neural Arch)	---	Height 3.5	0	0	
MOR 335 (2022-C-663)	Vert. Element (Centrum only)	---	Length 5.0, Width 4.1, Height 4.5	0	0	
MOR 355 (8-26-5-3)	Vert. Element (Centrum only)	---	Length 2.9, Width 7.2, Height 6.2	0	0	
MOR 355 (2022-C-650)	Vert. Element (Centrum only)	---	Length 2.1, Width 2.2, Height 1.9	3	1	
MOR 335 (8-26-5-16)	Vert. Element (Centrum + Neural arch)	---	Length 2.0, Width 1.9, Height 1.7	0	1	
MOR 355 (7-7-6-3)	Vert. Element (Haemal Arch/Chevron)	---	Length >14.2	0	0	
---	Vert. Element. (Centrum only)	---	Length 2.3, Width 4.9, Height >3.1	0	0	
MOR 355 (8-25-5-2)	Vert. Element (Centrum only)	---	Length 5.7, Width 15.1, Height 11.1	0	0	Adult
MOR 355 (8-24-5-22)	Vert. Element (Centrum only)	---	Length 6.1, Width 14.8, Height 12.2	0	0	Adult
MOR 355 (8-24-5-9)	Vert. Element (Neural Arch + Base of Spine)	---	Height >16.5	0	0	Adult
MOR 355 (8-22-5-16)	Vert. Element (Neural Arch + Spine)	---	Height >34.2	0	0	Adult
MOR 355 (8-25-5-10)	Vert. Element (Neural Arch + Spine)	---	Height 16.6	0	0	
MOR 355 (E-7-4-12)	Vert. Element (Neural Arch + Spine)	---	Height 22.9	0	0	

Specimen number	Bone	Side	Measurements (cm)	W	A	Notes
MOR 355 (8-25-5-3)	Vert. Element (Neural Arch + Spine)	---	Height 22.2	0	0	
MOR 355 (2022-C-676)	Vert. Elements (Centrum only)	---	Length 4.8, Width 4.7, Height 4.8	0	1	
MOR 355 (8-22-5-8)	Vert. Elements (Partially articulated vertebrae)	---	Length from 2.9 to 5.0	0	0-1/2	
---	Vert. Elements (Centra + Spines)	---	Length from 1.7 to 5.1	0	1	
---	Vert. Elements (Centra + Spines)	---		0	1	
---	Vert. Elements (Centra + Spines)	---		0	1	
---	Vert. Elements (Centra + Spines)	---		0	1	
---	Vert. Elements (Centra + Spines)	---		0	1	
---	Vert. Elements (Centra + Spines)	---		0	1	
---	Vert. Elements (Centra + Spines)	---		0	1	
---	Vert. Elements (Centra + Spines)	---		0	1	
---	Vert. Elements (Centra + Spines)	---		0	0	
---	Vert. Elements (Centra + Spines)	---		0	0	
---	Vert. Elements (Centra + Spines)	---		0	0	
---	Vert. Elements (Centra + Spines)	---		0	0	

Specimen number	Bone	Side	Measurements (cm)	W	A	Notes
---	Vert. Elements (Centra + Spines)	---		0	0	
---	Vert. Elements (Centra + Spines)	---		0	0	
---	Vert. Elements (Centra + Spines)	---		0	0	
---	Vert. Elements (Neural spine fragm.)	---		0	0	
---	Vert. Elements (Neural spine fragm.)	---		0	0	
---	Vert. Elements (Neural spine fragm.)	---		0	0	
---	Vert. Elements (Neural Arch)	---	Width >5.7	0	0	
---	Vert. Elements	---	---	0	0	
---	Vert. Elements	---	---	0	0	
---	Vert. Elements	---	---	0	0	
---	Vert. Elements	---	---	0	0	
---	Vert. Elements	---	---	0	0	
---	Vert. Elements	---	---	0	0	
MOR 355 (7-10-6-1)	Vert. Element (Haemal Arch/Chevron)	---	Length >28.1	0	0	
---	Vert. Elements	---	---	0	0	
---	Vert. Elements	---	---	0	0	
---	Vert. Elements	---	---	0	0	
---	Vert. Elements	---	---	0	0	
---	Vert. Elements	---	---	0	0	
---	Vert. Elements	---	---	0	0	
---	Vert. Elements	---	---	0	1	
---	Vert. Elements	---	---	0	1	
---	Vert. Elements	---	---	0	1	
---	Vert. Elements	---	---	0	1	

Specimen number	Bone	Side	Measurements (cm)	W	A	Notes
---	Vert. Elements	---	---	0	1	
---	Vert. Elements	---	---	0	1	
---	Vert. Elements	---	---	0	1	
---	Vert. Elements	---	---	0	1	
---	Vert. Elements	---	---	0	2	
---	Vert. Elements	---	---	0	2	
MOR 355 (7-21-6-3)	Vert. Element (Centrum + Neural arch)	---	Length 3.3, Width 5.2, Height 3.5	0	0	
MOR 335 (8-28-5-13)	Vert. Elements (Centrum + Neural Arch + Spine)	---	Length 4.7, Width 6.3, Height 6.8	0	0	
MOR 335 (2022-C-730)	Vert. Element (Centrum only)	---	Length >1.2, Width 2.7, Height 2.2	0	1	
MOR 355 (7-8-6-5)	Ilium	R	Length >16.0	0	0	Juvenile
MOR 355 (7-21-6-5)	Ilium	L	Length >32.3	0	0	Juvenile
MOR 355 (8-26-5-5)	Ilium	R?	Length >21.8	0	0	Juvenile
MOR 355 (7-17-6-2)	Ilium	L	Length >41.5	0	0	Juvenile
MOR 355 (8-22-5-3)	Ilium	L	Length >35.8	0	0	Juvenile
MOR 355 (8-22-5-13)	Ilium	L	Length >21.7	0	0	Juvenile
MOR 355 (8-22-5-12)	Ilium	R	Length >16.0	0	0	Juvenile
MOR 355 (8-22-5-21)	Ischium	R	Length >55.5	0	0	Adult
MOR 355 (8-22-5-71)	Ischium	R	Length >25.3	0	0	Juvenile
MOR 355 (8-24-5-5)	Ischium	R	Length >28.2	0	0	Juvenile
MOR 355 (8-22-5-5)	Ischium	L	Length >60.5	0	0	Juvenile
MOR 355 (2022-C-715)	Ischium	?	Length >17.9	0	0	Juvenile
MOR 355 (LE-7-14-4)	Metatarsal (IV?)	R	Length 17.3, Circumf. 9.6	0	0	Juvenile
MOR 355 (2022-C-671)	Metatarsal (II?)	R	Length >6.4, Circumf <10.8	0	1	Juvenile
MOR 355 (7-7-6-4)	Metatarsal (III)	L?	Length 24.3, Circumf. 12.7	0	0	Adult
MOR 355 (8-29-5-8)	Metatarsal (IV?)	L?	Length 19.0, Circumf. 10.7	0	0	Juvenile
MOR 355 (7-13-6-2)	Metacarpal (III)	R?	Length 14.0, Circumf. 5.2	0	0	
MOR 355 (2022-C-722)	Metacarpal (III?)	R?	Length >5.1, Circumf. 5.4	0	0	

Specimen number	Bone	Side	Measurements (cm)	W	A	Notes
MOR 355 (8-29-5-10)	Premaxilla	R	Length > 12.7, Pinch not measurable (<3.0)	0	1	Juvenile
MOR 355 (2022-C-718)	Premaxilla	R	Length >22.1, Pinch 4.4	0	0	
MOR 355 (7-11-6-1)	Maxilla	R	Length 17.9, Height >5.6	0	0	
MOR 355 (LE-6-22)	Maxilla	L?	Length >20.2, Height >6.5	0	0?	Adult
MOR 355 (8-20-5-1)	Dentary	R	Length 23.0, Height a coronoid >8.5	0	0	Juvenile
MOR 355 (8-29-5-5)	Ulna	R	Length >15.8, Circumf. 8.7	0	0?	Juvenile
MOR 355 (8-25-5-1)	Ulna	L?	Length 38.4, Circumf. 9.4	0	0	Juvenile
MOR 355 (8-26-5-12)	Ulna	L	Length 38.1, Circumf. 8.5	0	0	Juvenile
MOR 355 (8-25-5-7)	Radius	L	Length 35.4, Circumf. 7.2	0	0	Juvenile
MOR 355 (2022-C-653)	Prefrontal (?)	L	Length >5.5	0	1	Juvenile
MOR 355 (8-26-5-15)	Quadrate	R	Length 17.9	0	0	Adult
---	Postorbital	L	Length >13.2, Height >4.7	0	2	Adult
MOR 355 (8-28-5-11)	Pedal ungual (II-3)	R?	Length 4.5, Width 3.8	0	0	
MOR 355 (8-28-5-70	Pedal ungual (III-4)	R?	Length 3.9, Width 4.8	0	0	
MOR 355 (8-29-5-1)	Pedal phalanx (IV-3?)	L?	Length 1.8, Width 4.8	0	0	
MOR 355 (2022-C-719)	Pedal ungual (II-3?)	?	Length 4.6, Width 3.8	0	0	
MOR 355 (2022-C-720)	Pedal ungual (II-3?)	?	Length >2.4, Width 4.0	0	1	
MOR 355 (2022-C-721)	Pedal phalanx (IV-3?)	?	Length 1.4, Width 3.5	0?	0	
MOR 355 (2022-C-724)	Pedal phalanx (II-2?)	?	Length 1.9, Width 3.4	0	1	
MOR 355 (8-26-5-17)	Manual phalanx (V-2?)	?	Length 2.8	0	0	
---	Manual phalanx (V-1?)	?	Length 3.0	0	1	
---	Manual phalanx (II-3?)	?	Length from >2.0 to >3.0	0	1	
---	Manual phalanx (III-3)	?	Length >2.0	0	1	
---	Manual phalanx (V-2)	?	Length >2.1	0	0	
---	Manual phalanx	?	Length >2.2	0	1	
---	Manual phalanx	?	Length >2.3	0	1	
---	Manual phalanx	?	Length >2.4	0	2	
MOR 355 (2022-C-726)	Manual phalanx (V-1?)	?	Length >2.0	0	0	
---	Ribs	R	Length from >10.0 to >34.7	0	0	7 distinct ribs

Specimen number	Bone	Side	Measurements (cm)	W	A	Notes
---	Ribs	L	Length from >16.7 to >34.1	0	0	4 distinct ribs
---	Ribs	R	Length >22.2 and >21.1	0	0	2 distinct ribs
MOR 355 (8-24-5-6)	Ribs	L	Length >38.5	0	0	1 distinct rib
---	Rib fragments	---	---	0	0	8 fragm.
---	Rib fragments	---	---	0-1?	0	8 fragm.
---	Rib fragments	---		0	0	2 fragm.
---	Rib fragments	---	---	0	0	24 fragm.
MOR 355 (8-26-5-2)	Bone fragment	---	---	0	0	2 fragm.
---	Bone fragment	---	---	1	1-2	14 fragm.
---	Bone fragments	---	---	0	0	9 fragm.
---	Bone fragments	---	---	0	0	11 fragm.
---	Bone fragments	---	---	0-3	0-1	5 fragm.
MOR 355 (2022-C-654)	Bone fragment	---	---	0	1	1 fragm.
---	Bone fragments	---	---	0	0	32 fragm.
---	Bone fragments	---	---	0-1	0-1	3 fragm.
---	Bone fragments	---	---	1?	0	2 fragm.
---	Bone fragments	---	---	0	0	18 fragm.
---	Bone fragments	---	---	0	2-3	11 fragm.
---	Bone fragments	---	---	0	0-1	54 fragm.
---	Bone fragments	---	---	0	0	3 fragm.
---	Teeth	---	---	---	---	5 tyrannosaur (?) teeth
---	Turtle (?) elements	---	---	0	0-1	5 fragments
---	Fish plates	---	---	---	---	

APPENDIX D: OVERVIEW OF TAPHONOMIC SIGNATURES OF MONODOMINANT HADROSAURID BONEBEDS

Bonebed	Taxa	Type of BB	Formation	Age	Location	MNI	Grouwth stages	Biological age	Weathering	Abrasion	Breakage/Fractures	Other features	Reference
Devil's Coulee Juvenile Bonebed (JBB)	*Hypacrosaurus stebingeri*	Mass mortality	Oldman	late Campanian	Alberta (Canada)	4	Late juvenile	3	Little	Little to no	Transverse (56.0%), Spiral (6.0%)	Wet rot, Rare tooth marks (3 specimens)	This thesis
Spring Creek Bonebed	Lambeosaurine	Mass mortality	Wapiti	late Campanian	Alberta (Canada)	8	Late juvenile	Unknown (no LAG, but potentially around 2-3 years old)	Stage 0 = 72.9%, Stage 1 = 16.8%, Stage 2 = 10.3%	Stage 0 = 84.3%, Stage 1 = 13.9%, Stage 2 = 0.9%, Stage 3 = 0.9%	Complete = 44.2%, Spiral = 7.6%, Transverse = 9.3%, Mixed = 38.9%	Tooth marks on 3.8%, Parallel striae on 28.2%	Holland et al. (2021)
Blacktail Creek North (TM-066, MOR 548)	*Hypacrosaurus stebingeri*	Mass mortality	Two Medicine	late Campanian	Montana (USA)	23	"Yearlings" (early juveniles)	<1	Little to no	Little to no	Little to no		Varricchio and Horner (1993) & This thesis
Lambeosite (TM-019, MOR 355)	*Hypacrosaurus stebingeri*	Mass mortality	Two Medicine	late Campanian	Montana (USA)	5	Late juvenile (4), Adult (1)	3	Little to no	Little to no	Little to no		Varricchio and Horner (1993) & This thesis
Camposaur Bonebed (TM-003)	*Maiasaura peeblesorum*	Mass mortality	Two Medicine	late Campanian	Montana (USA)	20	Juvenile	Unknown (no histo data)	Most with weathered ends		Most with broken ends		Varricchio and Horner (1993)
West Hadrosaur Bonebed (TM-067)	*Maiasaura peeblesorum*	Mass mortality	Two Medicine	late Campanian	Montana (USA)	9	Juvenile (8), Adult (1)	Unknown (no histo data)	Little to no	Little to no	Little to no		Varricchio and Horner (1993)
Westside Quarry (TM-041)	*Prosaurolophus maximus* (*'blackfeetensis'*)	Mass mortality	Two Medicine	late Campanian	Montana (USA)	4	Subadult, Adult	Unknown (no histo data)	Little to no	Little to no	Little to no		Varricchio and Horner (1993) & Rogers (1990)
Blagoveschensk dinosaur locality (BDL)	*Amurosaurus riabinini*	Attritional	Udurchukan	?late Maaastrichtian	Russia	?	Late juvenile, Subadult	Unknown (no histo data)	Little to no (less than 2%)	Common (rounded broken edges)	Common	Rare tooth marks (less than 2%), No trample marks, No teeth in dentary battery	Lauters et al. (2008)
Dragon's Tomb	*Saurolophus angustirostris*	Mass mortality	Nemegt	Maastrichtian	Mongolia	21	Juvenile, Subadult, Adult (no hatchlings/ yearlings)	Unknown (no histo data)	No weathering (stage 0)	No abrasion (stage 0)	Undescribed	No tooth marks, Articulated and disarticulated individuals, Skin impressions	Bell et al. (2018)
Princess Bonebed	Lambeosaurine (likely *Lambeosaurus lambei*)	Mass mortality	Dinosaur Park	Campanian	Alberta (Canada)	3	Subadult, Adult	Unknown (no histo data)	Little to no	Uncommon (on broken edges of 8 elements)	Common (93% incomplete)	Rot (20 elements), Potential tooth mark on 1 element	Eberth et al. (2014)
Willow Creek Anticline Bonebed (MOR-TM-003)	*Maiasaura peeblesorum*	?	Two Medicine	Campanian	Montana (USA)	7	?	Unknown (no histo data)	Stage 0 = 37%, Stage 1 = 60%	Moderate	Mostly broken (84%)	Evidence of gnawing on 3.9%, Invert. borings on 1.6%, Root traces on 78.6%	Schmitt et al. (2014)
Kugou Quarry	*Shantungosaurus giganteus*	Mass mortality	Xingezhuang/ Hongtuya	Campanian	Shandong Province (China)	55	Adult	Unknown (no histo data)	?	?	Mostly complete		Hone et al. (2014)
Bleriot Ferry (BF)	*Edmontosaurus regalis*	Mass mortality (most likely)	Horseshoe Canyon	late Campanian	Alberta (Canada)	9	Late juvenile, Adult (mainly)	Unknown (no histo data)	Little to no (less than 1%)	stages 1-3	Both ends (more than 90%), Compression fract. (more than 80%)	Tooth marks (10%), Trample marks (more than 15%)	Evans et al. (2015)
Fox Coulee (FC)	*Edmontosaurus regalis*	Mass mortality (most likely)	Horseshoe Canyon	late Campanian	Alberta (Canada)	?	Juvenile, Subadult, Adult	Unknown (no histo data)	Little to no (less than 1%)	Minimal abrasion, stages 1-3	Both ends (more than 90%)		Evans et al. (2015)
Prehistoric Park (PP)	*Edmontosaurus regalis*	Mass moratlity (most likely)	Horseshoe Canyon	late Campanian	Alberta (Canada)	2	Subadult, Adult	Unknown (no histo data)	Little to no (less than 1%)	Minimal abrasion, stages 1-3	Both ends (more than 90%), Compression fract. (more than 80%)		Evans et al. (2015)
Danek Bonebed	*Edmontosaurus regalis*	Mass mortality	Horseshoe Canyon	late Campanian	Alberta (Canada)	12	Missing only hatchling-sized individuals	Unknown (no histo data)	Little to no (over 90% stage 0)	Early stages of abrasio (97% stages1 or 2)	Mostly broken	Tooth marks on 24.5% (mostly on tyrannosaurid)	Bell and Campione (2014)
Sun River Bonebed	Lambeosaurine	Mass mortality	Two Medicine	late Campanian	Montana (USA)	8	Late juvenile	Unknown (no histo data)	Stage 0 = 97%, rest is stage 1	stage 0 = 68%, stage 1 = 29.6%, stage 2 = 1.8%	Mostly complete (28% are fractured, mostly spiral and transverse)	Wet rot, Presence of 1 smaller humerus, Consistent taphonomic signatures	Scherzer and Varricchio (2010)

Bonebed	Taxa	Type of BB	Formation	Age	Location	MNI	Grouwth stages	Biological age	Weathering	Abrasion	Breakage/Fractures	Other features	Reference
Standing Rock Hadrosaur Site	*Edmontosaurus annectens*	Mass mortality	Hell Creek	Maastrichtian	South Dakota (USA)	44	Late early juvenile (7%), Late juvenile (12%), Subadult (51%), Adult (30%)	Unknown (no histo data)	Stage 0 = 96%, Stage 1 = 4%, Stage 2 = 0.1%, Stage 3 = 0.1%	Stage 0 = 92%, Stage 1 = 8%, Stage 2 = 0.2%, No stage 3	62% are complete (incompleteness of some bones may be due to excavation/preparation)	Tooth marks on 5.5% (100 bones), Trample marks on 2.5% (45 bones), Disarticulated/Disassociated, Most maxilla retain all or majority of their teeth, Dentaries don't retain teeth	Ullmann et al. (2017)
Concordia Hadrosaur Site	*Edmontosaurus annectens*	Attritional (most likely)	Hell Creek	Maastrichtian	South Dakota (USA)	?	?Adult	Unknown (no histo data)	Undescribed	Undescribed	Undescribed	Undescribed	Colson et al. (2004)
Wendy's Bonebed (WBB)	*Gryposaurus* sp.	Mass mortality	Oldman	Campanian	Alberta (Canada)	3	Juvenile	2 groups - <1 year, <2 year	Very little (less than 4% - stage 1 = 3 specimens, Stage 2 = 1 specimen)	Stage 0 = 55%, Stage 1 = 26%, Stage 2 = 15%, Stage 3 = 4%	Mostly incomplete (17% show no breakage)		Scott et al. (2022)
Hanson Ranch Bonebed (HR)	*Edmontosaurus annectens*	Mass mortality	Lance	late Maastrichtian	Wyoming (USA)	18	Late juvenile, ?Subadult, ?Adult	Unknown (no histo data)	Little (stage 0 = 98.5%)	Stage 0 = 97%, Stage 1 = 2%, Stage 2 = 0.7%, Stage 3 = 0.1%	48% unfractured		Snyder et al. (2020)
Liscomb Bonebed	*Edmontosaurus sp.*	Mass mortality	Prince Creek	late Campanian - early Maastrichtian	Alaska (USA)	19	Late juvenile	Unknown (no LAG)	Stage 0 = 74%	Mostly unabraded or very slight abrasion (stages 0-1), High abrasion = 1.2%	Highly fragmented, Transverse fractures (post-diagenesis), Very rare spiral fractures (fresh bone)	Rare tooth marks (1%), Disseminated pyrite in some bones	Gangloff and Fiorillo (2010)
Basturs Poble	*Pararhabdodon isonensis*	?Mass mortality	Tremp	Maastrichtian	Spain	22	?Juvenile, ?Subadult		Stage 0 = 66.67%, Stage 1 = 24.5%, Stage 2-3 < 9%	Stage 0 = 47.03%, Stage 1 = 39.28%, Stage 2 = 11.89%, Stage 3 = 1.81%			Gaete Harzenetter (2020) - PhD thesis
JDM Quarry (Malta Bonebed)	*Brachylophosaurus* sp.	?	Judith River	Campanian	Montana (USA)	6	Subadult (4), Adult (2)	Unknown (no histo data)	Minimal (Stage 0 = 88%, Stage 1 = 11.5%)	Absent	?	Tooth marks (5 bones)	LaRock (2000) - MSc thesis
Wulaga quarry	*'Sahaliyania elunchunorum' (Amurosaurus riabinini)*	Undescribed	Yuliangze	Maastrichtian	Heilongjiang Province (China)	?	?(Different sizes)	Undescribed	Undescribed	Undescribed	Undescribed	Undescribed	Godefroit et al. (2008)
	Probrachylophosaurus sp.	Undescribed	Foremost	middle Campanian	Alberta (Canada)	?	Undescribed	Undescribed	Undescribed	Undescribed	Undescribed	Undescribed	Thompson et al. (2020, 2021)
	Hypacrosaurus altispinus	Undescribed	Horseshoe Canyon	late Campanian - Maastrichtian	Alberta (Canada)	?	Undescribed	Undescribed	Undescribed	Undescribed	Undescribed	Undescribed	